Supporting Information

Co-modified Nickel Ferrite Magnetic Nanomaterials: A Green, Cost-Effective, and Functional Catalytic Platform for Suzuki-Miyaura Cross-Coupling Reaction

Jyotismita Bora[a], Mayuri Dutta[a], Aquif Suleman[a], Gunjan Hazarika[a], Tikendrajit Chetia[a], Rituparna Chutia[b], Bolin Chetia[a]*

[a]Department of Chemistry, Dibrugarh University, Dibrugarh, Assam-786004, India

[b]Guwahati College, Guwahati, Assam-781021

*E-mail: bolinchetia@dibru.ac.in

Sl. No.	Contents	Page No.
1	d-spacing calculation of Co-$NiFe_2O_4$ NPs from SAED pattern	2
2	Histogram statistics from TEM image and Polydispersity metrices	2
3	Recyclability of the Co-$NiFe_2O_4$ Catalyst for the SMC reaction	3-5
4	Hot-filtration and Leaching test of the Co-$NiFe_2O_4$ nanocatalyst for the SMC reaction	6-7
5	Testing of reaction efficiency in presence of 95% ethanol	7-8
6	Green chemistry matrix calculations	8-10
7	Pd-scavenging experiments	10
8	S17. Comparison of some Pd-based catalysts and the present Co-containing catalyst in Suzuki-Miyaura coupling	11
9	S18. Analytical data of some representative compounds	12-46
10	References	47

Table S1: d-spacing calculation of Co-$NiFe_2O_4$ NPs from SAED pattern

Sl. No.	1/2r(nm^{-1})	1/r (nm^{-1})	r (nm)	d-spacing(Å)	(h k l)
1	6.044	3.022	0.330907	3.309067	(2 2 0)
2	7.762	3.881	0.25766	2.5766	(3 1 1)
3	8.889	4.445	0.2249	2.249	(2 2 2)
4	12.086	6.043	0.165481	1.654807	(4 2 2)
5	13.277	6.638	0.1506	1.506	(5 1 1)
6	16.376	8.188	0.1222	1.222	(4 4 0)

2. Histogram statistics from TEM image and Polydispersity metrices:

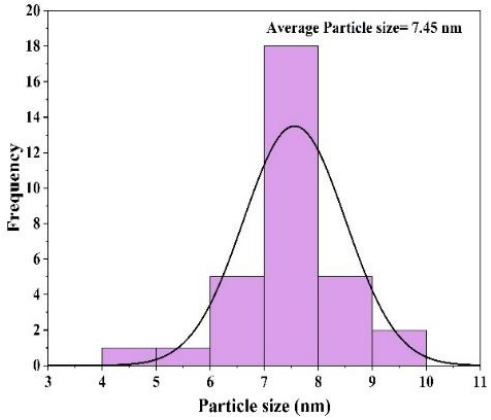

S2: Average particle size distribution curve from relevant Co-$NiFe_2O_4$ TEM image

Histogram statistics from TEM image,

Standard deviation, SD = 1.13

Percentile Diameter, d10= 6.02

d50= 7.69

d90=8.84

Polydispersity metrices: Polydispersity index,

Span= $\frac{d90-d10}{d50}$ = 0.37

Lower the value of span, narrower is the size distribution and it implies narrow and uniform particle growth.

Coefficient of variation (CV)= $\frac{SD}{d} = \frac{1.13}{7.45} = 0.15$

CV<0.10, highly monodisperse

CV= 0.10-0.20, moderately polydisperse

CV>0.20, polydisperse. Since, the value of CV=0.15, hence the particles are moderately dispersed.

3. Recyclability of the Co-$NiFe_2O_4$ Catalyst for the Suzuki-Miyaura Cross-coupling (SMC) reaction:

One of the most important characteristics of a heterogeneous catalyst is its recyclability. For the recyclability test, 4-methylphenylboronic acid and bromobenzene were selected as the model substrates. The magnetic nan catalyst was isolated via an external magnet. This method was repeated for four consecutive cycles. The catalyst can be successfully used up to 6th catalytic cycle with negligible loss in the product yield. The TEM and PXRD analysis were performed for the reused catalyst. FESEM (Fig. S6), TEM analysis (Fig. S7) of the reused catalyst (after 6th cycle) showed nearly identical morphology of the nanocrystals i.e. retained its spherical nature. The average particle size (Fig. S8) was found to be nearly same after 6th cycle (7.89 nm). The PXRD analysis (Fig. S9) showed the existence of all the planes as the fresh catalyst in the recycled (6th cycle) catalyst. The VSM data of the recycled catalyst showed a negligible drop in saturation magnetization value (Fig. S10). The XPS spectrum of recycled catalyst showed presence of Ni (2p), Co (2p),Fe (2p) and O (1s) as the main elements in the sample. The XPS sprectrum showed Co, Ni in +2 state and also showed peaks for Fe (2p). This means the metals of the catalyst restored its original oxidation state after sixth cycle (Fig. S11). For the better assessment of catalyst's reusability and to evaluate the stability and usefulness over time the amount of catalyst recovered after each run was measured and the reactants were weighed on the basis of amount of catalyst recovered.

Table S3: Recovery of catalyst after each run

Cycle	Catalyst Used (mg)	Catalyst Recovered (mg)	Recovery (%)	Yield (%)
1st	10	9.7	97	95
2nd	9.7	9.3	95.87	94
3rd	9.3	8.7	93.54	92
4th	8.7	8.0	91.95	90
5th	8.0	7.3	91.25	87
6th	7.3	6.5	89.04	84

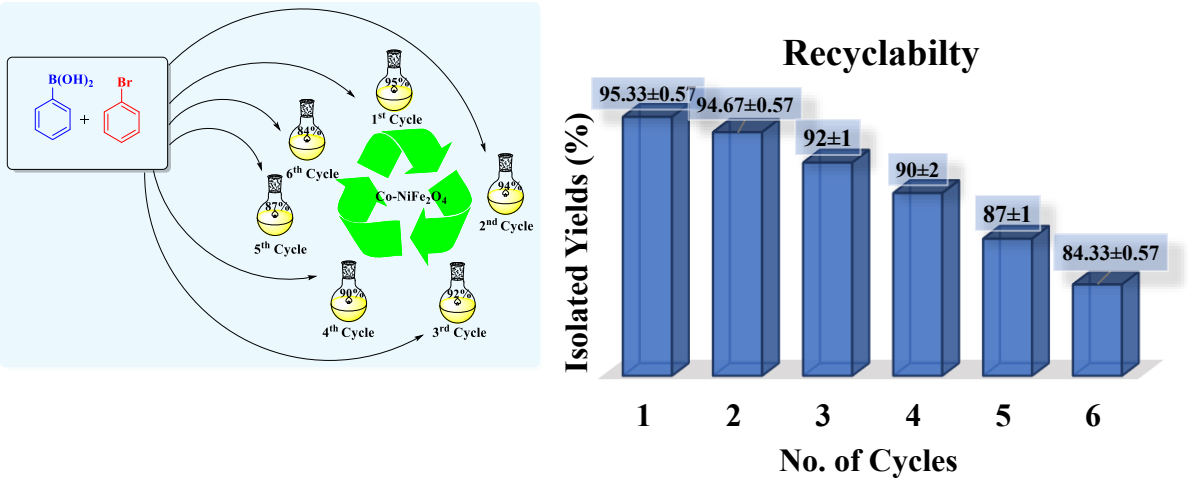

S4: Schematical and graphical representation of recyclability of the Catalyst

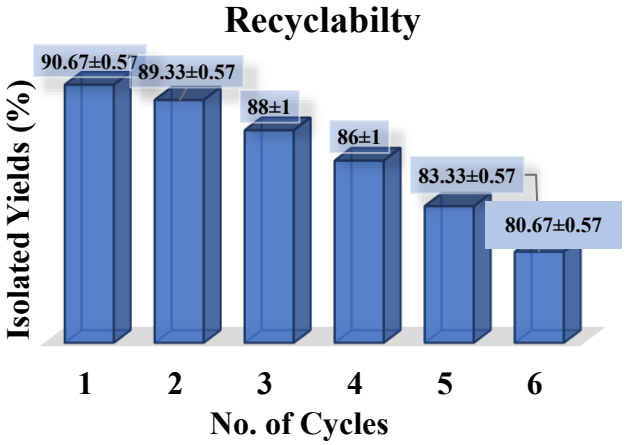

S5: Graphical representation of recyclability of the catalyst (reaction between Chlorobenzene and phenylboronic acid)

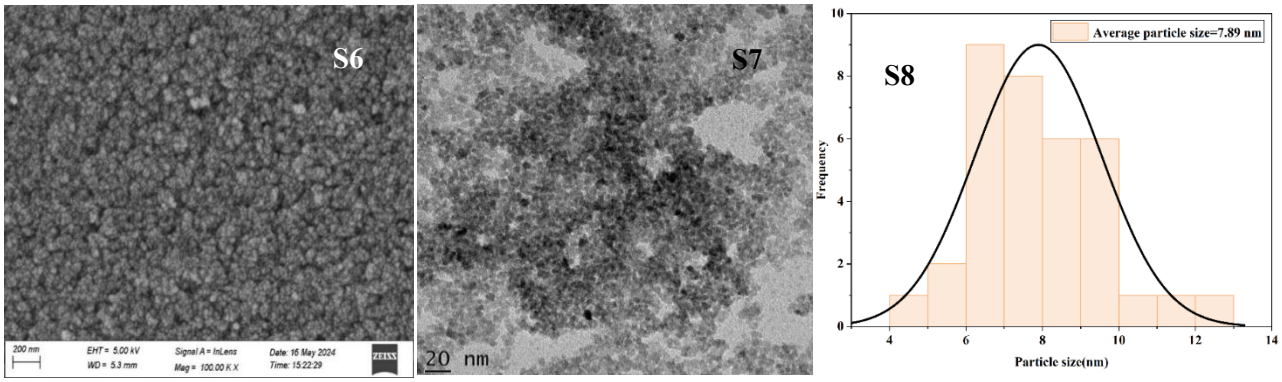

S6, S7: FESEM and TEM image of recycled Co-$NiFe_2O_4$ nanocatalyst

S8: Average size distribution of recycled Co-$NiFe_2O_4$ nanocatalyst

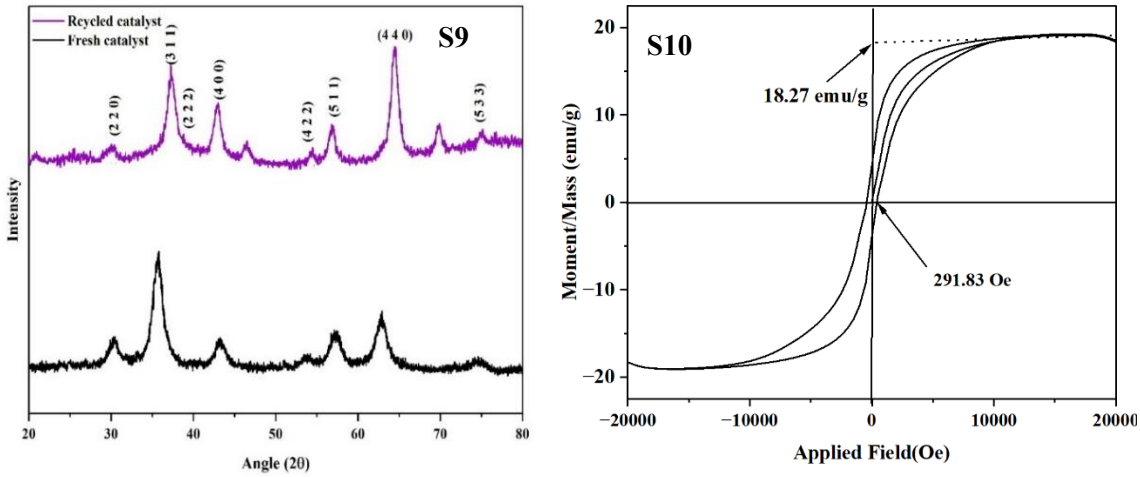

S9, S10: PXRD pattern and VSM data of recycled Co-$NiFe_2O_4$ nanocatalyst

Table S11: ICP-MS analysis of fresh and recycled catalyst

Sl No.	Sample name	Ni	Co	Fe	Pd
1	Co-$NiFe_2O_4$ (Fresh)	4.68	3.87	13.11	-
2	Co-$NiFe_2O_4$ (Recycled)	4.39	3.56	12.98	-
Unit		%	%	%	%
Detection Limit (ppm)		0.01	0.01	0.1	0.01

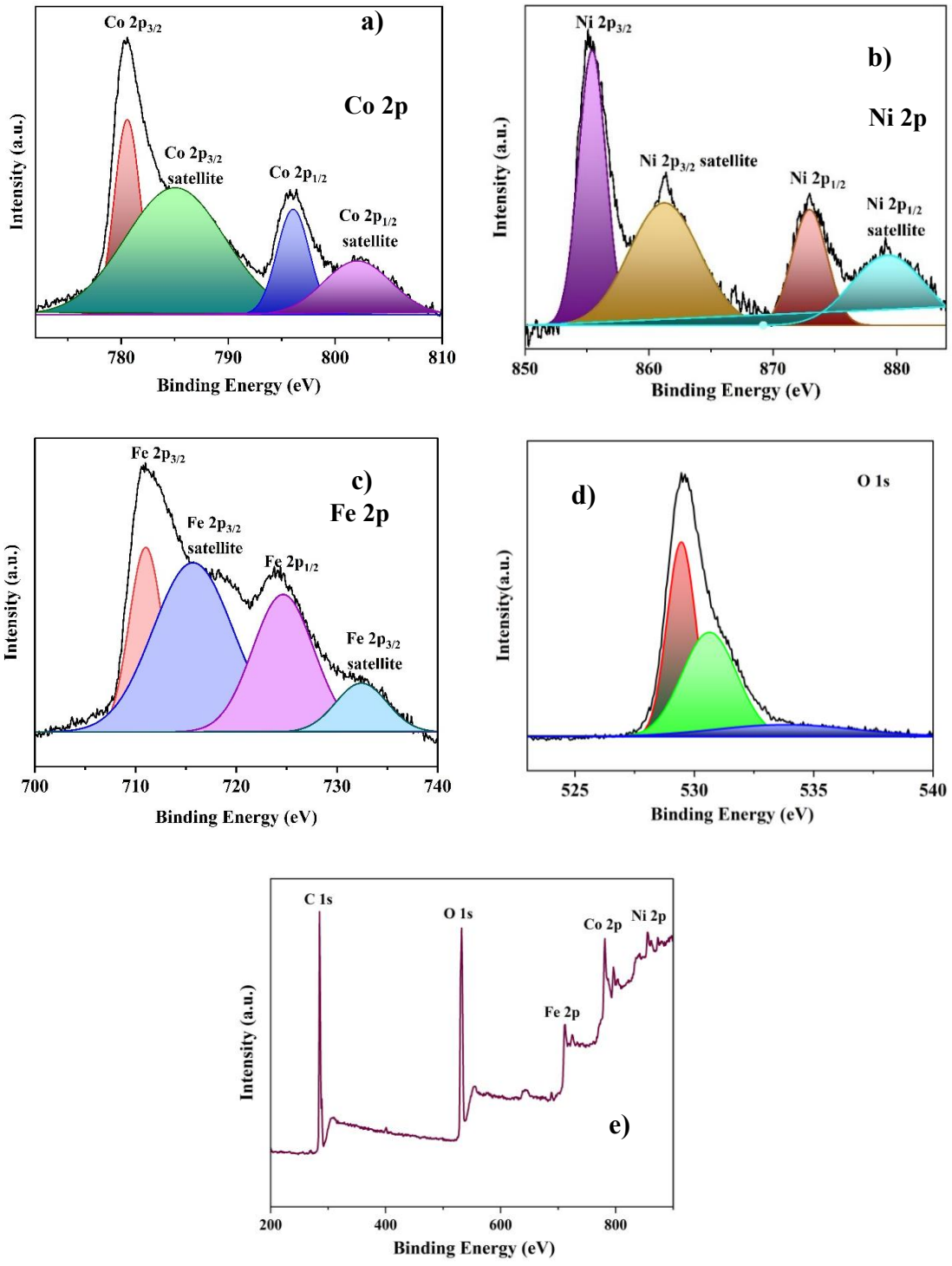

S12: XPS spectrum of recycled Co-$NiFe_2O_4$ (a) XPS spectrum of Co 2p b) XPS spectrum of Ni 2p c) XPS spectrum of Fe 2p d) XPS spectrum of O 1s (e) Wide survey scan XPS spectrum of recycled Co-$NiFe_2O_4$ sample

4. Hot-filtration and Leaching test of the Co-$NiFe_2O_4$ nanocatalyst for the SMC reaction: Hot-filtration test or leaching test is generally used to figure out whether the nature of catalyst is heterogeneous or homogeneous. The hot filtration test was performed for the SMC reaction using 4-methylphenylboronic acid and bromobenzene with the optimized reaction condition and progress of the reaction was monitored by TLC. After 45 mins or half conversion; the catalyst was removed via magnetic separation and the mixture was filtered. The reaction was continued for additional 3h with the filtrate and no significant progress of the reaction was detected. These findings clearly nullify homogeneous nature of catalysis.

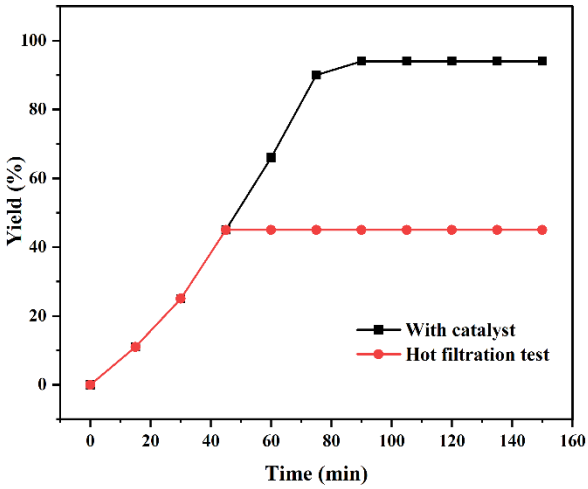

S13: Hot filtration test for the SMC reaction

To address the issue of metal leaching, quantitative analysis of dissolved Ni, Co and Fe species in the reaction media was performed using ICP-MS.

1. **Fresh catalyst reaction filtrate (FCF):**
   After hot filtration at the reaction temperature, the clear filtrate was analysed for Ni and Co content. Both metals were found to be present at trace levels.
2. **Recycled catalyst reaction filtrates (RCF):**
   After each catalytic cycle were similarly filtered and analyzed. No quantifiable accumulation of Ni or Co metal was detected over successive runs, indicating negligible metal leaching during recycling.
3. **Time-resolved analysis (TR):**
   Aliquots withdrawn at different reaction times (e.g., 30 min and 60 min) showed no Ni and Co content, supporting the absence of leaching under operating conditions.

Table S14: ICP-MS analysis of FCF, RCF and TR samples

Sl No.	Sample name	Ni	Co	Fe	Pd
1	FCF	-	-	-	-
2	RCF	-	-	-	-
3	TR_{30}	-	-	-	-
4	TR_{60}	-	-	-	
Unit		%	%	%	%
Detection Limit in ppm		0.01	0.01	0.1	0.1

These results, along with the hot-filtration test (no further product formation after catalyst removal), clearly demonstrate that the catalytic activity arises from the heterogeneous solid catalyst rather than dissolved metal species.

ICP-MS analysis of the post-reaction filtrate obtained after hot filtration. (Table S14, Entry 1). The concentrations of Ni and Co were found to be below the detection limit ruled out the leaching of catalytically active species under the reaction conditions.

Catalyst deactivation is governed by surface-level phenomena-primarily fouling, aggregation, and subtle surface reconstruction-rather than bulk phase instability or dominant metal leaching.

The correlation between catalyst deactivation with structural changes, the characterization of the recovered catalyst. Comparative XRD, VSM, average particle size distribution, XPS and ICP-MS analysis of the recycled catalyst reveal that the spinel structure and magnetic properties are largely retained after repeated cycles, suggesting that the observed decline in yield is primarily due to surface partial aggregation rather than metal loss. FESEM and TEM image of recycled catalyst showed retention of morphology with slight aggregation.

Taken together, the combination of hot filtration, ICP-MS leaching analysis, and characterization of recycled catalyst provides strong evidence for the heterogeneous nature and stability of the catalyst.

5. Testing of reaction efficiency in presence of 95% ethanol:

The catalytic activity of the Co-containing catalyst was evaluated in 95% ethanol as a reaction medium. Both boronic acid substrates with electron donating and withdrawing groups were tested along with heterocyclic boronic acids. However, the results showed lower yields, likely due to reduced solubility of base and/or unfavourable interaction with the catalyst surface.

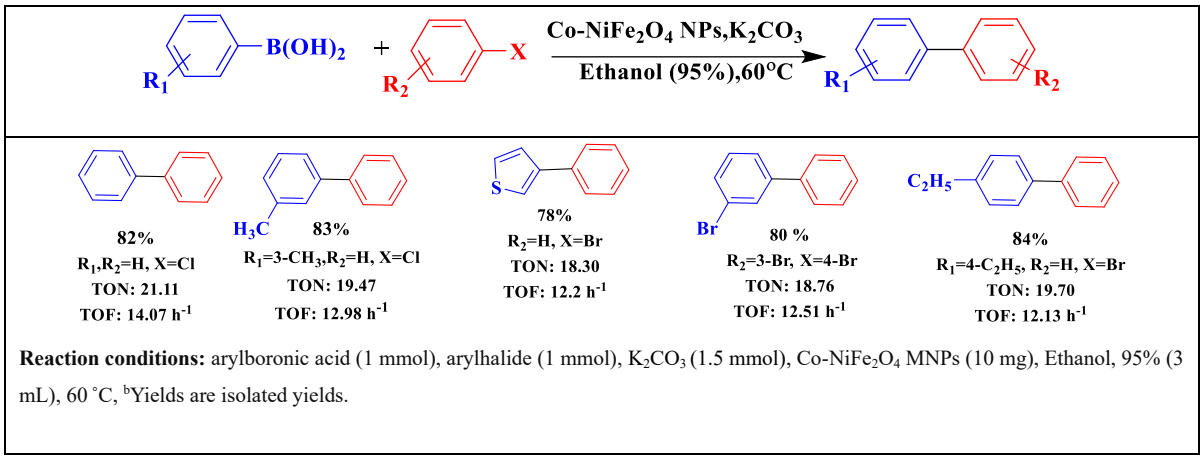

Reaction conditions: arylboronic acid (1 mmol), arylhalide (1 mmol), K_2CO_3 (1.5 mmol), Co-$NiFe_2O_4$ MNPs (10 mg), Ethanol, 95% (3 mL), 60 °C, [b]Yields are isolated yields.

Table S15: Substrate scope for biaryl synthesis via SMC reaction in presence of 95% ethanol as a reaction medium

6. Green chemistry matrix calculation:

Environmental factor (E-factor): E-factor of a reaction can be defined as the ratio of mass of the total waste and mass of the product. It is a simple metric used to define greenness of a reaction.

$$\text{E-factor}=\frac{Mass\ of\ total\ waste}{Mass\ of\ the\ product}$$

$$\text{Or E-factor}=\frac{Mass\ used-Mass\ recovered}{Mass\ of\ the\ product}$$

With decrease in E-factor value, greenness of a reaction increases.

a) E-factor Calculation for Synthesis of biaryls:

Substrates

Phenylboronic acid (1 mmol)	0.121 g
Chlorobenzene (1 mmol)	0.113 g
K_2CO_3 (1.5 mmol)	0.207 g

Catalyst, $Ni_{0.6}Co_{0.4}Fe_2O_4$ NPs	0.010g
Solvent: Ethanol: H_2O mixture (3 ml)	2.68 g
Wash solvent	6 g
Product:	0.138 g

E-factor=$\frac{(0.121+0.113+0.207+0.010+2.68+6)-(0.138+0.010+2.68+6)}{0.138}$

E-factor=2.19

b) Reaction mass efficiency (RME):

$$\textbf{RME}=\frac{\boldsymbol{Mass\ of\ product}}{\sum(\boldsymbol{Mass\ of\ stoichiometic\ reactants})}\times \mathbf{100}$$

Greenness of a reaction is directly proportional to RME value.

Substrates

	Phenylboronic acid (1 mmol)	0.121 g
	Chlorobenzene (1 mmol)	0.113 g
Product:	1,1´-biphenyl	0.138 g

$$\textbf{RME}=\frac{\mathbf{0.138}}{(\mathbf{0.121+0.113})}\times\mathbf{100 = 58.97\%}$$

Green chemistry matrix calculation for Co-$NiFe_2O_4$:

i) E-factor Calculation:

$$\text{E-factor}=\frac{Mass\ of\ total\ waste}{Mass\ of\ the\ product}$$

$$\text{Or E-factor}=\frac{Mass\ used-Mass\ recovered}{Mass\ of\ the\ product}$$

Reactants	Amount(g)
$NiCl_2.6H_2O$	0.285
$CoCl_2.6H_2O$	0.191
$Fe(NO_3)_3.9H_2O$	0.810
$(NH_4)_2CO_3$	0.480
Ascorbic acid	1.76
Water used	75.00
Ethanol Used	35.50
Water recovered	75.00
Ethanol recovered	1.116
Mass of the product obtained	0.390

$$\text{E-factor}=\frac{Mass\ used-Mass\ recovered}{Mass\ of\ the\ product}$$

$$=\frac{(0.285+0.191+0.810+0.480+1.76+75+35.50\ )-(1.116+75+35.50+1.60)}{1.116}$$

=0.726 (Less waste generation)

ii) **Reaction Mass Efficiency (RME):**

$$\text{RME}=\frac{Mass\ of\ product}{\sum(Mass\ of\ stoichiometic\ reactants)}\times 100\ \%$$

$$RME=\frac{1.116}{(0.285+0.191+0.810)}\times 100\%$$

=86.78% (>70%, highly sustainable)

7. **Pd-scavenging experiments:**

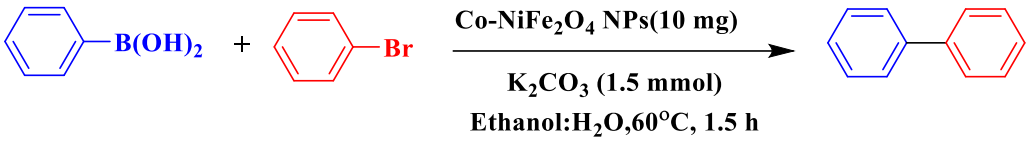

Table S16: Control experiments for Pd-scavenging

Sl. No.	Pd-scavengers	Yield (%)
1	-	94±1
2	SiliaMetS Thiol (50 mg)	94±1
3	SiliaMetS Thiourea (50 mg)	94±1

To ruled out the fact of presence of Pd in trace amount, we have carried out Pd- scavenging experiments. We performed the reaction in presence of metal scavengers SiliaMetS Thiol and SiliaMetS Thiourea, it was observed that same yield of product was obtained after 1.5 h both in presence of Pd- scavengers as well as in absence of scavengers. These findings confirm the absence of Pd in the protocol.

Table S17. Comparison of some Pd-based catalysts and the present Co-containing catalyst in Suzuki-Miyaura coupling

Pd-based catalytic systems (literature)	Catalyst type	Cost consideration	Recyclability	Sustainability aspect	Substrate scope
Pd- Embedded Triptycene-Based Porous Organic Polymer	Heterogeneous (15 mg) Tedious synthetic procedure of catalyst	Precious metal (Pd), but efficient at low loading	Up to 5th cycles	Efficient but not always sustainable, mild reaction conditions. Possibility of metal contamination	Iodo and bromo derivatives
Xerogel G8Pd NPs	Heterogeneous (20 mg) Facile synthetic procedure of catalyst	Precious metal (Pd), but efficient at low loading	Up to 5th cycles	Efficient but not much sustainable (since acetonitrile is used) Possibility of metal contamination	Only iodo derivatives
Pd@CMC-CA-PVA	Heterogeneous (40 mg) Tedious synthetic procedure of catalyst	Precious metal (Pd), but efficient at low loading	Up to 6th cycles	Not sustainable (since DMF is used) Possibility of metal contamination	Only iodo derivatives
Fe-based MOFs @Pd@COFs	Heterogeneous (20 mg) Tedious synthetic procedure of catalyst	Precious metal (Pd), but efficient at low loading	Up to 5th cycles	Mild reaction conditions Possibility of metal contamination	Iodo and bromo derivatives
Co-$NiFe_2O_4$ NPs	Heterogeneous (10 mg) Facile synthetic procedure of catalyst	Earth-abundant, low-cost metal	Up to 6th cycles	More aligned with green chemistry principles, mild reaction conditions. Lower risk of metal contamination	Iodo, bromo and chloro derivatives

S18: Analytical Data of the representative compounds: (NMR and LCMS analysis)

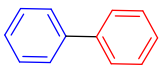	**1,1'-biphenyl** White coloured powder, m.p. 69˚C ^{1}H NMR (500 MHz, $CDCl_3$) δ 8.27 (d, J=7 Hz, 4H), 7.63 (t, J = 7 Hz, 2H), 7.54 (t, J=7 Hz,4H) ppm, $^{13}C\{^1H\}$ NMR (125 MHz, $CDCl_3$) δ 141.93, 135.66, 132.71,128.00 ppm.
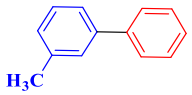	**3-methyl-1,1'-biphenyl** Off-white coloured oily liquid, m.p. 29˚C ^{1}H NMR (500 MHz, $CDCl_3$) δ 8.02(s, 1H), 7.92 (d, J = 8.5 Hz, 2H), 7.86 (d, J = 8 Hz, 2H), 7.69 (d, J = 8 Hz, 1H), 7.64 (t, J=7 Hz, 1H), 7.58 (d, J= 7.5 Hz, 1H), 7.53 (t, J= 7 Hz, 1H), 2.48 (s, 3H) ppm.
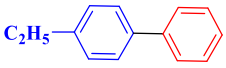	**4-ethyl-1,1'-biphenyl** Off-white coloured powder, m.p. 40˚C ^{1}H NMR (500 MHz, $CDCl_3$) δ 7.73(t, J=7.5 Hz, 1H), 7.54 (d, J = 8 Hz, 2H), 7.37(t, J= 7.5 Hz, 2H), 7.13(d, J=8 Hz, 2H), 7.08 (d, J= 8 Hz, 2H), 2.04 (q, J=6.5 Hz,2H), 1.38-1.42 (m, J= 7 Hz, 3H) ppm. $^{13}C\{^1H\}$ NMR (125 MHz, $CDCl_3$) δ 156.37, 149.58, 140.64, 133.44,129.33,126.73, 124.84,119.48,30.07, 23.06 ppm
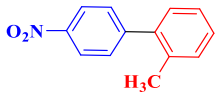	**2-methyl-4'-nitro-1,1'-biphenyl** Yellow coloured powder ^{1}H NMR (500 MHz, $CDCl_3$) δ 8.39(d, J=6.5 Hz, 2H), 8.19(d, J=5 Hz, 1H), 8.17(t, J= 4.5 Hz, 1H), 7.84(d, J = 6.5 Hz, 1H), 7.83(t, J= 8Hz, 1H), 7.45(d, J= 7.5 Hz, 2H), 2.17 (s, 3H) ppm.$^{13}C\{^1H\}$ NMR (125 MHz, $CDCl_3$) δ 149.28, 145.97, 133.56,132.76, 129.81, 129.10, 128.87,126.89, 126.36, 123.52, 20.41 ppm
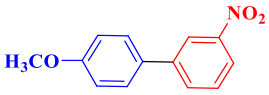	**4'-methoxy-3-nitro-1,1'-biphenyl** Yellow coloured powder ^{1}H NMR (500 MHz, $CDCl_3$) δ 8.05(s,1H), 7.56 (d, J=7.5 Hz, 2H), 7.53(t, J = 6.5 Hz, 1H), 7.42(t, J = 4.5 Hz, 1H), 7.31(d, J= 6.5Hz,1H), 6.68(d, J=7.5 Hz, 2H), 3.79 (s, 3H) ppm. $^{13}C\{^1H\}$ NMR (125 MHz, $CDCl_3$) δ 164.66, 146.56, 141.44, 134.38, 130.04, 129.64, 127.95, 125.96, 124.98, 121.18, 114.07 ppm
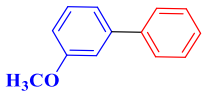	**3-methoxy-1,1'-biphenyl** Off-white coloured powder, m.p. 51˚C ^{1}H NMR (500 MHz, $CDCl_3$) δ 7.85 (s,1H), 7.77 (d, J=7 Hz, 2H), 7.47 (t, J = 7.5 Hz, 1H), 7.36 (t, J = 7.5 Hz, 1H), 7.31 (d, J= 7 Hz,2H), 7.17 (d, J=7.5 Hz, 1H), 7.06 (d, J=7 Hz, 1H), 3.86 (s, 3H) ppm. $^{13}C\{^1H\}$ NMR (125 MHz, $CDCl_3$) δ 165.44, 145.16, 140.98, 128.64, 128.42, 126.89, 126.72, 115.41, 115.07, 113.38, 53.00 ppm.
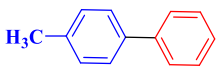	**4-methyl-1,1'-biphenyl** White coloured powder, m.p. 49˚C ^{1}H NMR (500 MHz, $CDCl_3$) δ 8.15 (d, J = 8 Hz, 2H), 7.70 (d, J = 8.5 Hz, 2H), 7.51 (d, J= 8.5 Hz,2H), 7.42 (d, J=8 Hz, 2H), 7.20 (t, J=6.5 Hz, 1H), 2.20 (s, 3H) ppm. $^{13}C\{^1H\}$ NMR (125 MHz, $CDCl_3$) δ 139.27, 138.32, 136.86, 134.90, 133.63, 128.93, 128.34, 128.10, 30.83 ppm
	4'-methyl-3-nitro-1,1'-biphenyl Yellow coloured powder ^{1}H NMR (500 MHz, $CDCl_3$) δ 8.25 (d, J = 7 Hz, 2H), 7.49 (d, J = 7.5 Hz, 1H), 7.35 (d, J= 7.5 Hz, 2H), 7.31-7.32 (t, J=5 Hz, 1H), 7.29 (d,

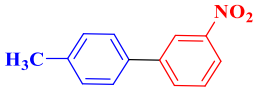	J=6.5 Hz, 1H), 6.75 (s, 1H) 2.21 (s, 3H) ppm. $^{13}C\{^{1}H\}$ NMR (125 MHz, $CDCl_3$) δ 146.16, 137.12, 133.49, 132.09, 134.47, 130.00, 129.69, 125.41, 125.08, 22.98 ppm
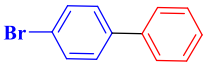	**4-Bromo-1,1'-biphenyl** Off-white coloured powder, m.p. 78˚C ^{1}H NMR (500 MHz, $CDCl_3$) δ 8.24 (d, J=7.5 Hz, 2H), 7.73 (d, J=7.5 Hz, 2H), 7.61 (d, J=7.5 Hz, 2H), 7.52 (t, J=6 Hz, 2H), 7.41 (t, J=5.5 Hz, 1H), ppm. $^{13}C\{^{1}H\}$ NMR (125 MHz, $CDCl_3$) δ 141.93, 139.81, 135.66, 133.45, 132.71, 128.00, 122.64, 121.70 ppm
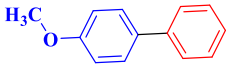	**4-Methoxy -1,1'-biphenyl** Off white coloured powder, m.p. 50 ˚C ^{1}H NMR (500 MHz, $CDCl_3$) δ 8.51 (d, J=9 Hz, 2H), 7.95 (d, J=8.5 Hz, 2H), 7.79 (t, J= 7.5 Hz, 2H), 7.48 (t, J=7.5 Hz, 1H), 6.98 (d, J= 9 Hz, 2H), 3.82(s, 3H) ppm. $^{13}C\{^{1}H\}$ NMR (125 MHz, $CDCl_3$) δ 160.38, 150.96, 133.99, 130.78, 130.23, 128.43, 127.12, 113.99, 55.38 ppm
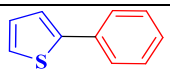	**2-phenylthiophene** Off-white coloured oily liquid, m.p. 69˚C ^{1}H NMR (500 MHz, $CDCl_3$) δ 7.53 (d, J=8.5 Hz, 1H), 7.44 (t, J=8.5 Hz, 1H), 7.41 (t, J=7.5 Hz, 2H), 7.25 (t, J= 7.5 Hz, 1H), 6.91 (t, J=7.5 Hz, 1H), 6.88 (d, J=7.5 Hz, 2H) ppm. $^{13}C\{^{1}H\}$ NMR (125 MHz, $CDCl_3$) δ 156.43, 145.73, 130.01, 129.55, 127.98, 127.79, 127.42, 115.45 ppm
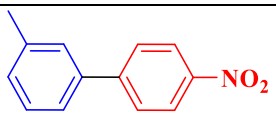	**3-methyl-4'-nitro-1,1'-biphenyl** Yellow oily liquid ^{1}H NMR (500 MHz, $CDCl_3$) δ 8.23(s, J=7.5 Hz, 1H), 8.12 (d, J=8.5 Hz, 2H), 7.70 (d, J=9 Hz, 2H), 7.48 (d, J= 7.5 Hz, 1H), 7.33 (t, J=7.5 Hz, 1H), 7.29 (d, J=7.5 Hz, 1H), 2.84 (s, 3H) ppm. $^{13}C\{^{1}H\}$ NMR (125 MHz, $CDCl_3$) δ 147.58, 146.30, 140.63, 137.26, 132.65, 132.23, 130.61, 130.03, 125.21, 125.04, 23.14 ppm
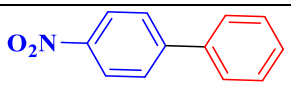	**4-nitro-1,1'-biphenyl** Yellow coloured powder ^{1}H NMR (500 MHz, $CDCl_3$) δ 8.27 (d, J=7.5 Hz, 2H), 8.00 (t, J=7 Hz, 1H), 7.78 (d, J=7 Hz, 2H), 7.64 (d, J= 7.5 Hz, 2H), 7.55 (t, J=7.5 Hz, 2H) ppm.$^{13}C\{^{1}H\}$ NMR (125 MHz, $CDCl_3$) δ 148.85, 146.87, 139.64, 130.15, 129.64, 128.51, 127.17, 123.46 ppm
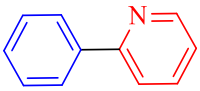	**2-phenylpyridine** Off-white coloured powder ^{1}H NMR (500 MHz, $CDCl_3$) δ 8.73 (d, J=6.5 Hz, 1H), 8.40 (d, J=8 Hz, 1H), 8.02 (d, J=8.5 Hz, 2H), 7.77 (t, J= 7.5 Hz, 1H), 7.52 (t, J=7 Hz, 2H), 7.28 (t, J=9 Hz, 1H), 6.89 (t, J= 7.5 Hz, 1H) ppm.$^{13}C\{^{1}H\}$ NMR (125 MHz, $CDCl_3$) δ 157.54, 149.52, 142.23, 138.62, 128.37, 127.04, 122.26, 120.93 ppm
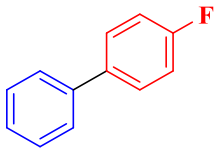	**4-fluoro-1,1'-biphenyl** Off-white coloured powder ^{1}H NMR (500 MHz, $CDCl_3$) δ 8.28 (d, J=7.5 Hz, 2H), 8.24 (d, J=7 Hz, 2H), 7.79 (t, J=8 Hz, 1H), 7.24 (d, J= 7.5 Hz, 2H), 7.14 (t, J=8.5 Hz, 2H) ppm.$^{13}C\{^{1}H\}$ NMR (125 MHz, $CDCl_3$) δ 153.12, 147.67, 135.23, 134.81, 131.30, 130.38, 127.76, 113.32 ppm.

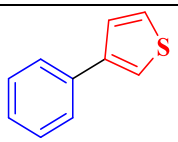	**3-phenylthiophene** Off-white coloured powder ^{1}H NMR (500 MHz, $CDCl_3$) δ 7.63 (d, J=9 Hz, 2H), 7.48 (d, J=6 Hz, 1H), 7.46 (s, 1H)7.43 (m, J=6 Hz, 2H), 7.38 (t, J= 6 Hz, 1H), 7.35 (t, J=5.5 Hz, 1H) ppm.^{13}C{^{1}H} NMR (125 MHz, $CDCl_3$) δ 142.38, 135.87,128.82, 127.15, 126.47, 126.36, 119.79 ppm.
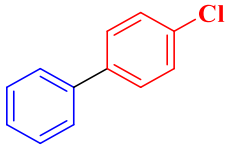	**4-chloro-1,1'-biphenyl** White coloured powder ^{1}H NMR (500 MHz, $CDCl_3$) δ 7.39 (t, J=7 Hz, 1H), 7.27 (d, J=7 Hz, 2H), 7.11 (d, J=8 Hz, 2H), 6.78 (d, J= 9.5 Hz, 2H), 6.74 (t, J= 9.5 Hz, 2H) ppm.^{13}C{^{1}H} NMR (125 MHz, $CDCl_3$) δ 141.68, 137.79,134.45, 131.78, 128.30, 127.55, 127.26,126.53 ppm.
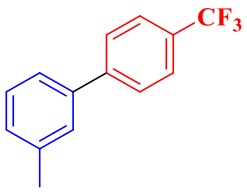	**3-methyl-4'-(trifluoromethyl)-1,1'-biphenyl** White coloured powder ^{1}H NMR (500 MHz, $CDCl_3$) δ 7.76 (d, J=7.5 Hz, 1H), 7.74 (d, J= 7 Hz, 2H) 7.58 (d, J=7.5 Hz, 2H), 7.51(s, J=7.5 Hz, 1H) 7.49 (t, J=7.5 Hz, 1H), 7.33 (d, J= 8.5 Hz, 1H), 2.58 (s, 3H) ppm.^{13}C{^{1}H} NMR (125 MHz, $CDCl_3$) δ 141.50, 141.38, 138.44,128.84, 128.82, 128.76, 128.15, 128.12,128.07, 127.32, 124.43 ppm.
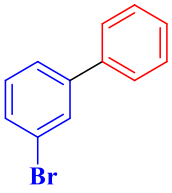	**3-bromo-1,1'-biphenyl** White coloured powder ^{1}H NMR (500 MHz, $CDCl_3$) δ 7.81 (d, J=6 Hz, 2H), 7.71(t, J= 7 Hz, 2H) 7.42 (t, J=10 Hz, 1H), 7.21 (d, J=8.5 Hz, 1H), 7.20 (d, J=7.5 Hz, 1H), 7.19 (d, J=7.5 Hz, 1H), 6.75 (s, 1H) ppm.^{13}C{^{1}H} NMR (125 MHz, $CDCl_3$) δ 143.39, 139.75,130.36, 130.22, 129.38, 128.89, 127.92, 127.16,126.26, 123.00 ppm.
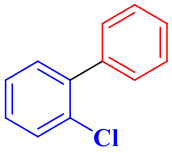	**2-chloro-1,1'-biphenyl** White coloured powder ^{1}H NMR (500 MHz, $CDCl_3$) δ 7.01 (d, J=11 Hz, 1H), 7.02 (t, J=10.5 Hz, 1H), 6.46 (d, J=9 Hz, 2H),6.15 (t, J=10.5 Hz, 2H), 6.07 (t, J= 9 Hz, 1H), 6.03 (d, J=10 Hz, 1H), 5.90 (t, J=9 Hz, 1H) ppm.^{13}C{^{1}H} NMR (125 MHz, $CDCl_3$) δ 144.98, 141.32,138.89, 129.68, 128.61, 128.34, 127.79, 124.39, 124.27,124.06 ppm.
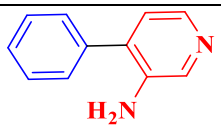	**4-phenylpyridin-3-amine** Light brown coloured powder ^{1}H NMR (500 MHz, $CDCl_3$) δ 8.02 (d, J=5.5 Hz, 1H), 7.96 (d, J=7 Hz, 1H), 7.43 (d, J=6 Hz, 2H), 7.25 (t, J=7.5 Hz, 1H), 6.83 (d, J= 5.5 Hz, 1H), 6.69 (t, J=7.5 Hz, 2H), 5.06 (s, 2H) ppm.^{13}C{^{1}H} NMR (125 MHz, $CDCl_3$) δ 158.49, 147.12,134.55, 133.62, 129.80, 129.67, 127.65, 117.18, 112.36 ppm.
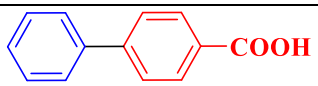	**[1,1'-biphenyl]-4-carboxylic acid** White coloured powder ^{1}H NMR (500 MHz, $CDCl_3$) δ 9.97 (s, 1H), 7.75(d, J=8 Hz, 2H), 7.71(d, J=7.5 Hz, 2H), 7.49 (t, J=10.5 Hz, 2H), 7.41 (t, J=10.5 Hz, 1H), 7.25 (d, J=7 Hz, 2H).^{13}C{^{1}H} NMR (125 MHz, $CDCl_3$) δ 191.35, 150.64, 135.02, 133.44, 132.49, 131.57, 131.05, 129.91, 127.98.
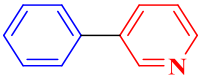	**3-phenylpyridine** Off-white coloured powder ^{1}H NMR (500 MHz, $CDCl_3$) δ 9.04 (s, 1H), 8.77 (d, J=6.5 Hz, 1H), 8.15(d, J=7.5 Hz, 2H), 8.10(t, J=7.5 Hz, 1H), 7.49(t, J= 8.5 Hz, 2H), 7.21(t, J=7.5 Hz, 1H), 6.94(d, J=7.5 Hz, 1H) ppm. ^{13}C{^{1}H} NMR (125

	MHz, $CDCl_3$) δ 153.86, 146.24, 142.49, 133.75, 129.83, 128.82, 128.40, 127.68, 125.82 ppm.
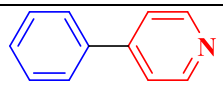	**4-phenylpyridine** Off-white coloured powder ^{1}H NMR (500 MHz, $CDCl_3$) δ 7.72 (d, J=8 Hz, 2H), 7.34 (d, J=7.5 Hz, 2H),7.24 (d, J=7.5 Hz, 2H), 7.11 (t, J=7.5 Hz, 2H), 6.87 (t, J=8 Hz, 1H) ppm. $^{13}C\{^1H\}$ NMR (125 MHz, $CDCl_3$) δ 150.08 141.19, 137.49, 130.91, 130.25, 127.47, 124.37 ppm.
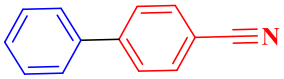	**[1,1'-biphenyl]-4-carbonitrile** White coloured powder ^{1}H NMR (500 MHz, $CDCl_3$) δ 7.90 (d, J=7.5 Hz, 2H), 7.50 (d, J=7.5 Hz, 2H), 7.39(t, J=7.5 Hz, 2H), 7.39(t, J=7 Hz, 2H), 7.14 (t, J=7.5 Hz, 1H), 6.81.$^{13}C\{^1H\}$ NMR (125 MHz, $CDCl_3$) δ 149.18, 140.31, 134.11, 131.67, 130.43, 129.58, 129.38, 118.67, 111.53.
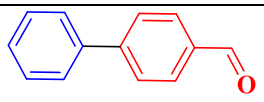	**[1,1'-biphenyl]-4-carbaldehyde** Light yellow coloured powder ^{1}H NMR (500 MHz, $CDCl_3$) δ 8.05 (s, 1H), 7.61 (t, J=8.5 Hz, 1H), 7.19 (d, J=7 Hz, 2H), 6.86 (d, J=7.5 Hz, 2H), 6.79(d, J=7.5 Hz, 2H), 6.65(t, J=7 Hz, 2H).$^{13}C\{^1H\}$ NMR (125 MHz, $CDCl_3$) δ 185.83, 146.36, 143.81, 133.26,131.46, 129.69, 128.47, 127.22, 126.52.

(The minor signals observed in the region of 4-5 ppm in the ^{1}H NMR spectra are likely due to trace amounts of residual moisture. The signals observed in the 1-3 ppm region in the ^{1}H NMR spectra can be attributed to residual solvents (e.g., hexane, acetone, ethyl acetate) or aliphatic contaminants introduced during sample handling, purification or washing of NMR tubes.

The signals observed in the 10-60 ppm region of the ^{13}C NMR spectra are primarily attributed to aliphatic carbon environments; however, minor additional unwanted peaks in this region may also arise from residual solvent (such as traces of hexane, ethyl acetate, acetone during purification or washing of NMR tubes).

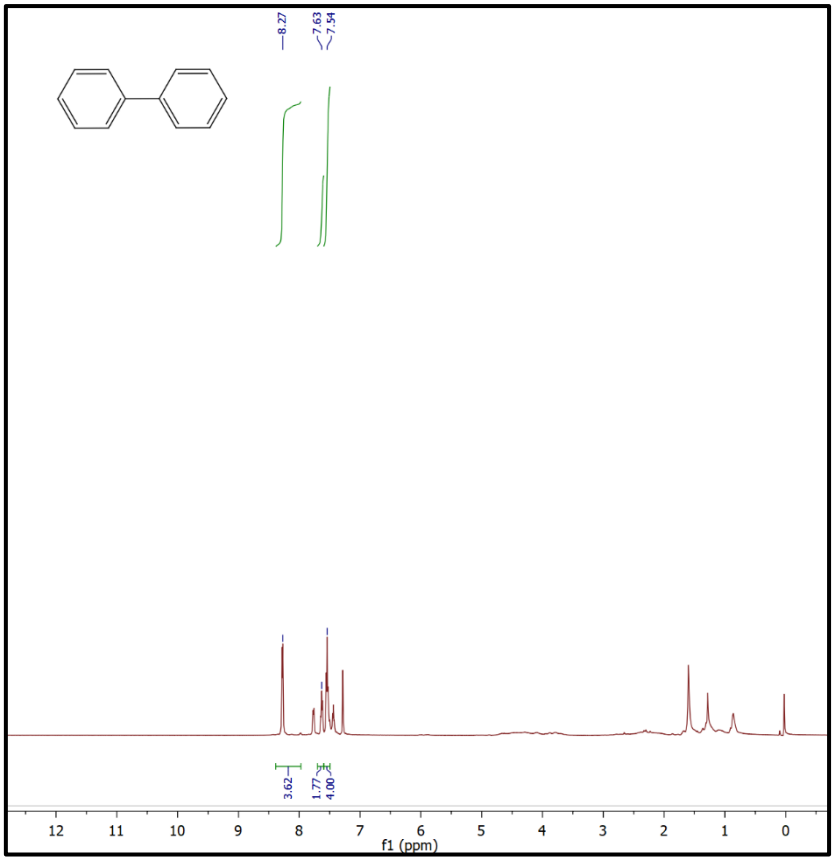

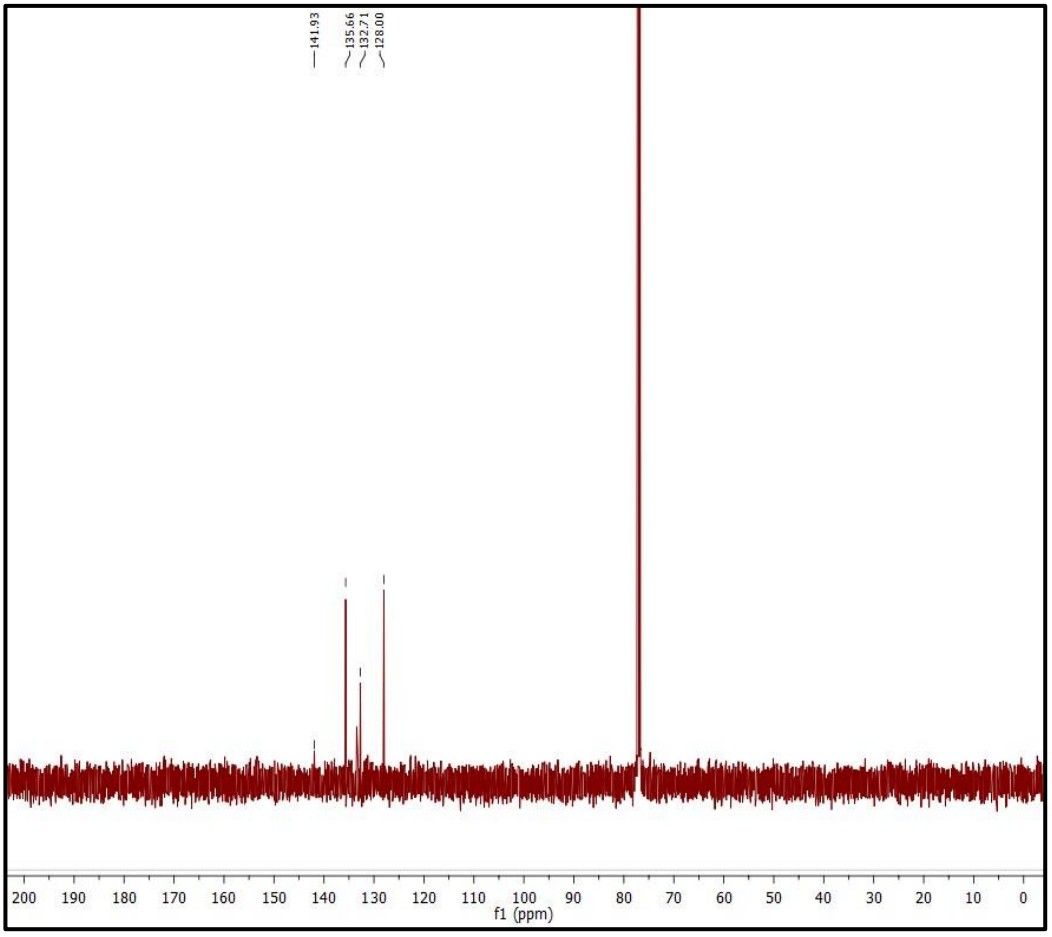

^{1}H and ^{13}C{^{1}H} NMR spectrum of 1,1'-biphenyl

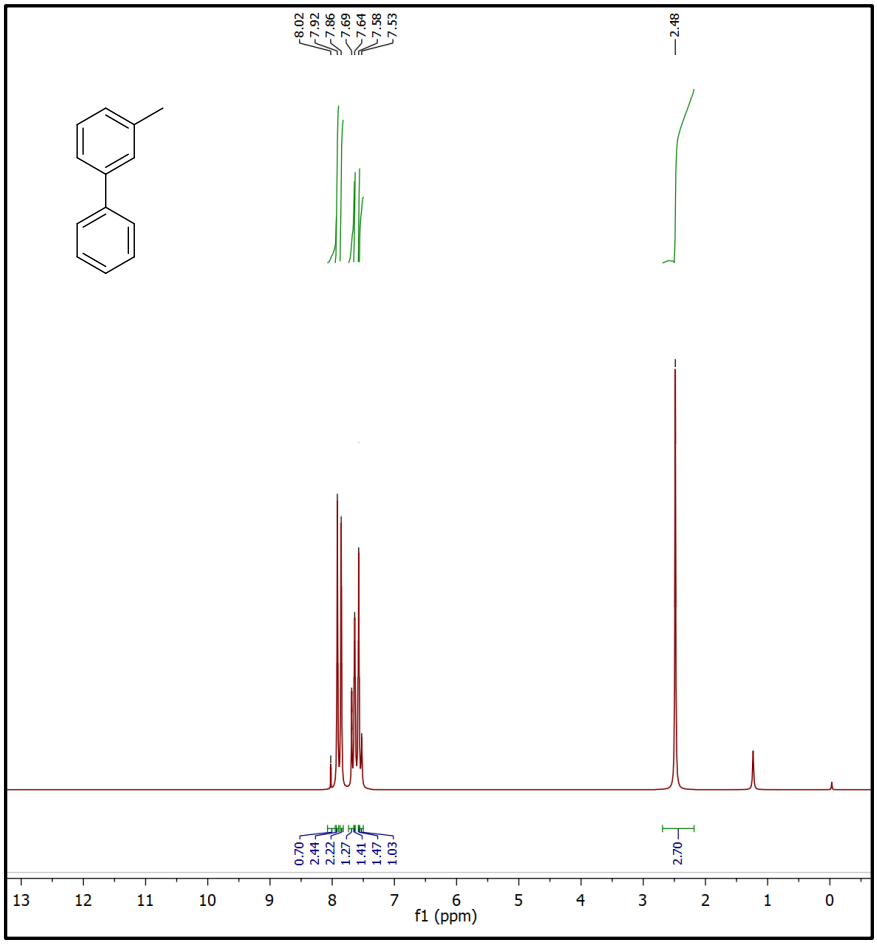

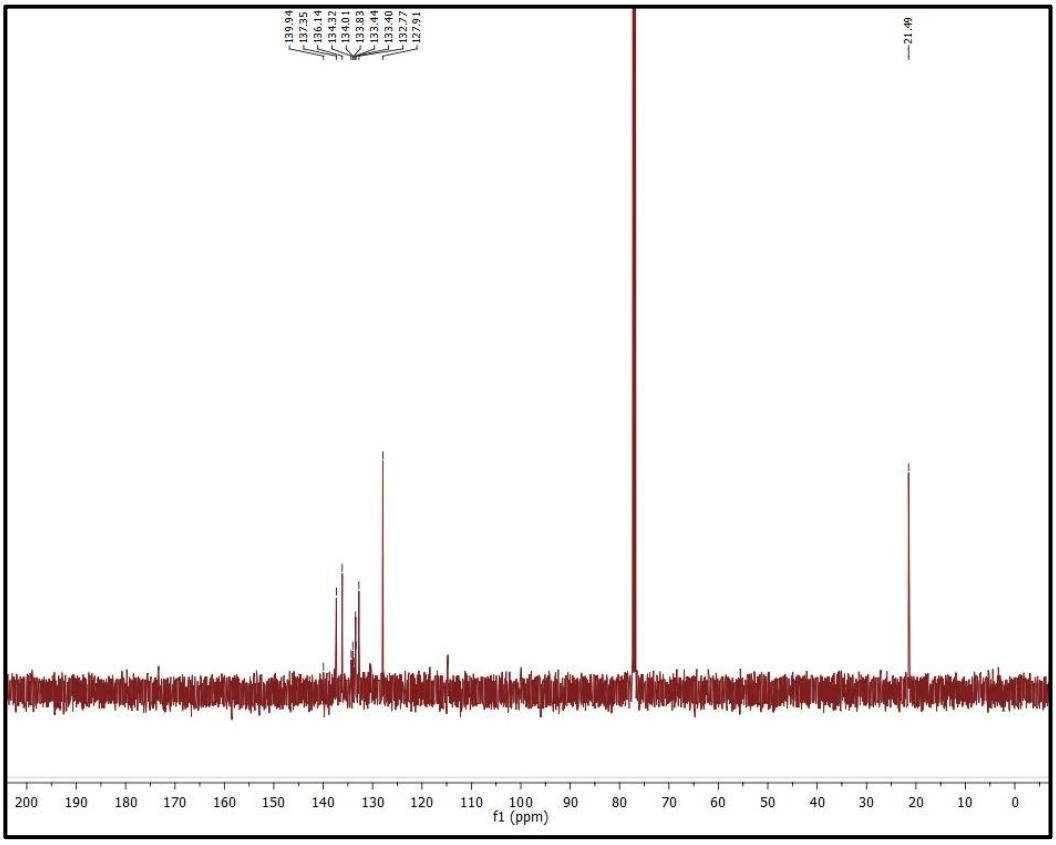

^{1}H and ^{13}C{^{1}H} NMR spectrum of 3-methyl-1,1'-biphenyl

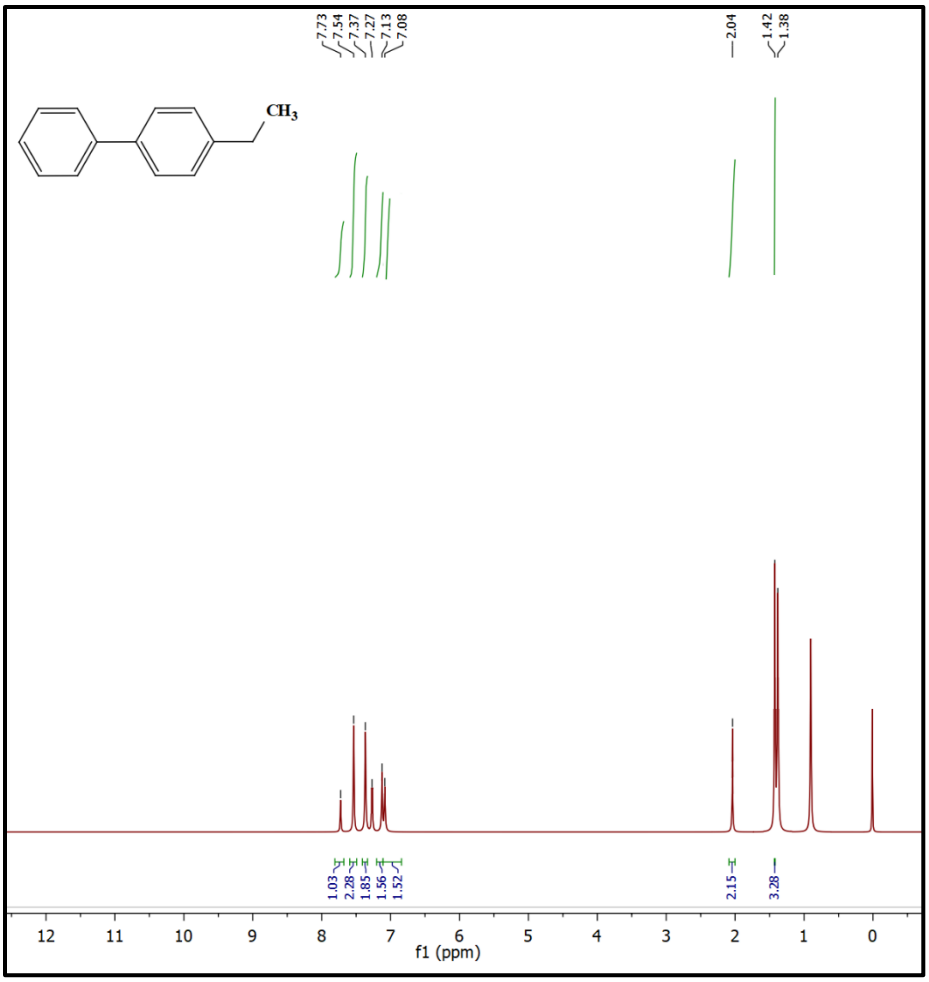

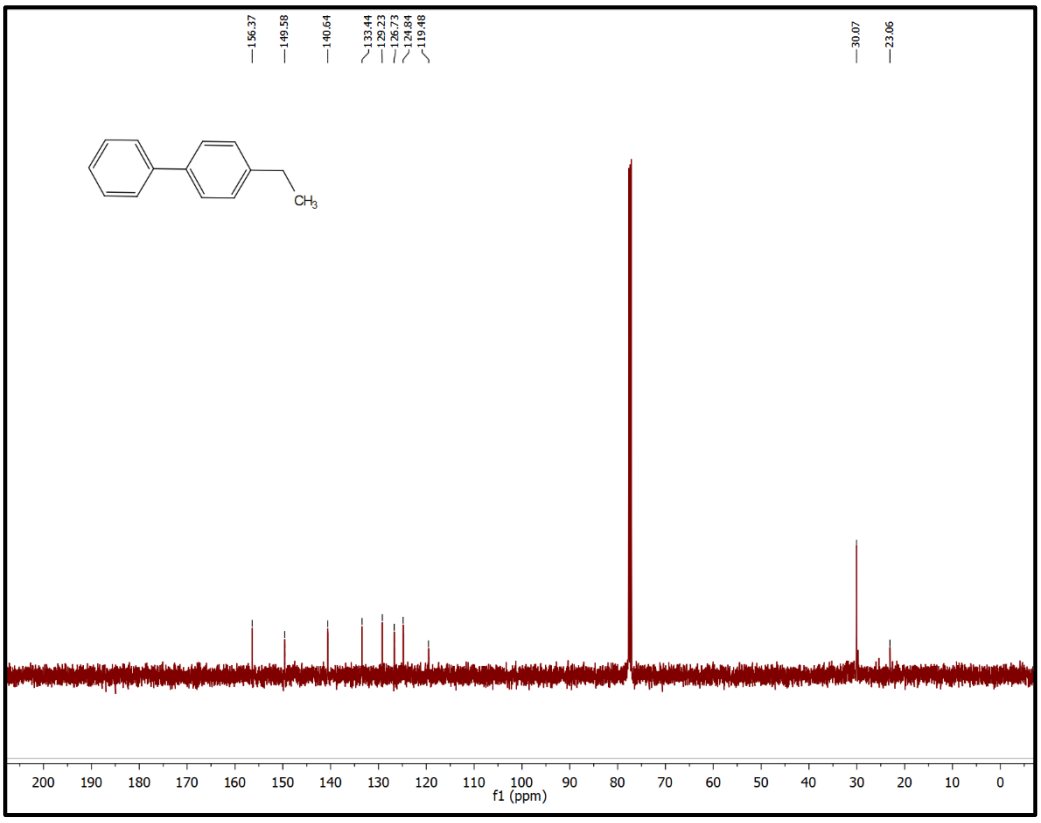

^{1}H and ^{13}C{^{1}H} NMR spectrum of 4-ethyl-1,1'-biphenyl

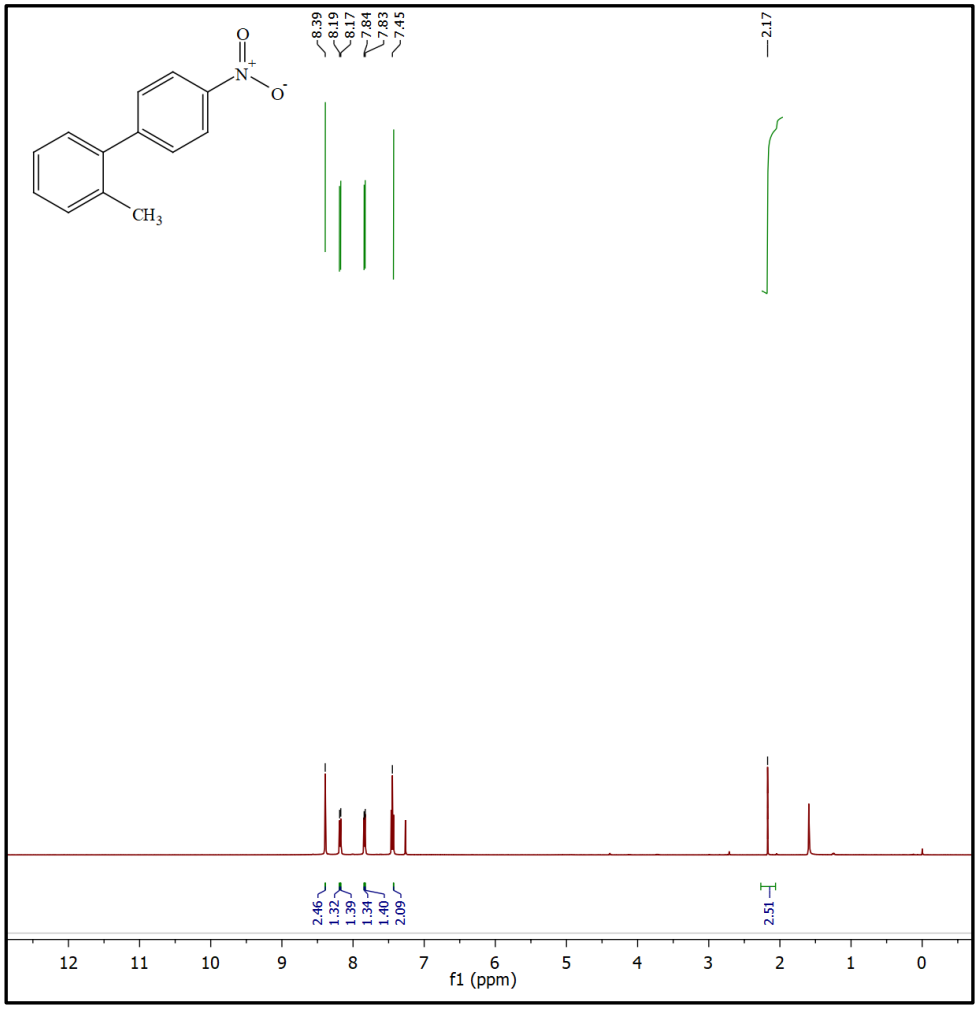

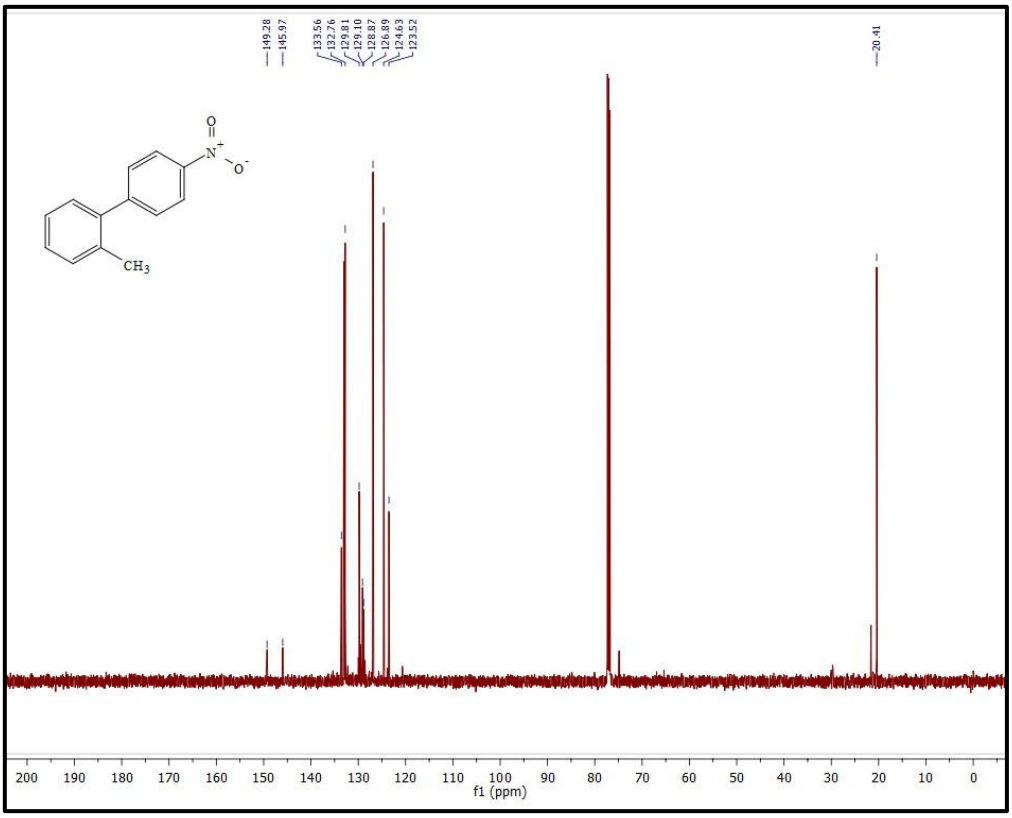

^{1}H and ^{13}C{^{1}H} NMR spectrum of 2-methyl-4'-nitro-1,1'-biphenyl

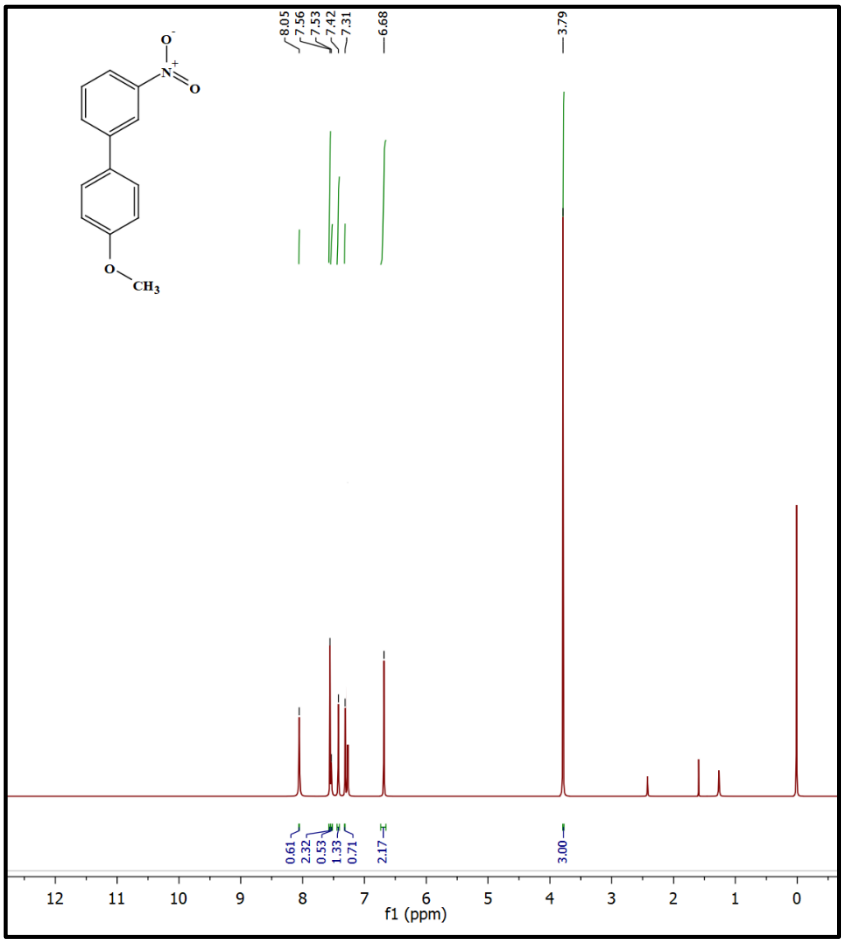

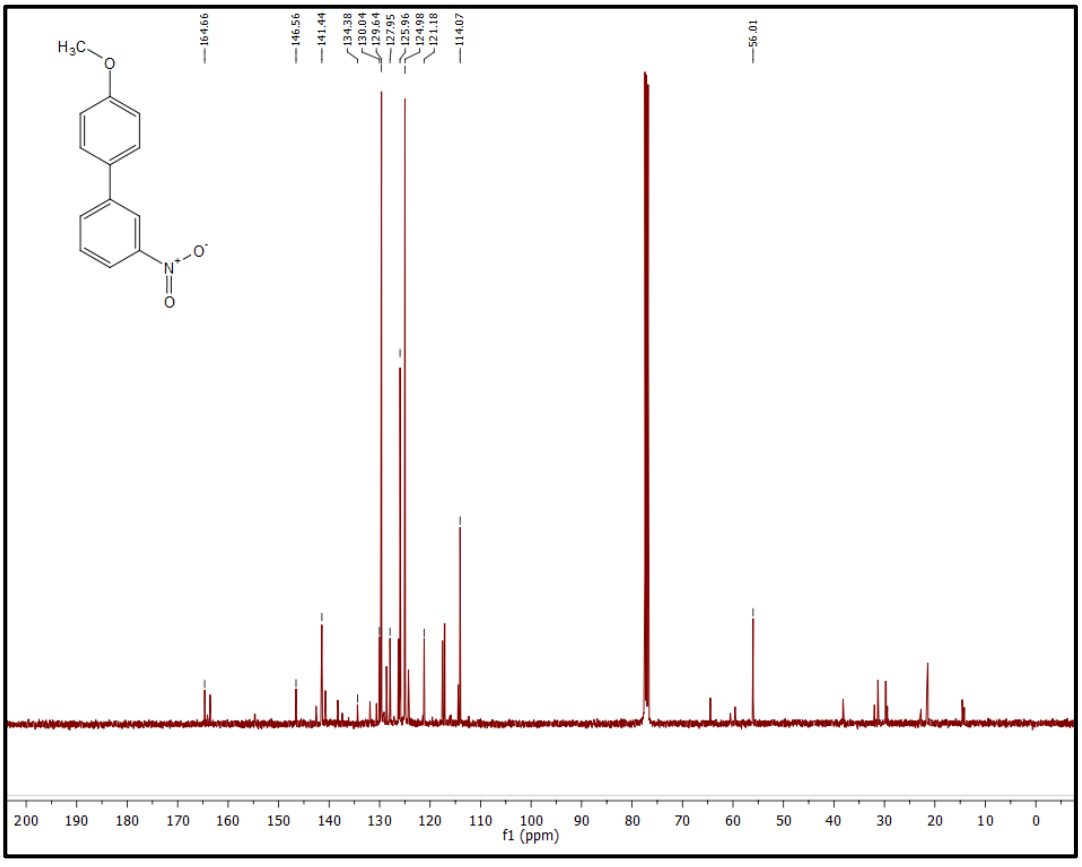

^{1}H and ^{13}C{^{1}H} NMR spectrum of 4'-methoxy-3-nitro-1,1'-biphenyl

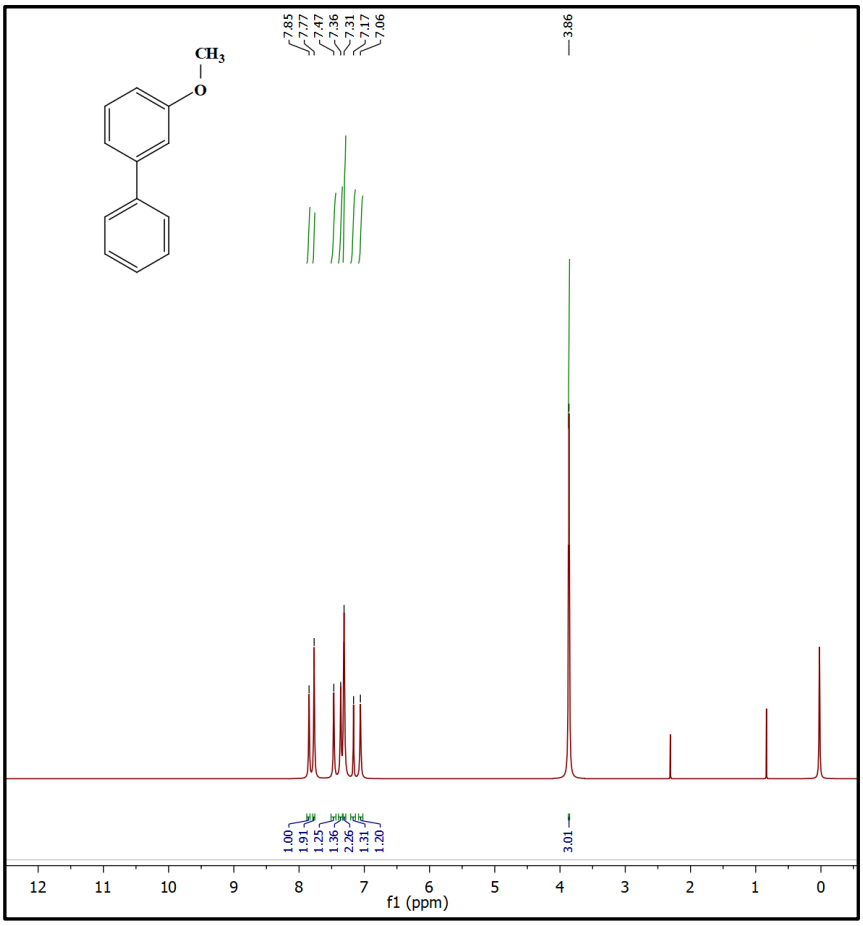

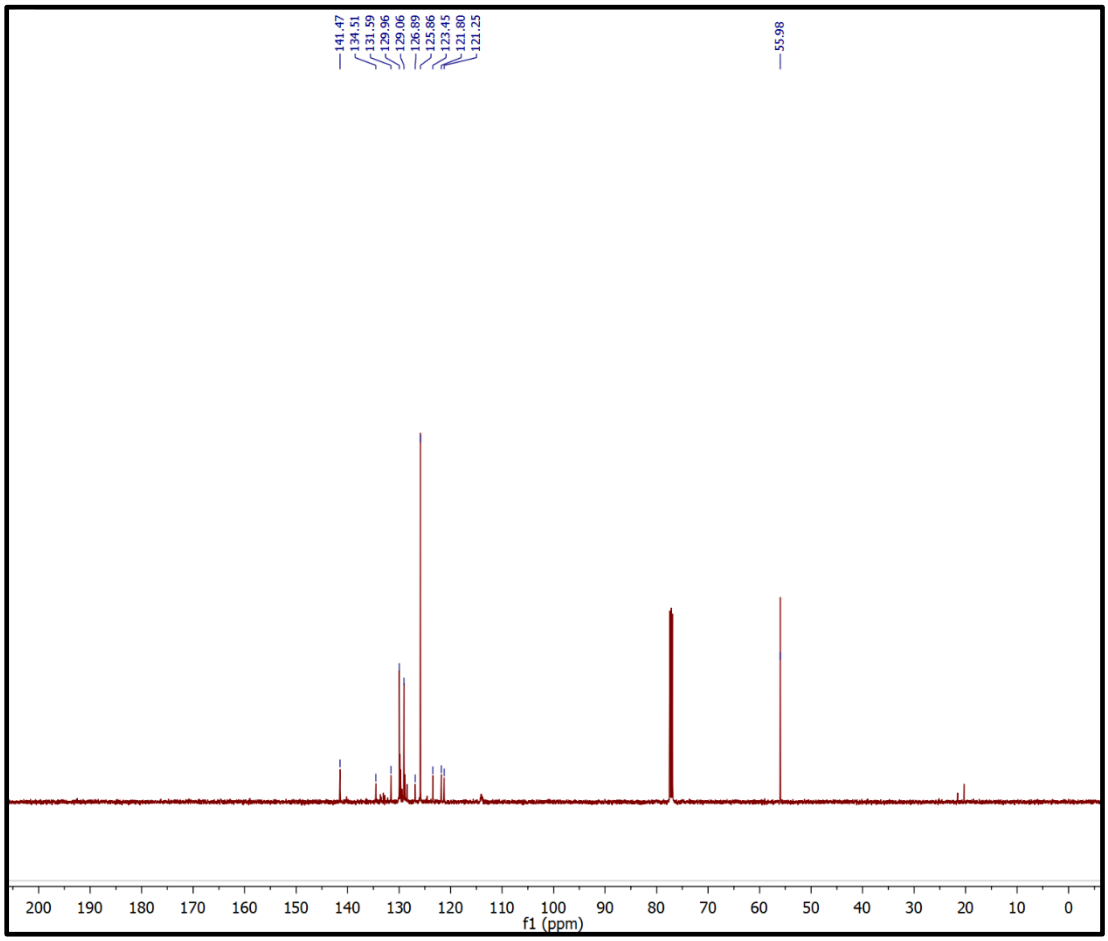

^{1}H and ^{13}C{^{1}H} NMR spectrum of 3-methoxy-1,1'-biphenyl

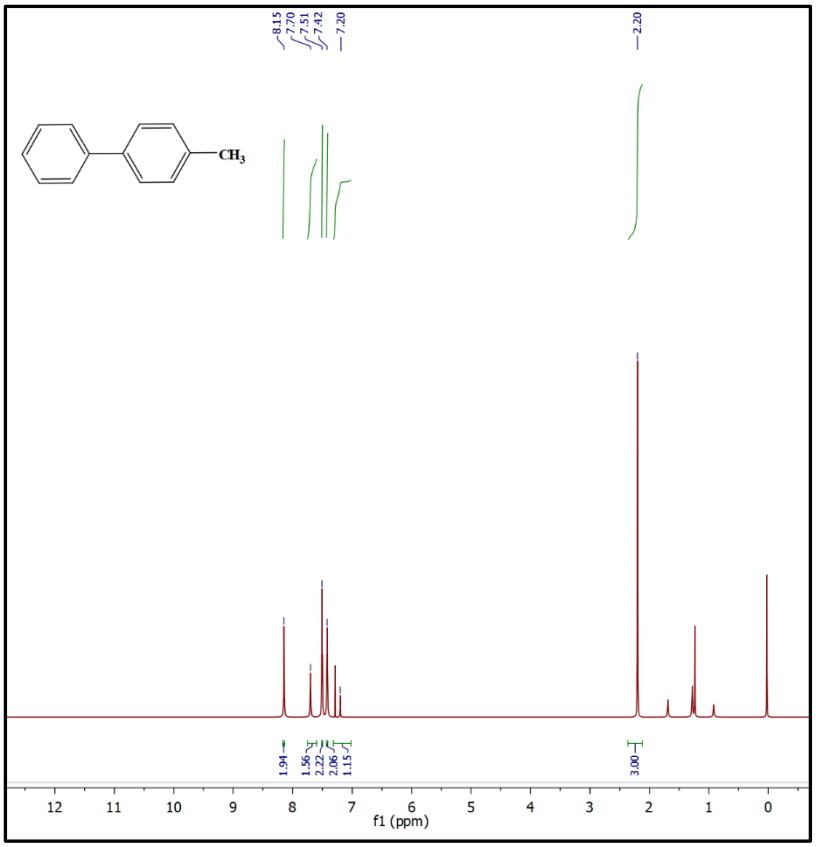

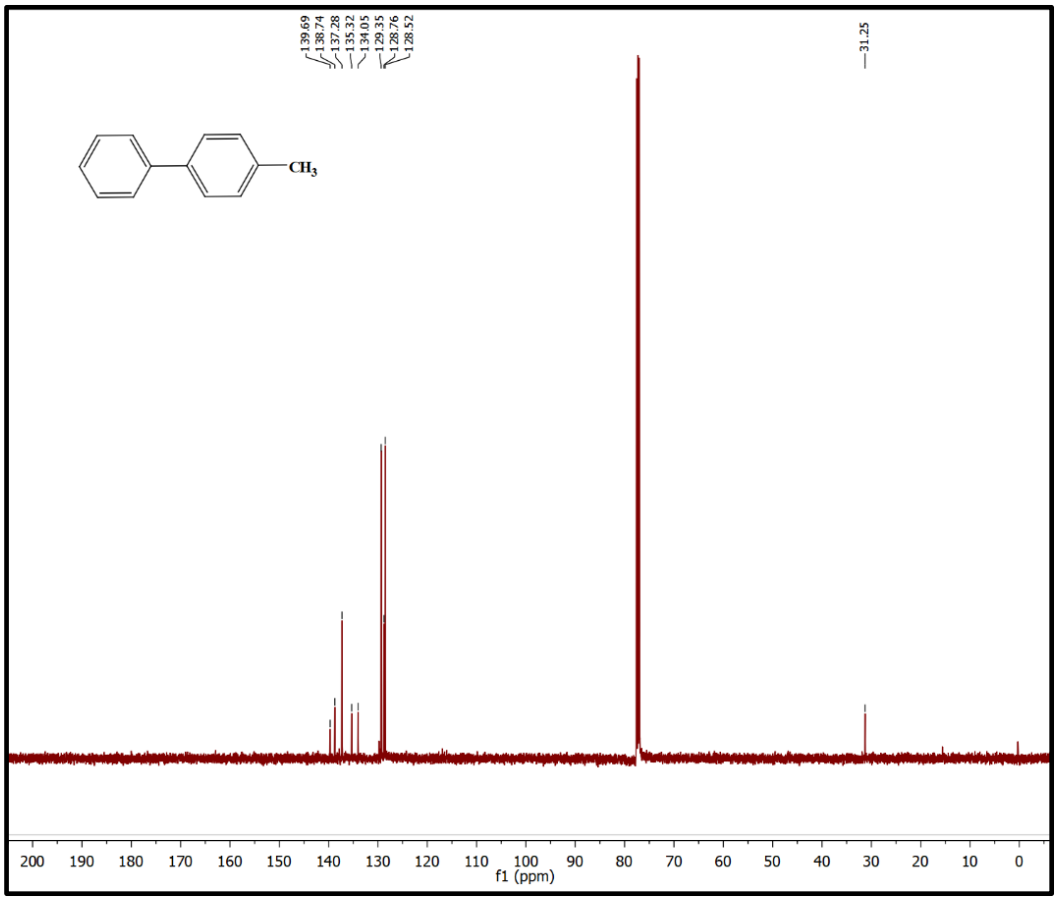

^{1}H and ^{13}C{^{1}H} NMR spectrum of 4-methyl-1,1'-biphenyl

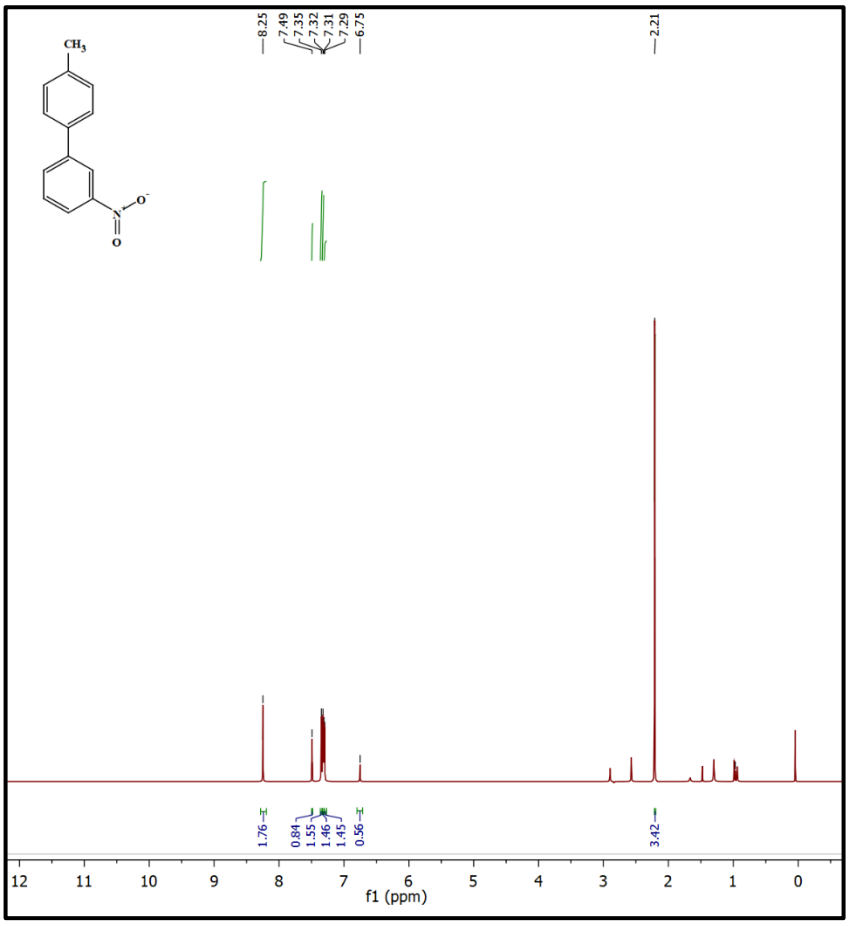

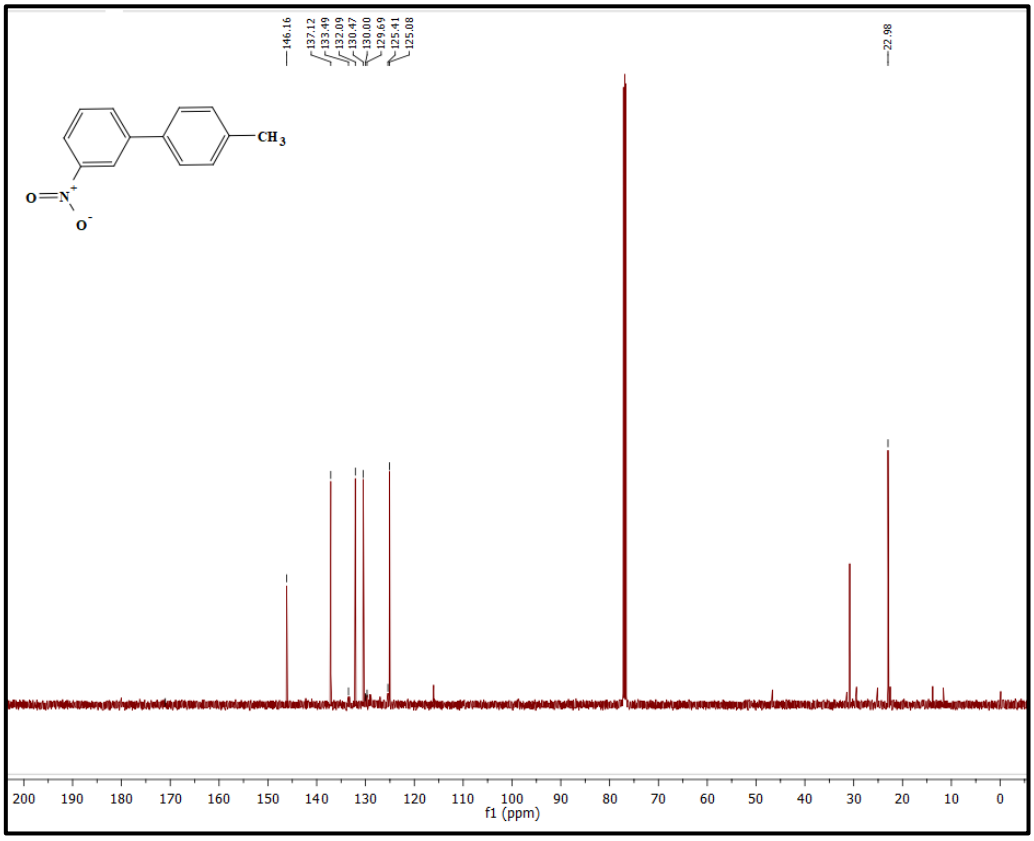

^{1}H and ^{13}C{^{1}H} NMR spectrum of 4'-methyl-3-nitro-1,1'-biphenyl

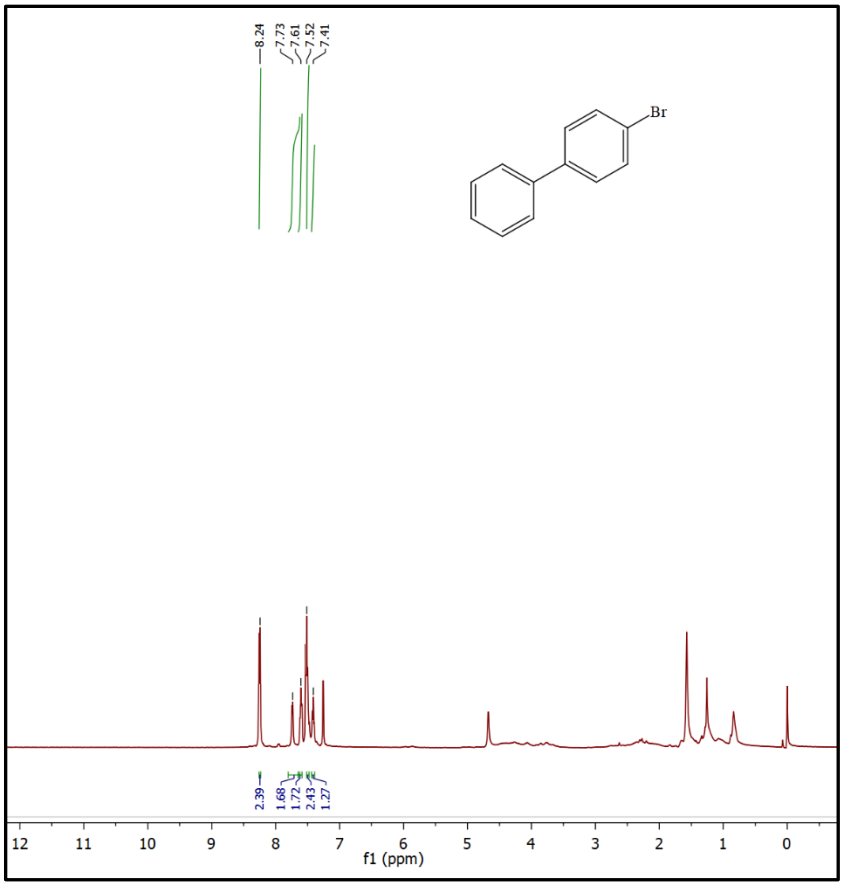

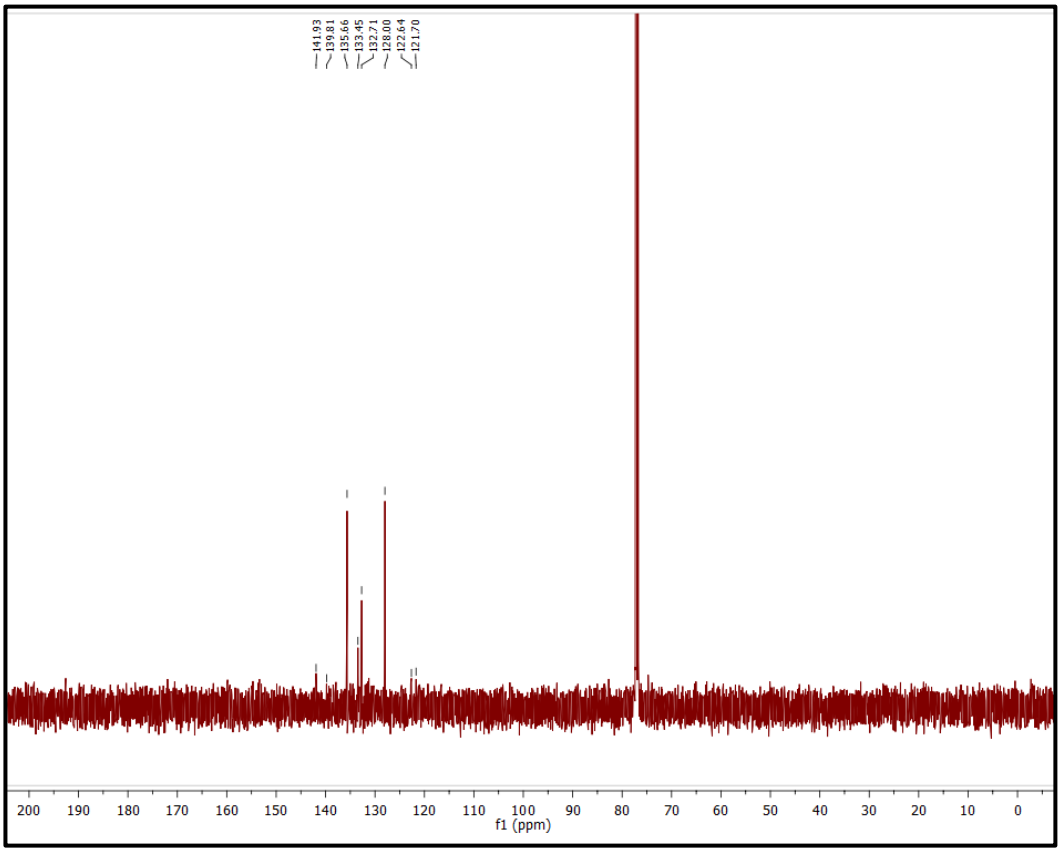

^{1}H and ^{13}C{^{1}H} NMR spectrum of 4-Bromo -1,1'-biphenyl

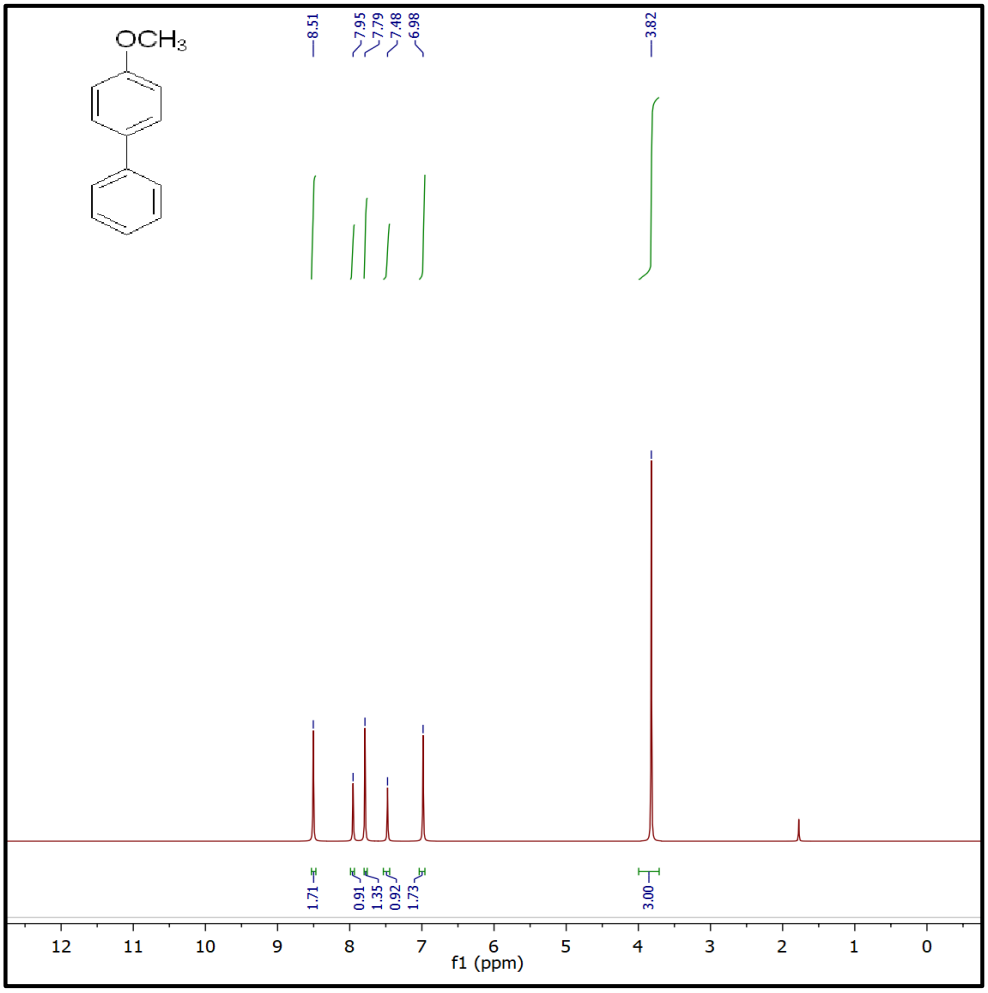

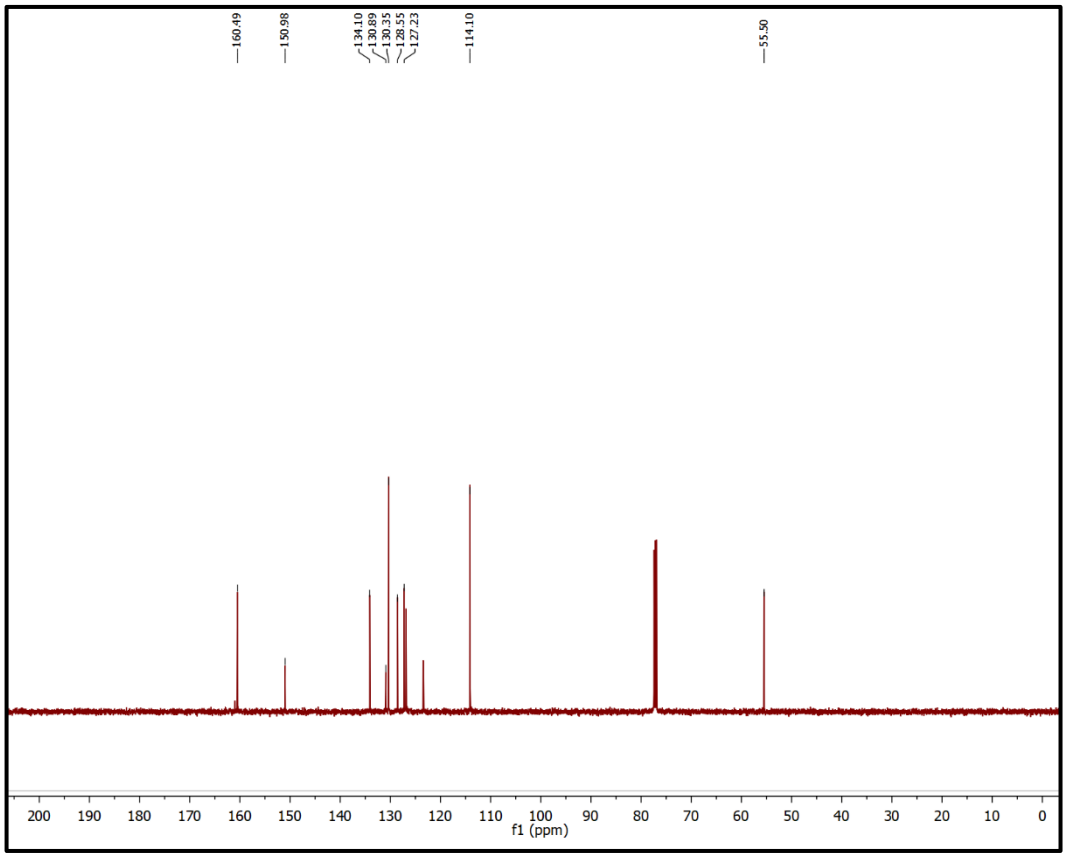

^{1}H and ^{13}C{^{1}H} NMR spectrum of 4-Methoxy -1,1'-biphenyl

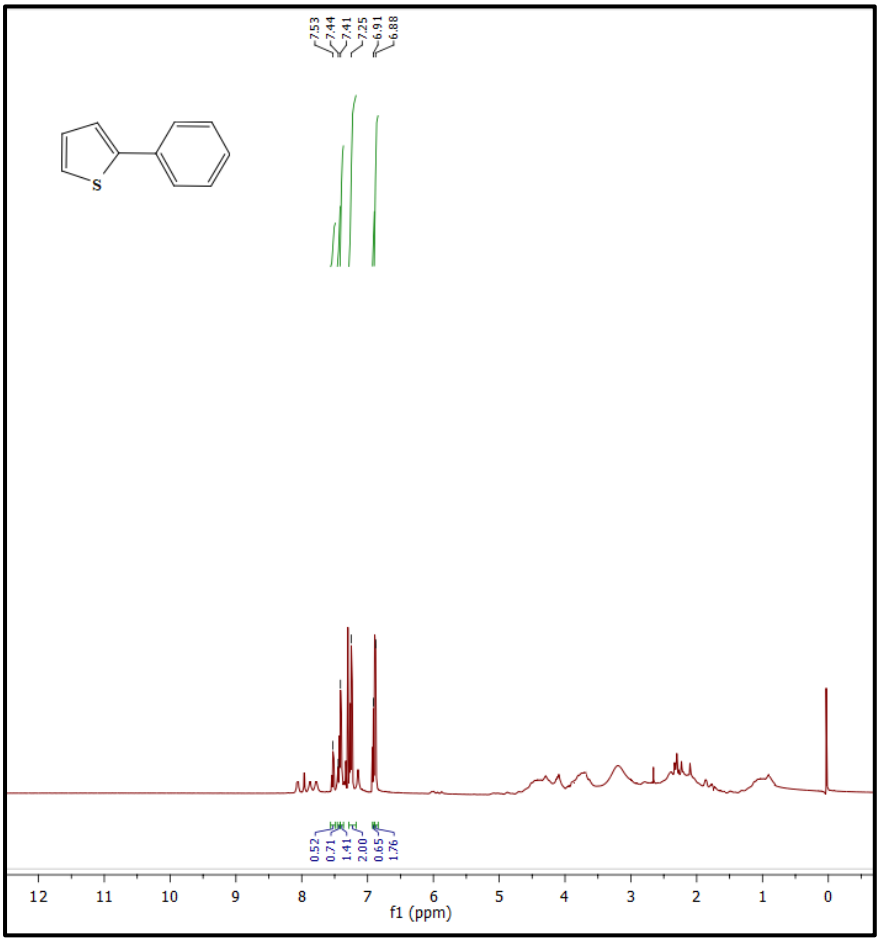

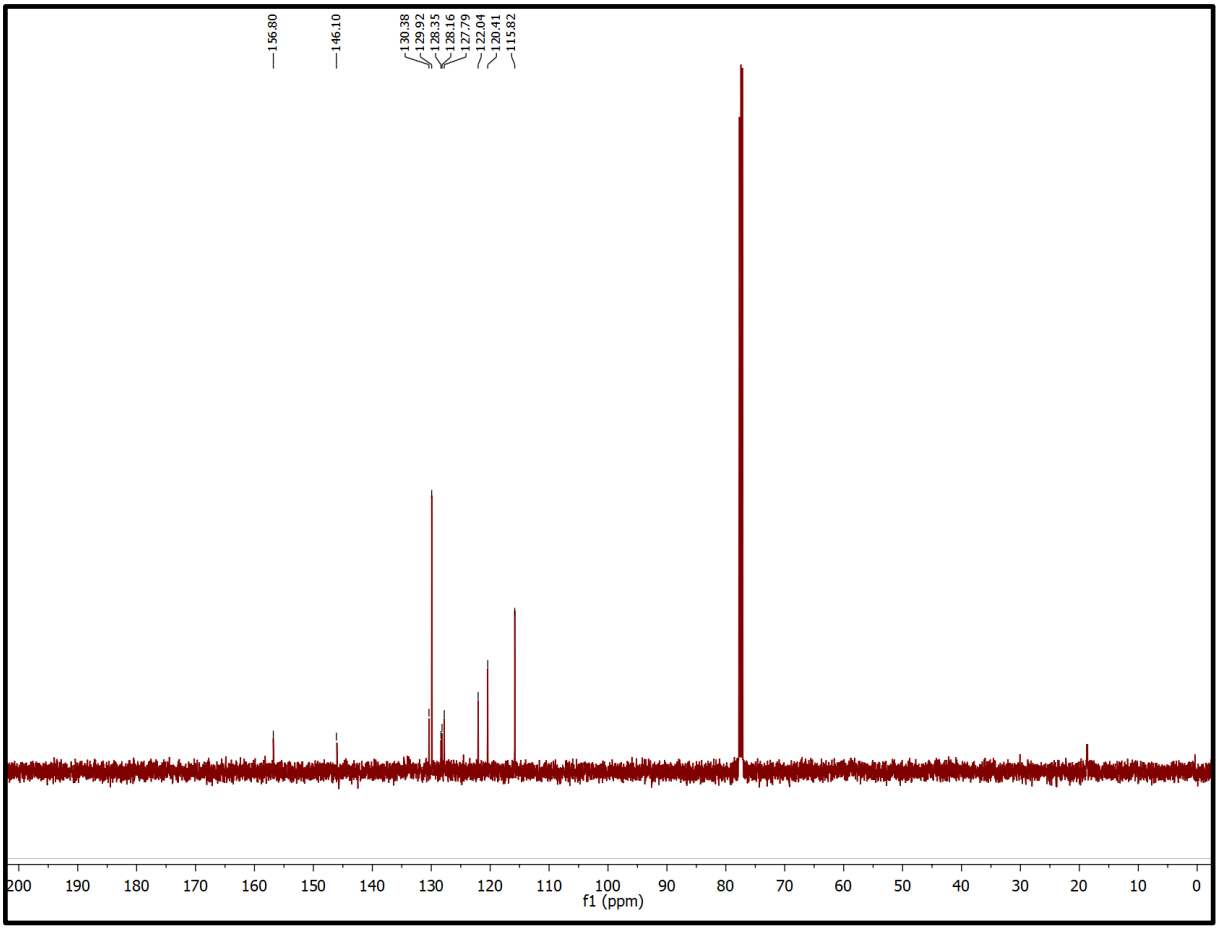

^{1}H and ^{13}C{^{1}H} NMR spectrum of 2-phenylthiophene

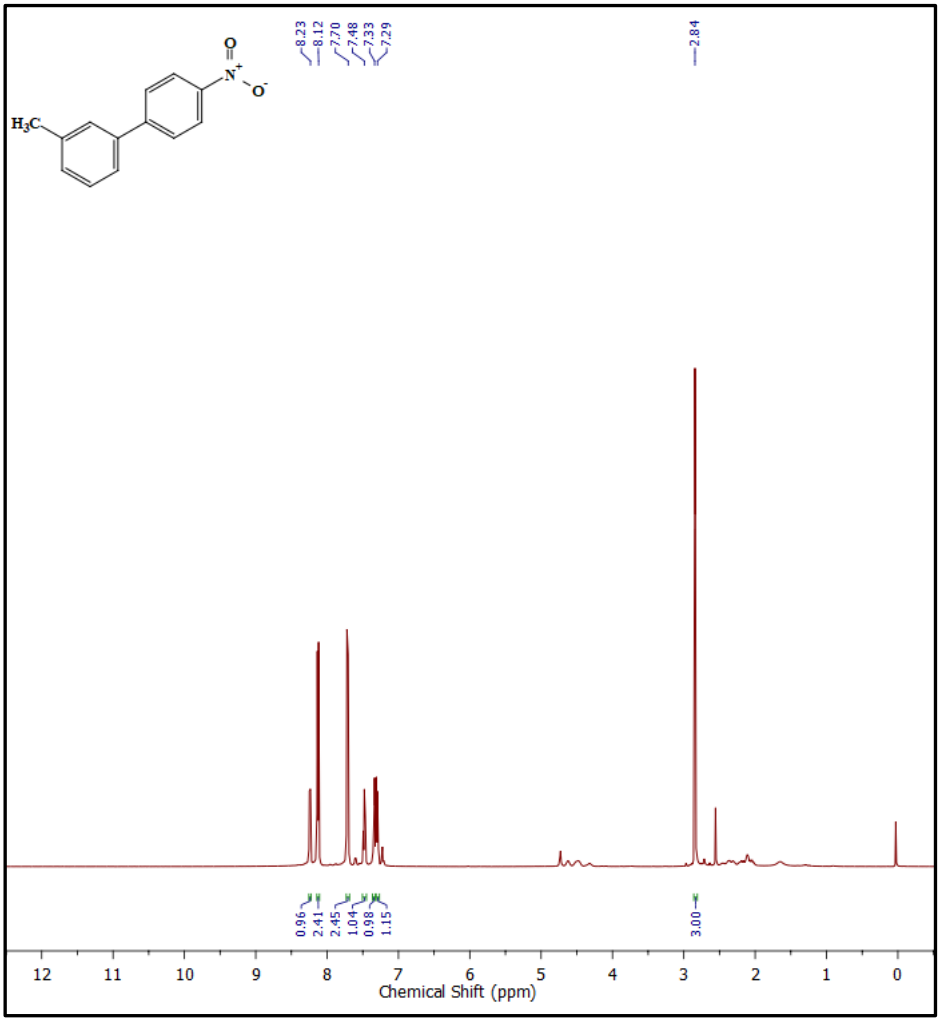

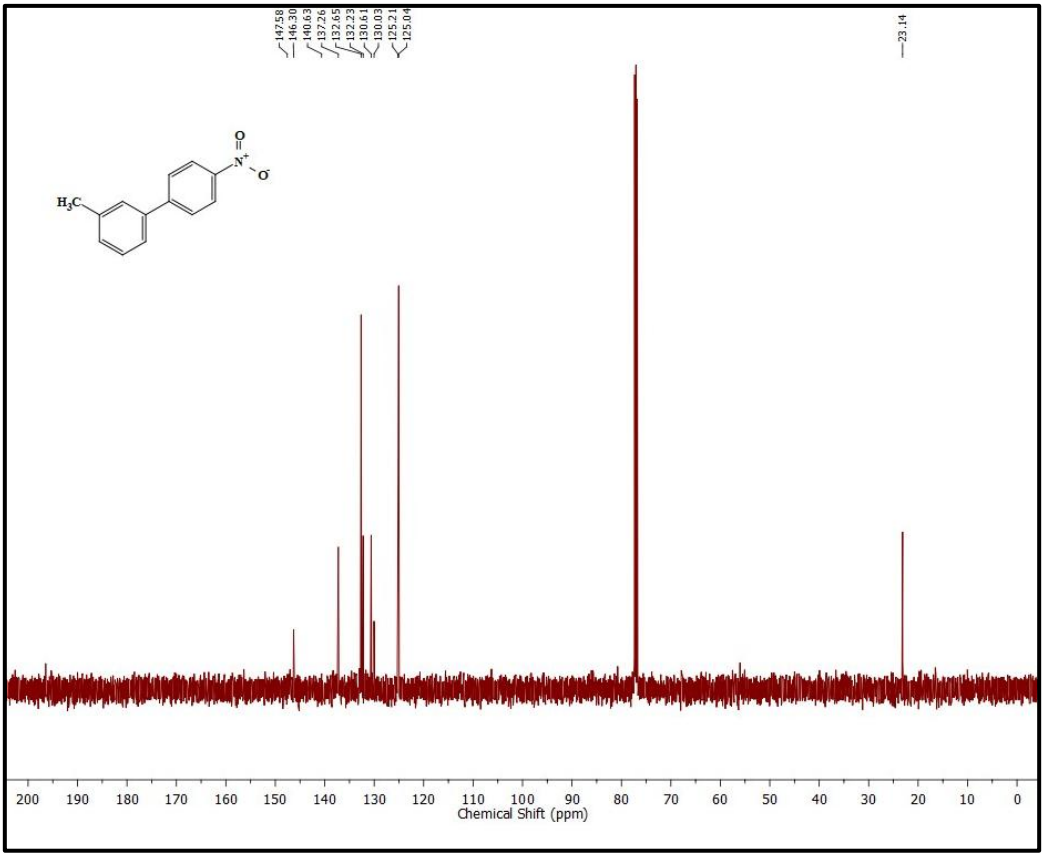

^{1}H and ^{13}C{^{1}H} NMR spectrum of 3-methyl-4'-nitro-1,1'-biphenyl

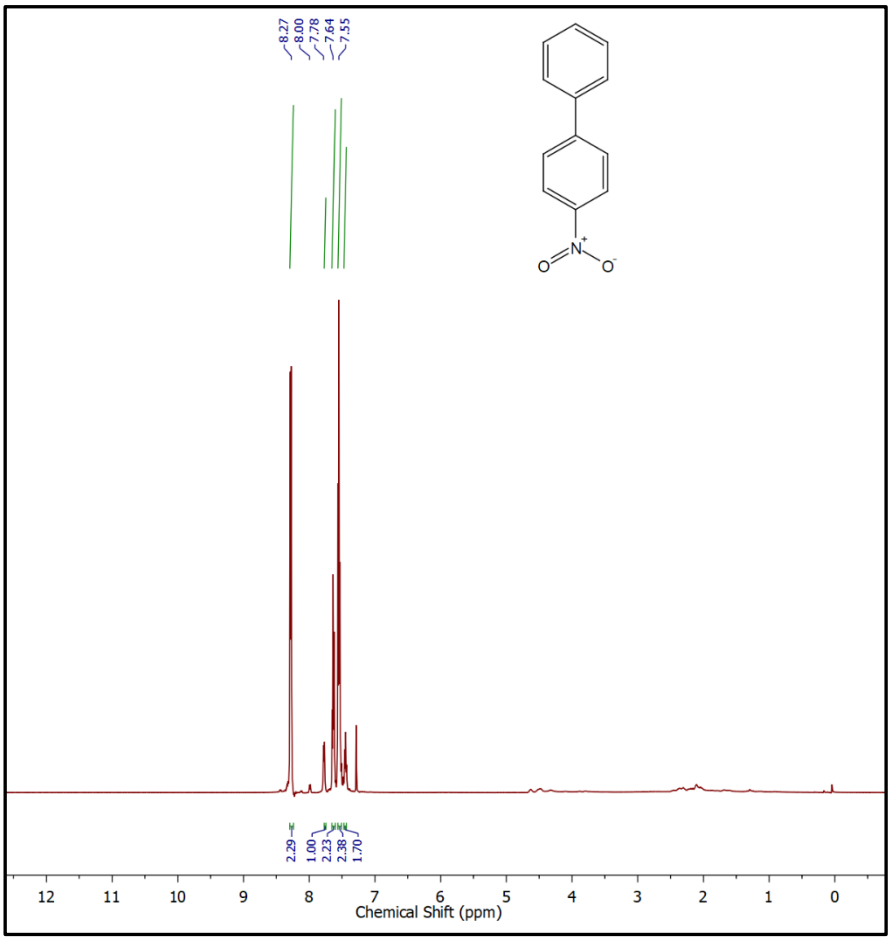

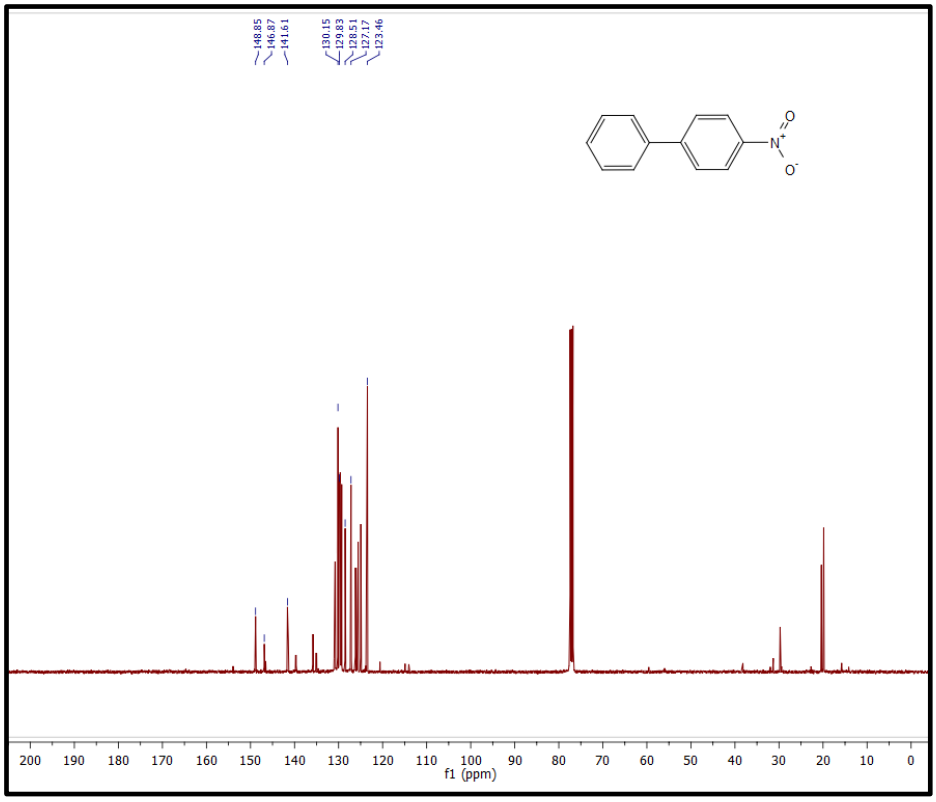

^{1}H and ^{13}C{^{1}H} NMR spectrum of 4-nitro-1,1'-biphenyl

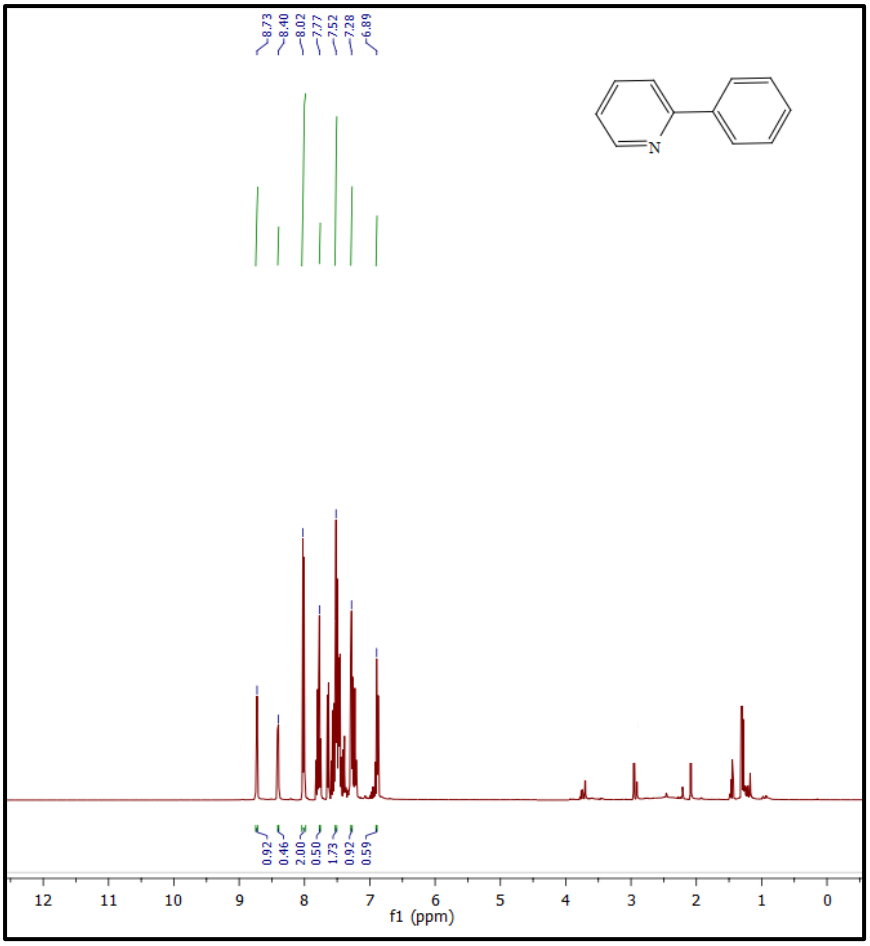

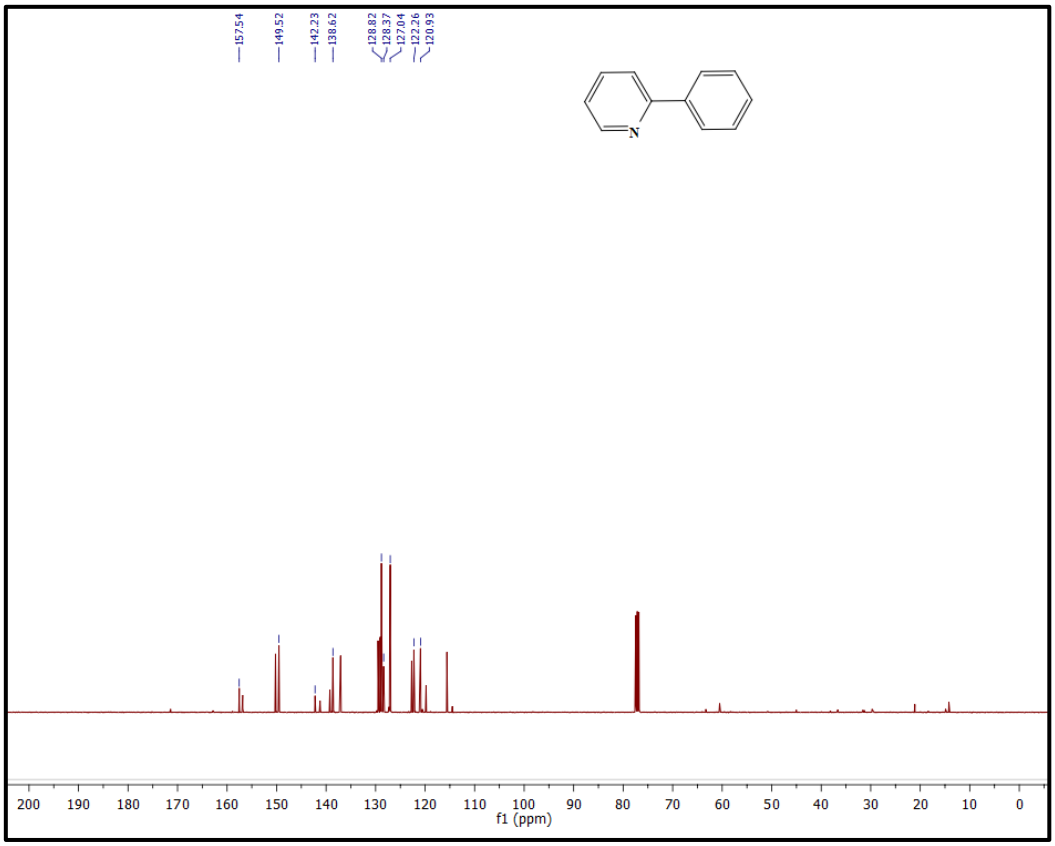

^{1}H and ^{13}C{^{1}H} NMR spectrum of 2-phenylpyridine

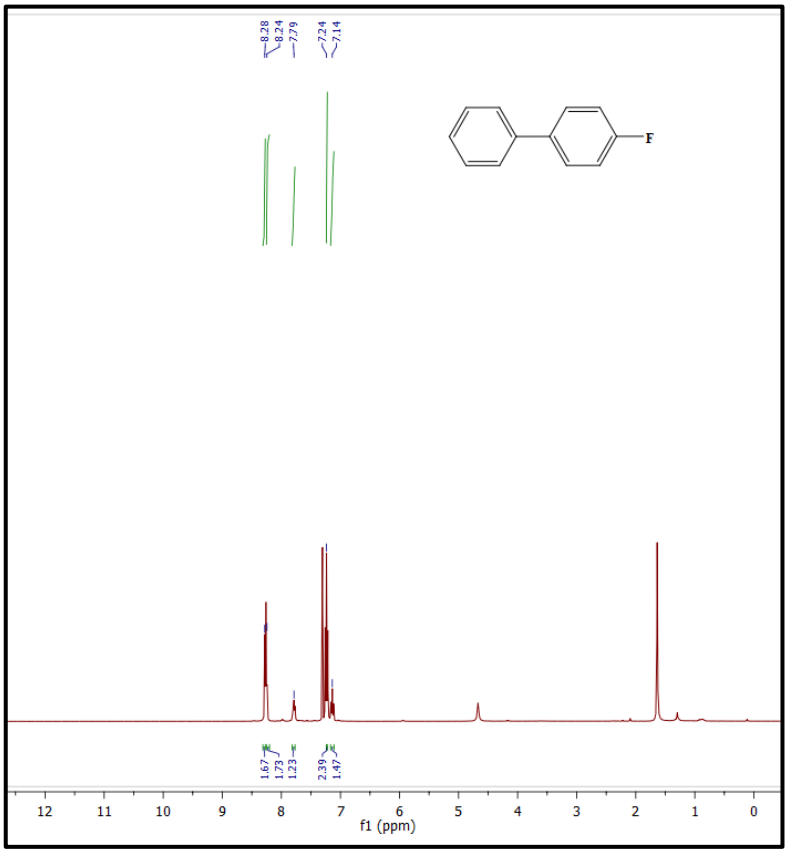

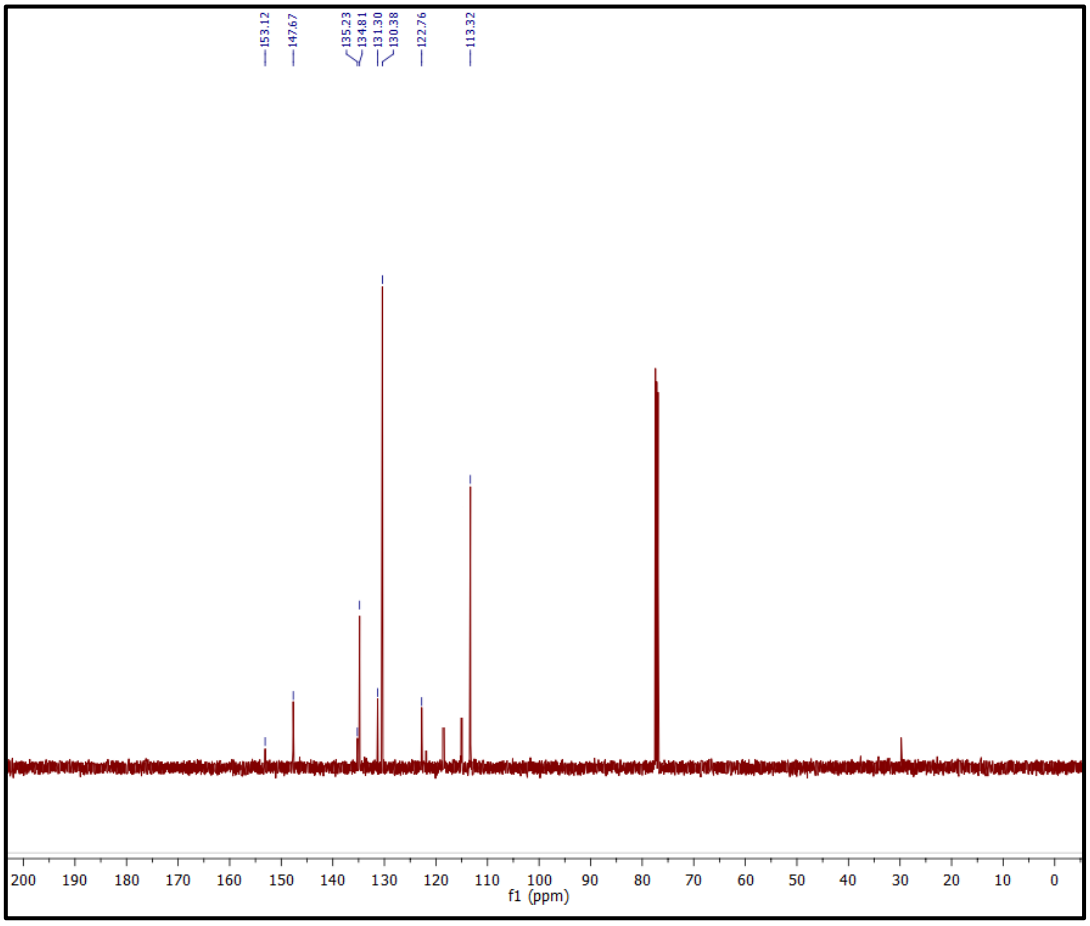

^{1}H and ^{13}C{^{1}H} NMR spectrum of 4-fluoro-1,1'-biphenyl

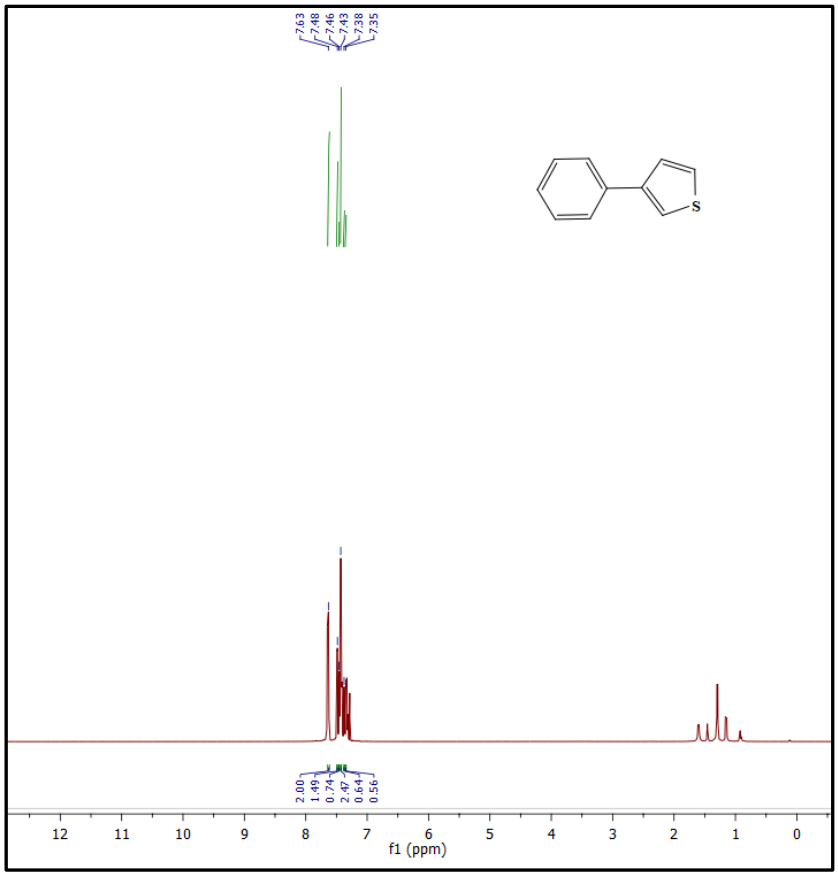

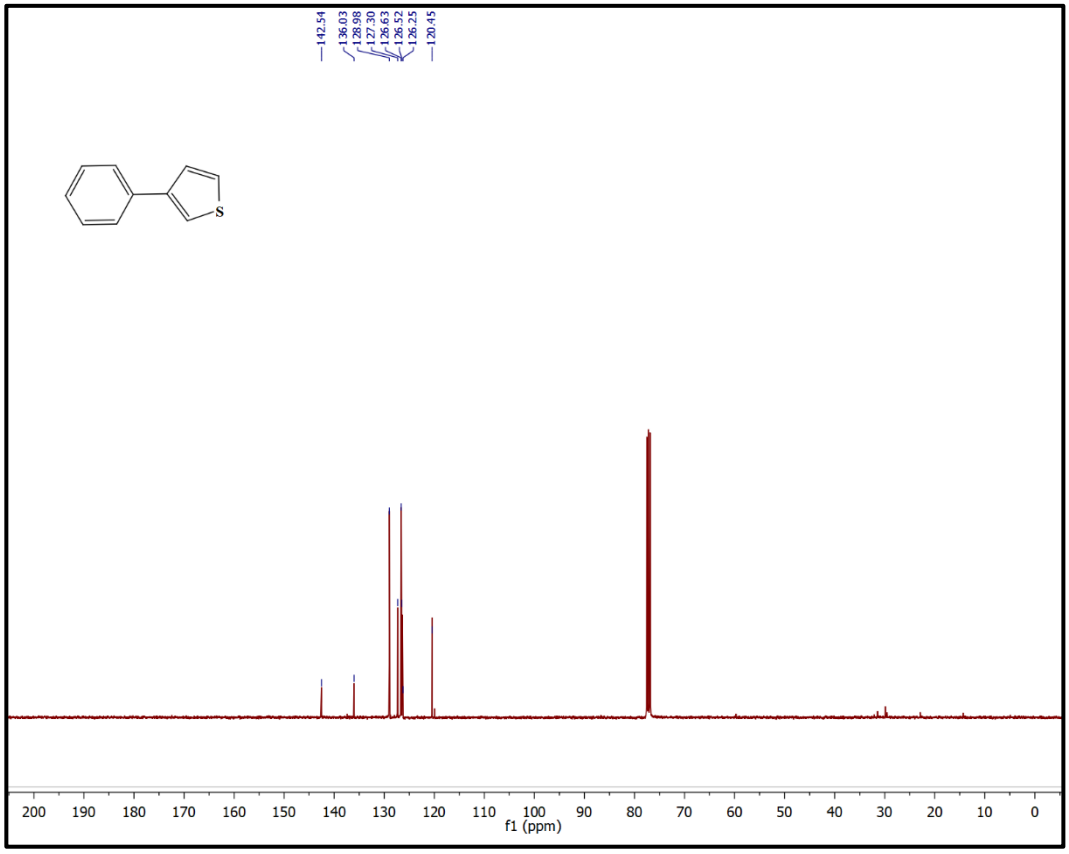

^{1}H and ^{13}C{^{1}H} NMR spectrum of 3-phenylthiophene

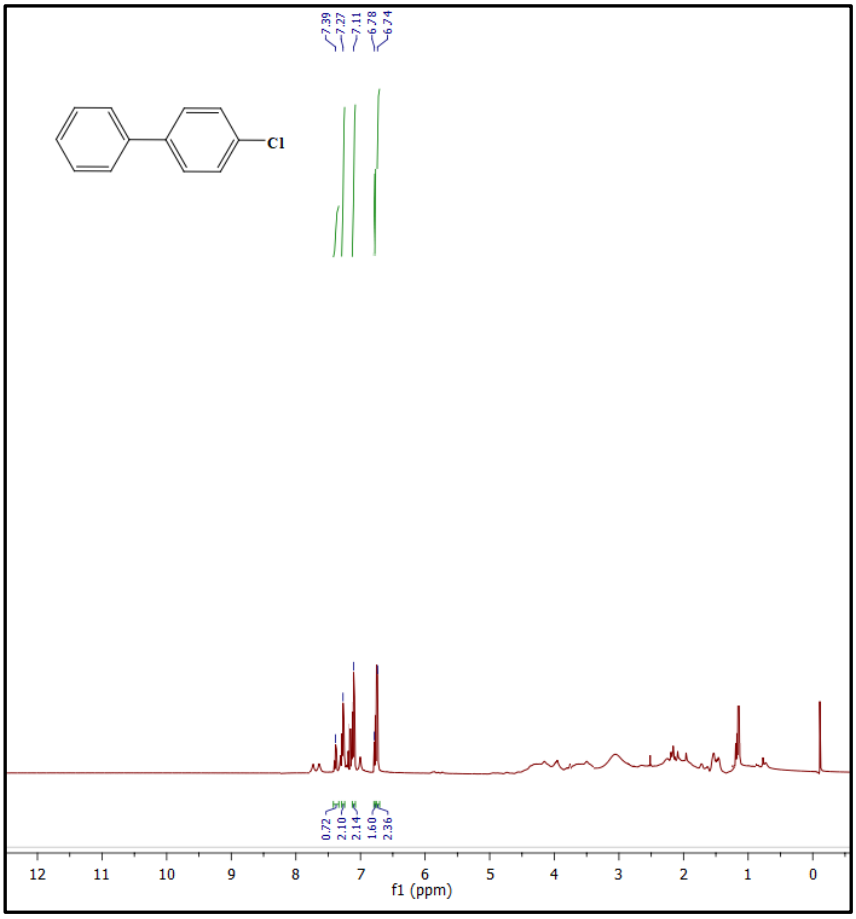

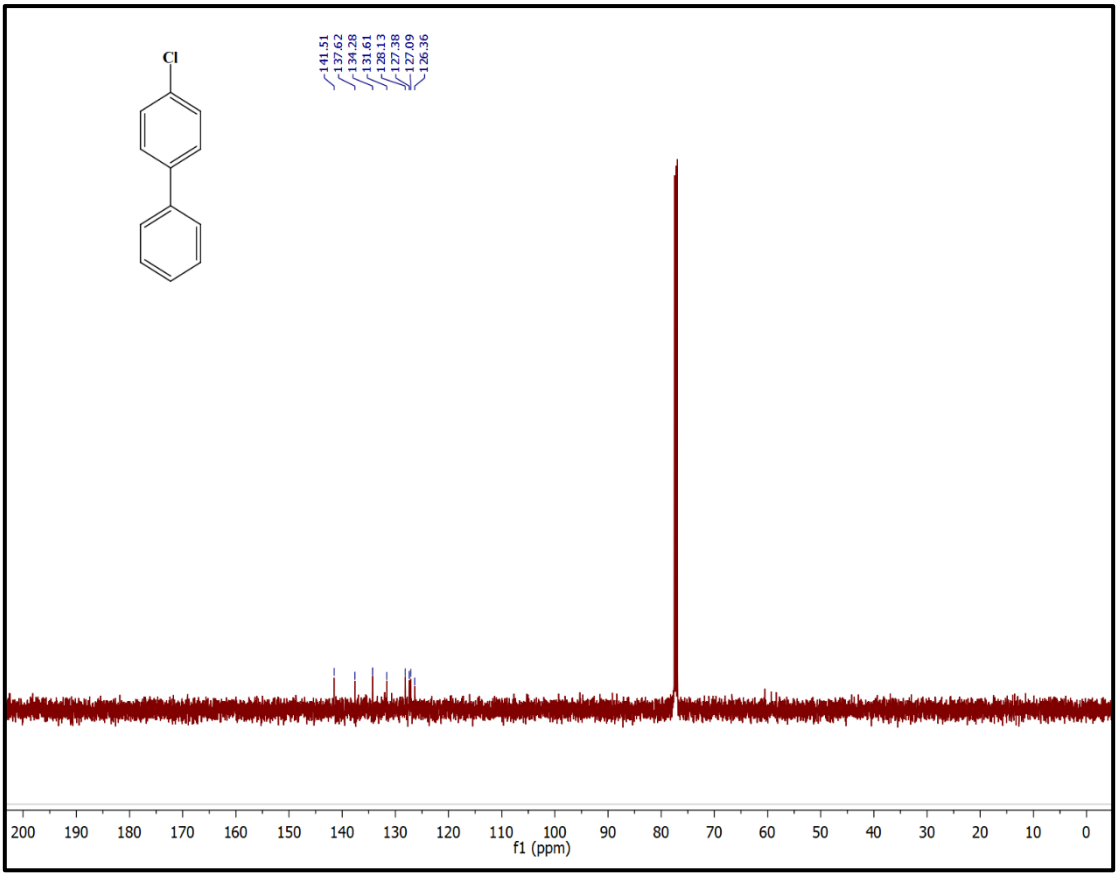

^{1}H and ^{13}C{^{1}H} NMR spectrum of 4-chloro-1,1'-biphenyl

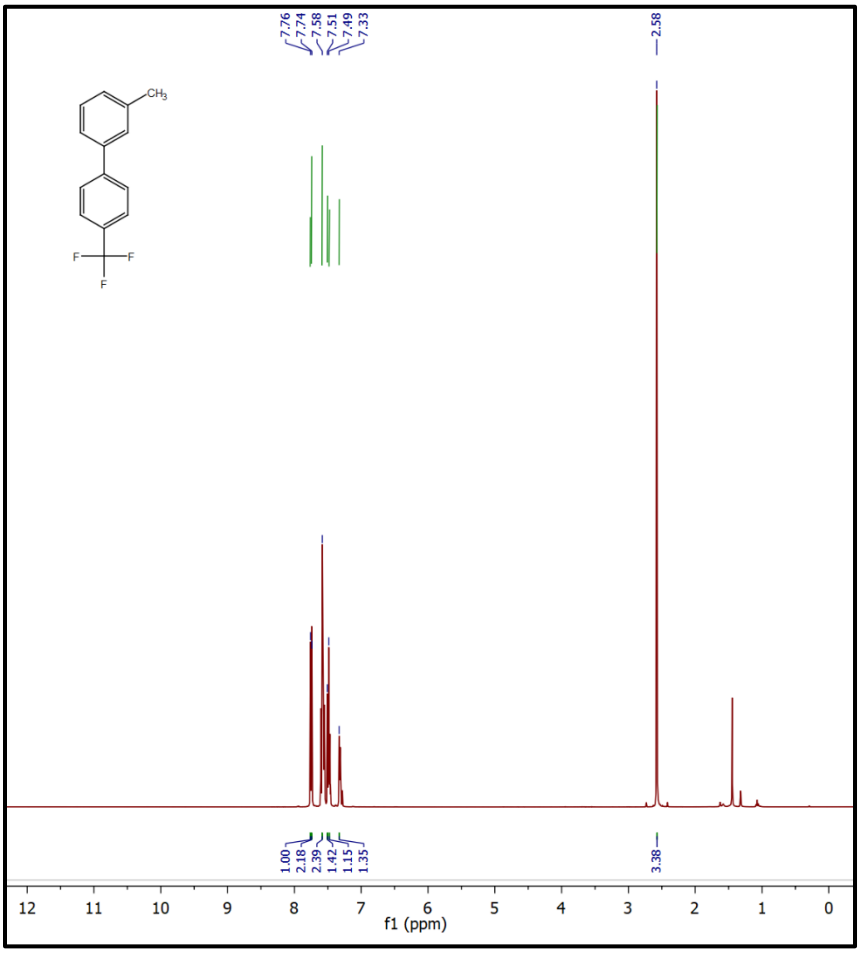

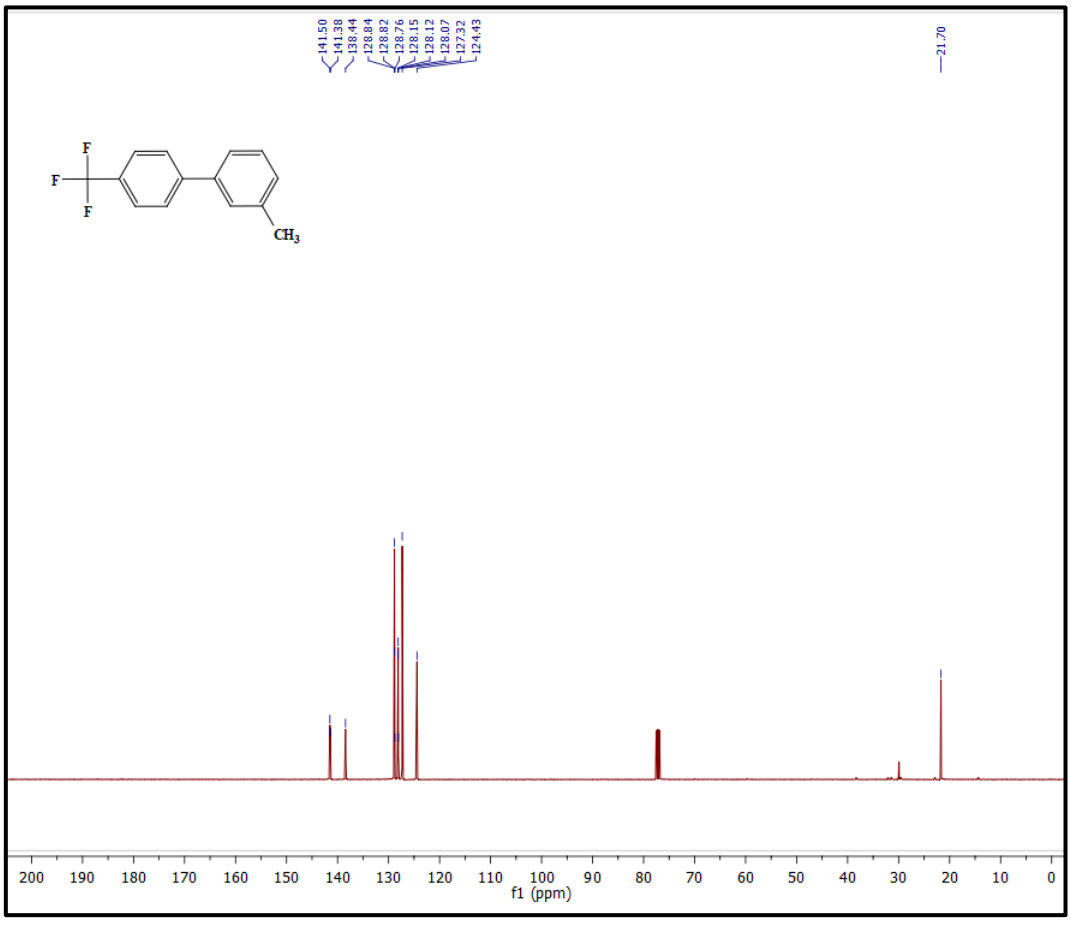

^{1}H and ^{13}C{^{1}H} NMR spectrum of 4-(trifluoromethyl)-1,1'-biphenyl

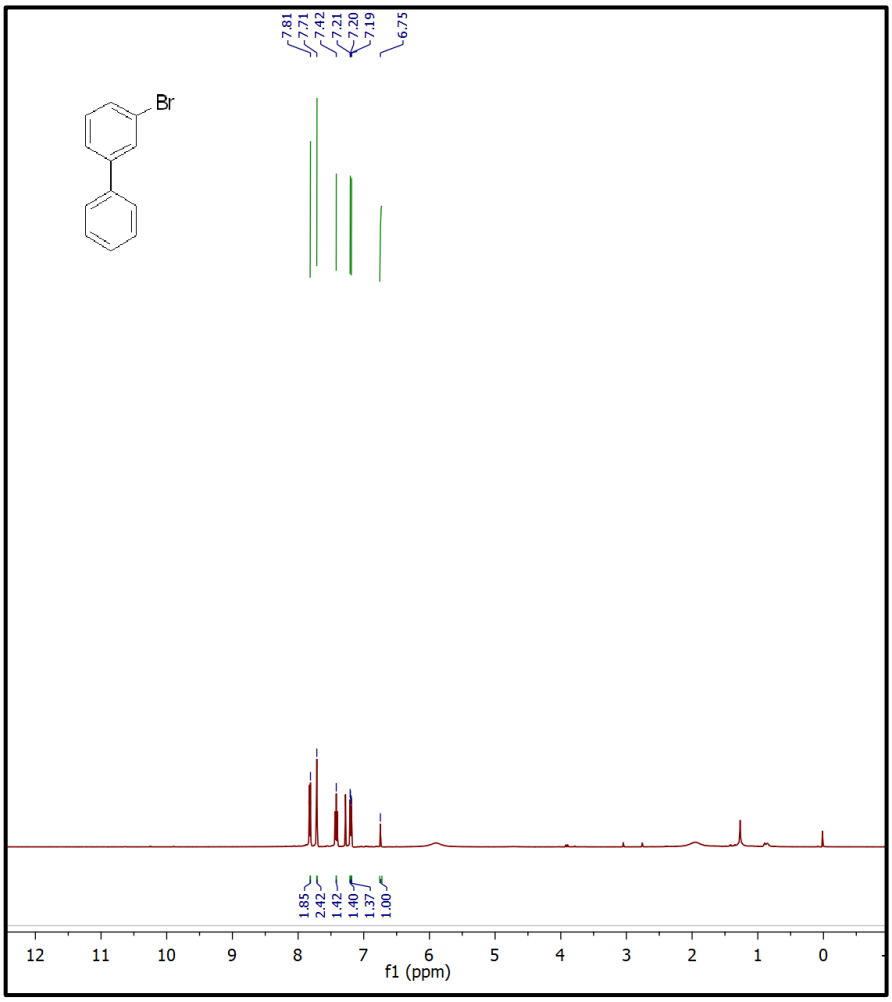

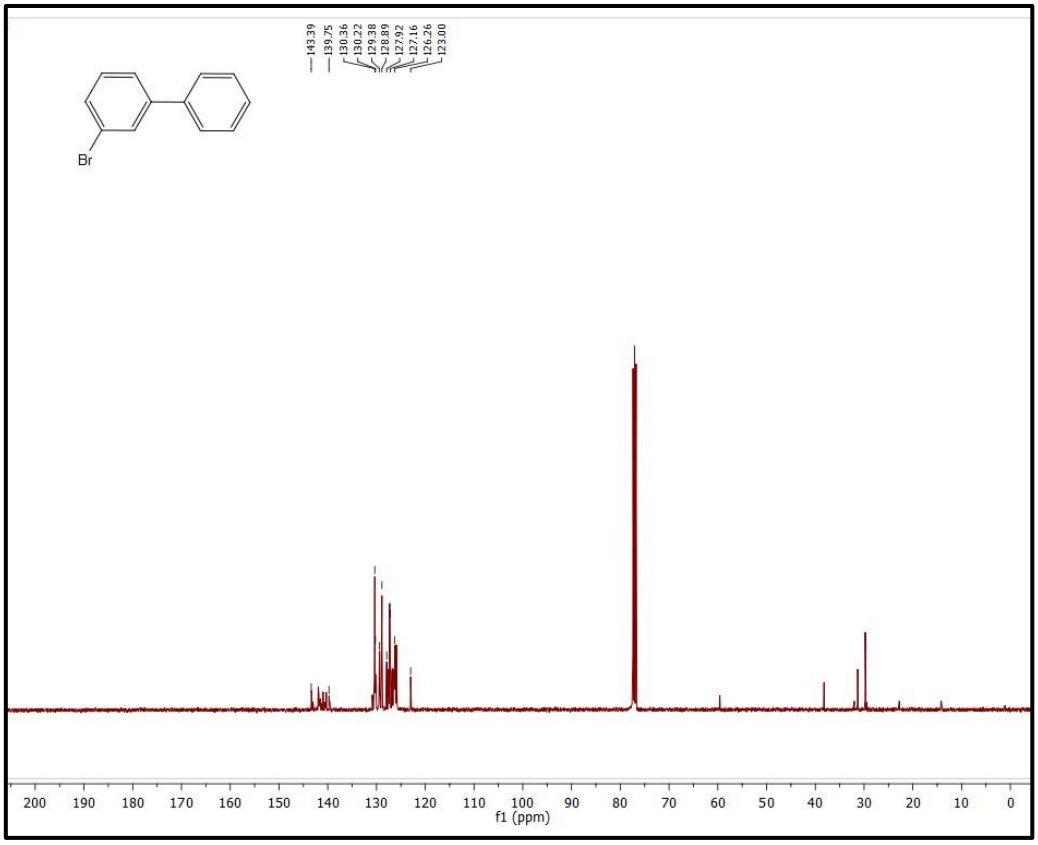

^{1}H and ^{13}C{^{1}H} NMR spectrum of 3-bromo-1,1'-biphenyl

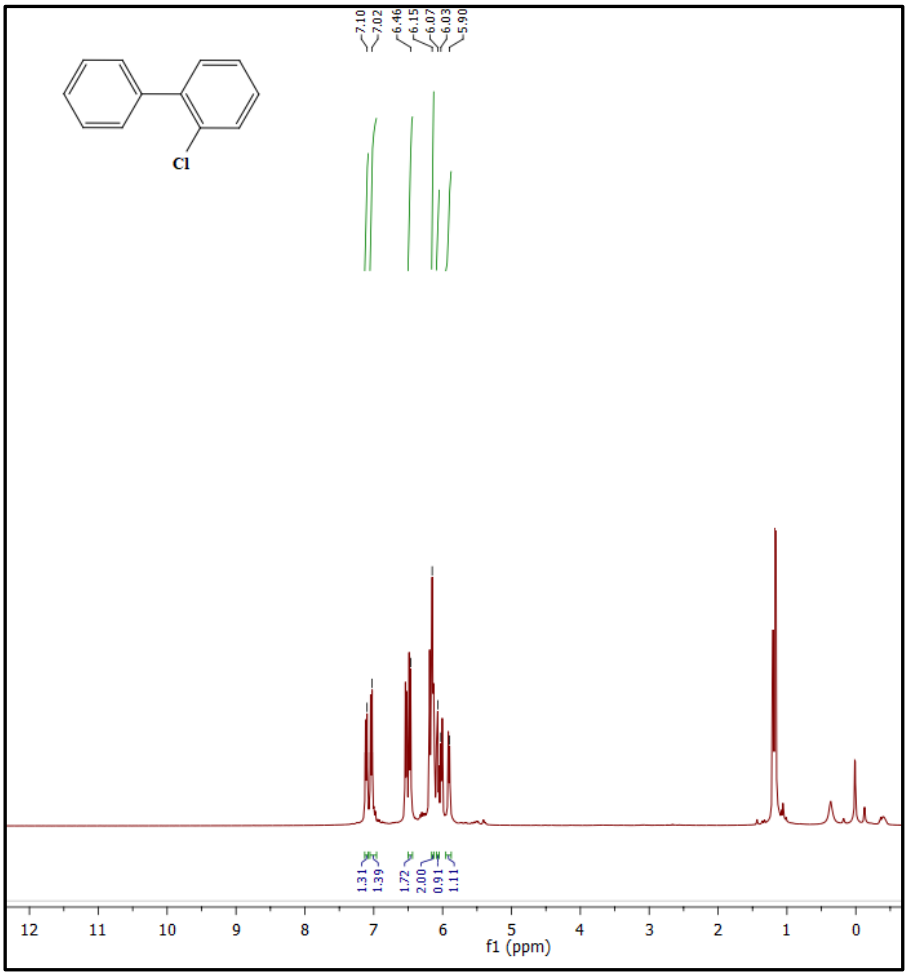

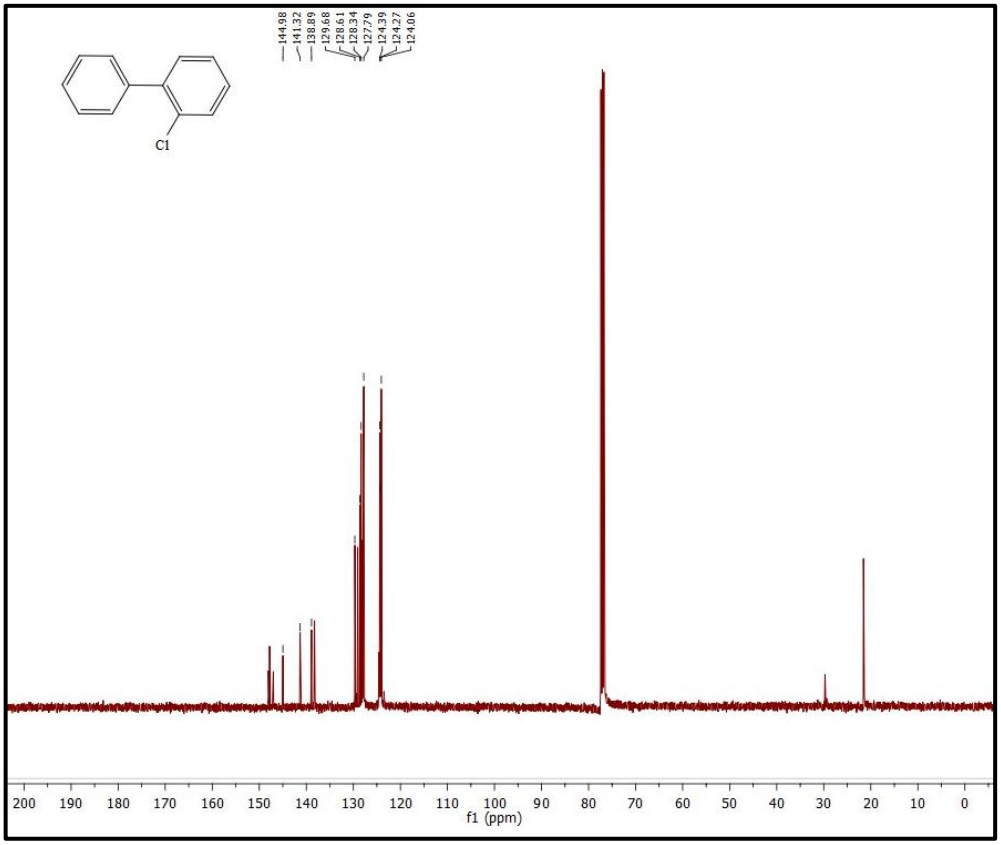

^{1}H and ^{13}C{^{1}H} NMR spectrum of 2-chloro-1,1'-biphenyl

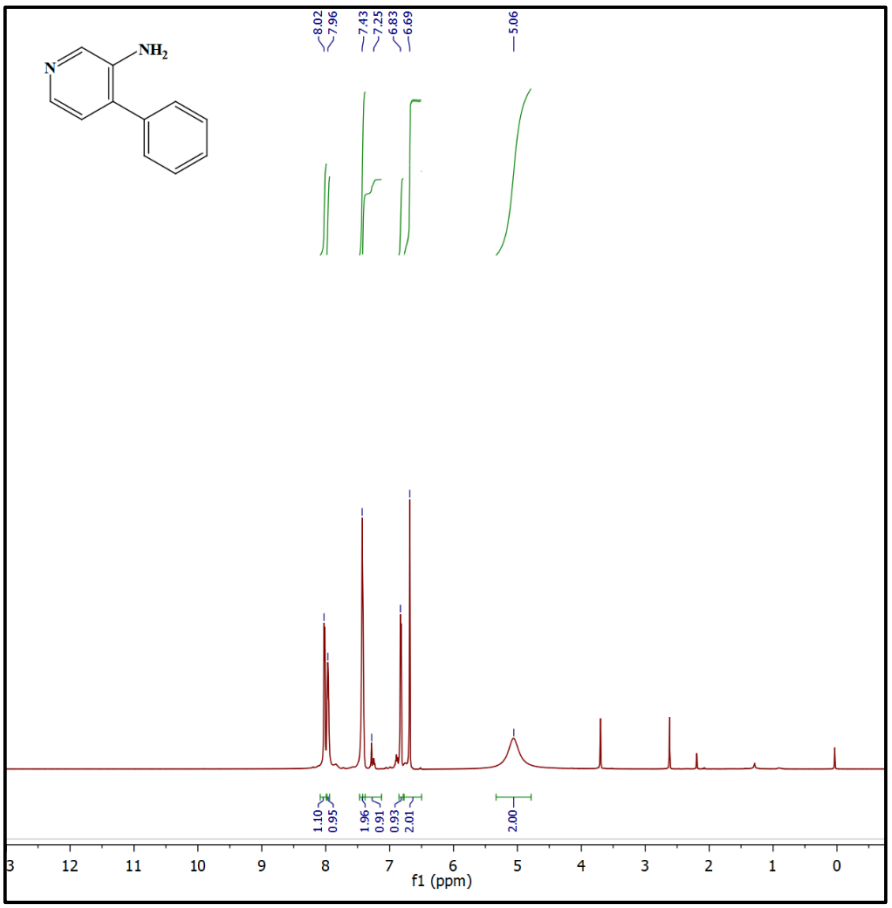

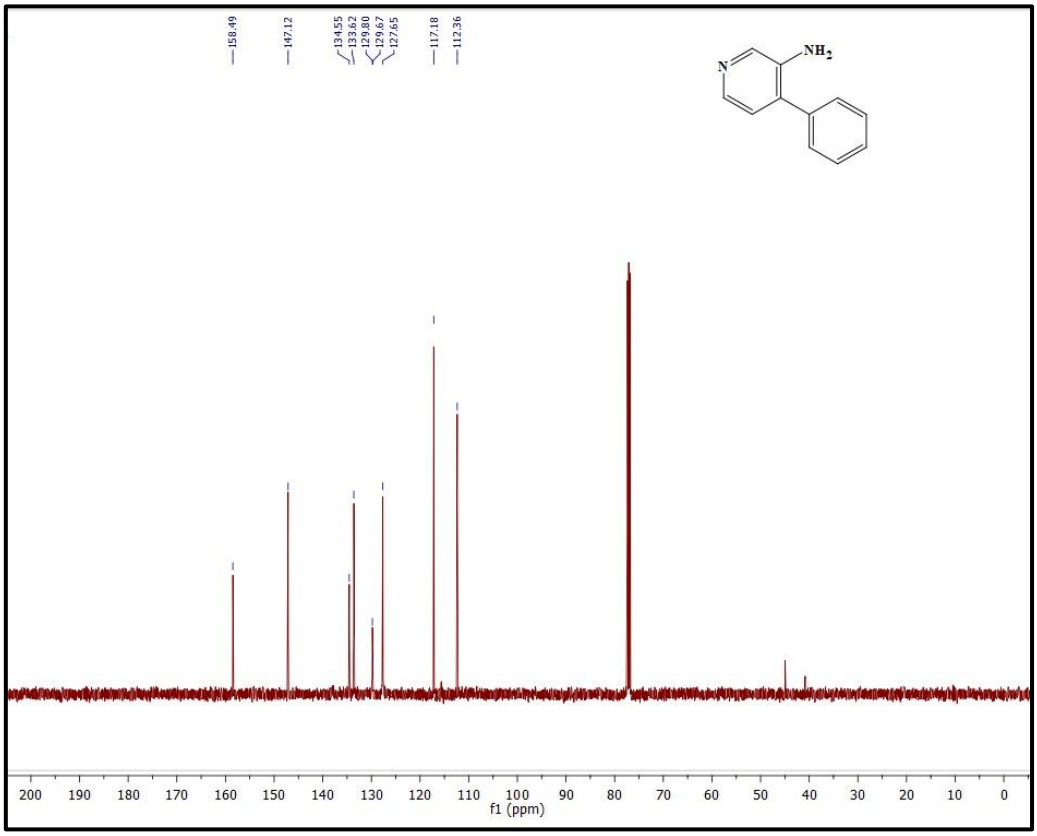

^{1}H and ^{13}C{^{1}H} NMR spectrum of 4-phenylpyridin-3-amine

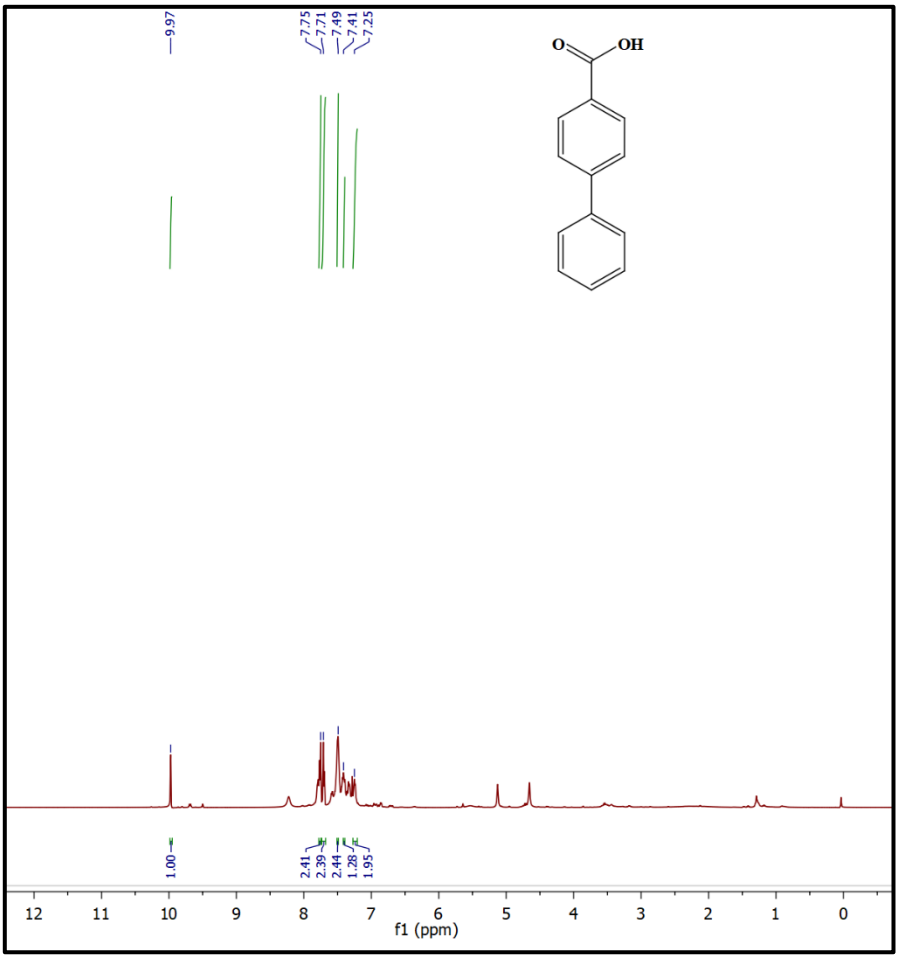

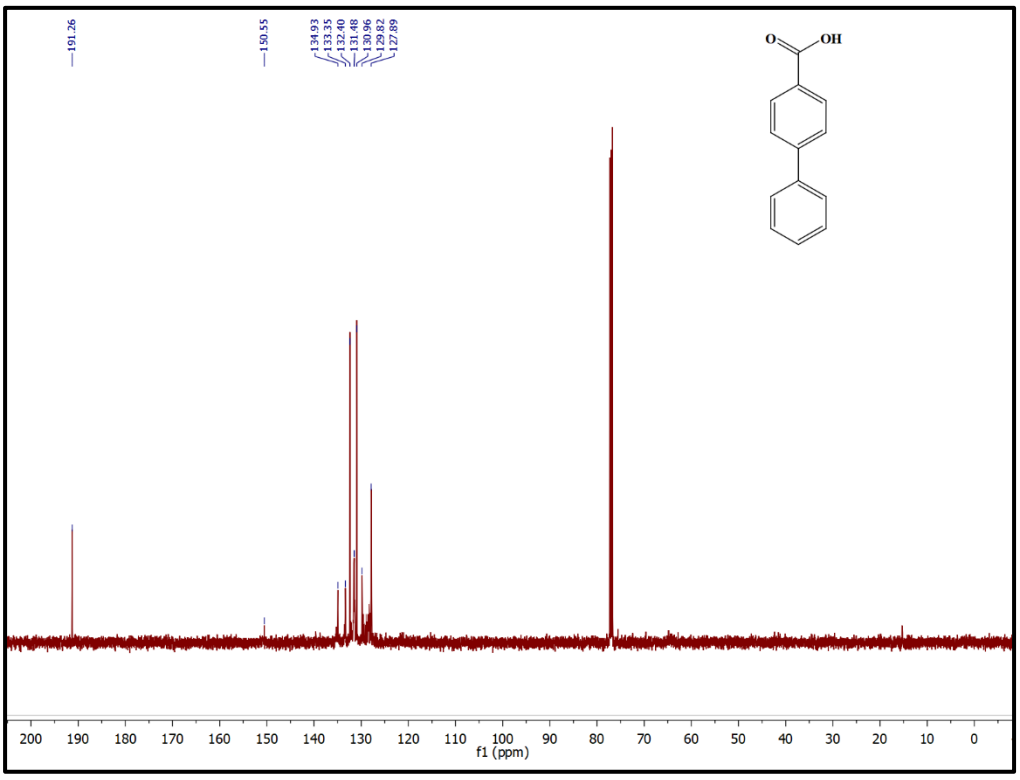

^{1}H and ^{13}C{^{1}H} NMR spectrum of [1,1'-biphenyl]-4-carboxylic acid

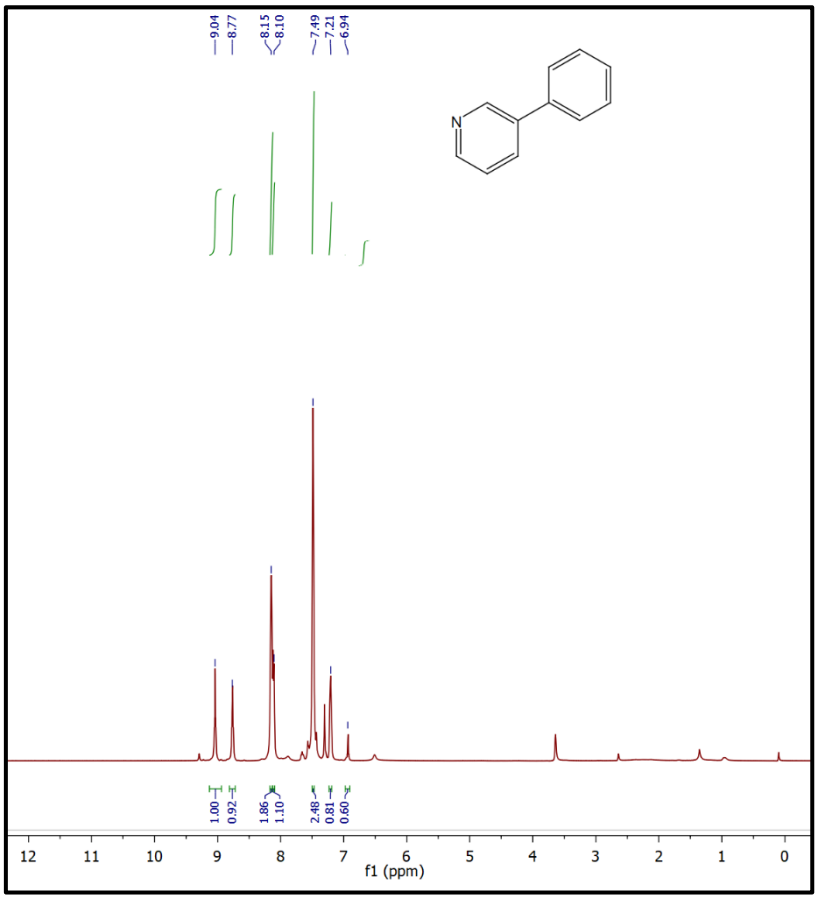

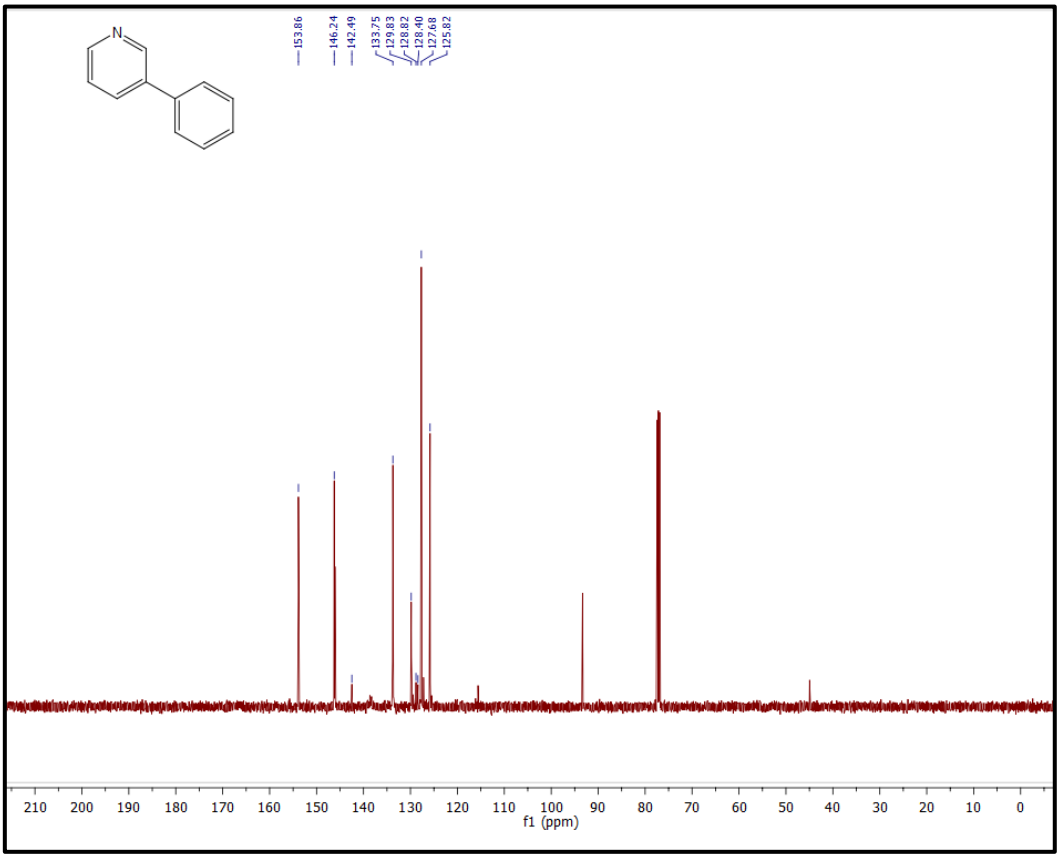

^{1}H and ^{13}C{^{1}H} NMR spectrum of 3-phenylpyridine

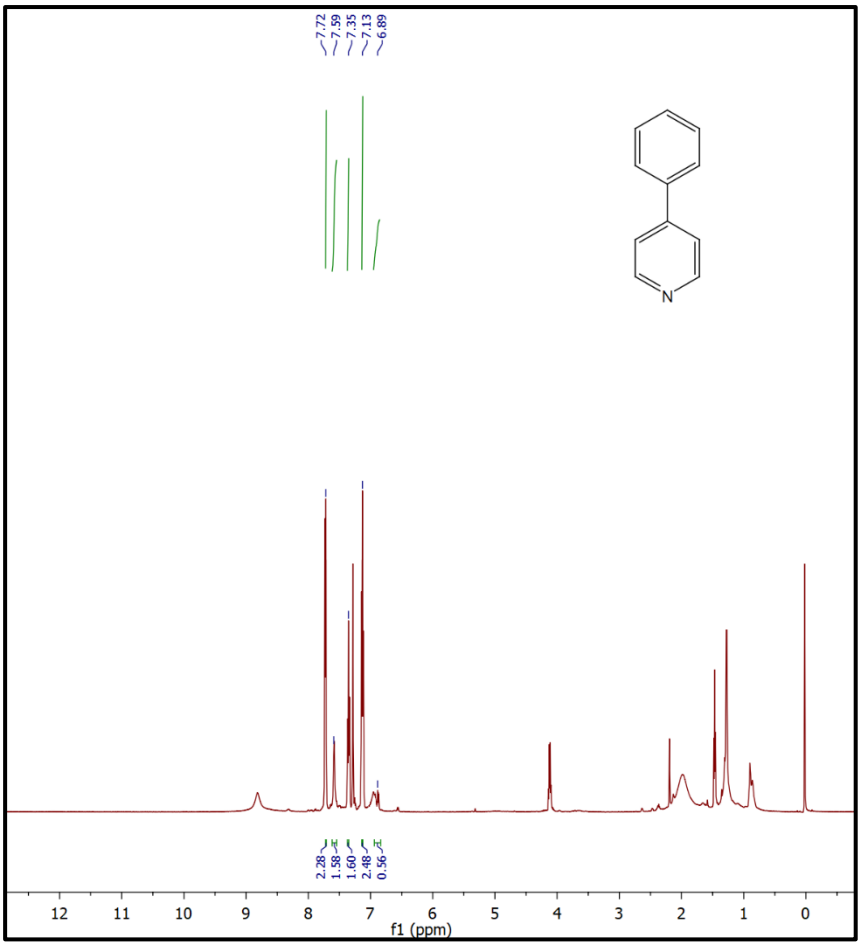

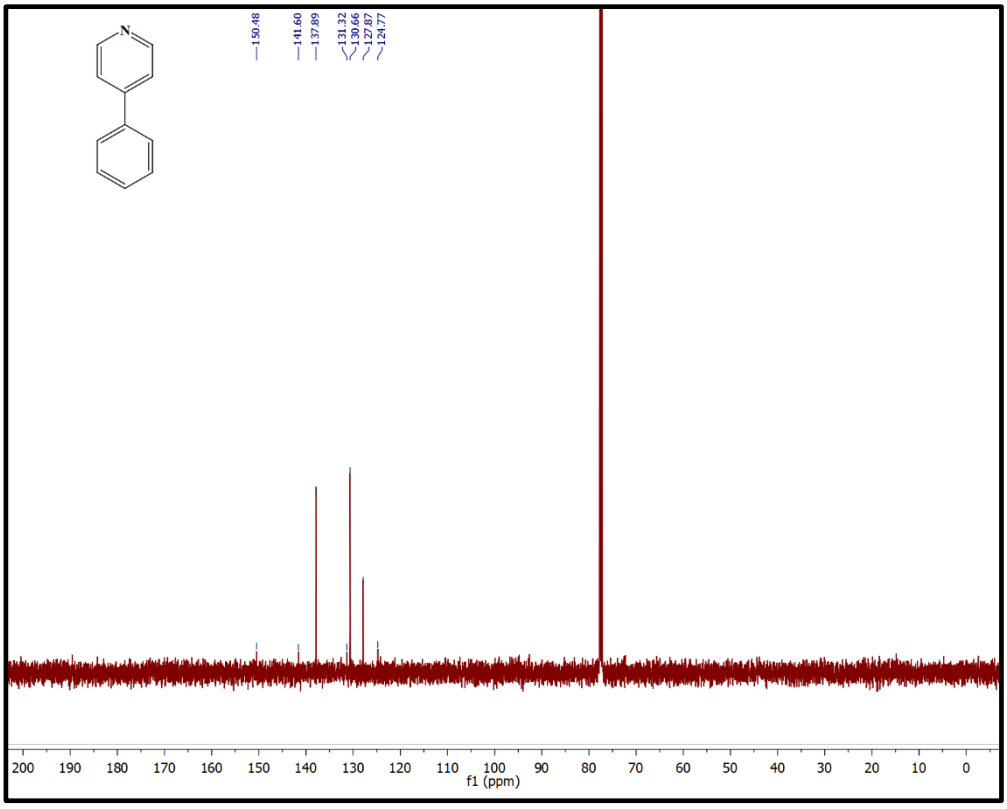

^{1}H and ^{13}C{^{1}H} NMR spectrum of 4-phenylpyridine

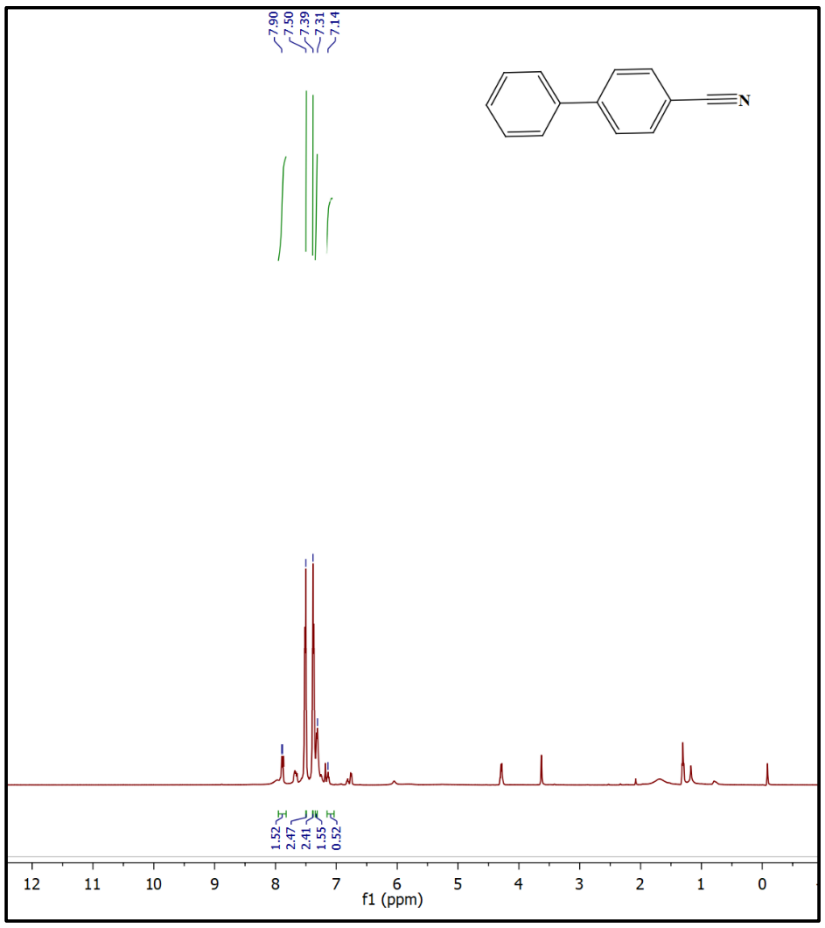

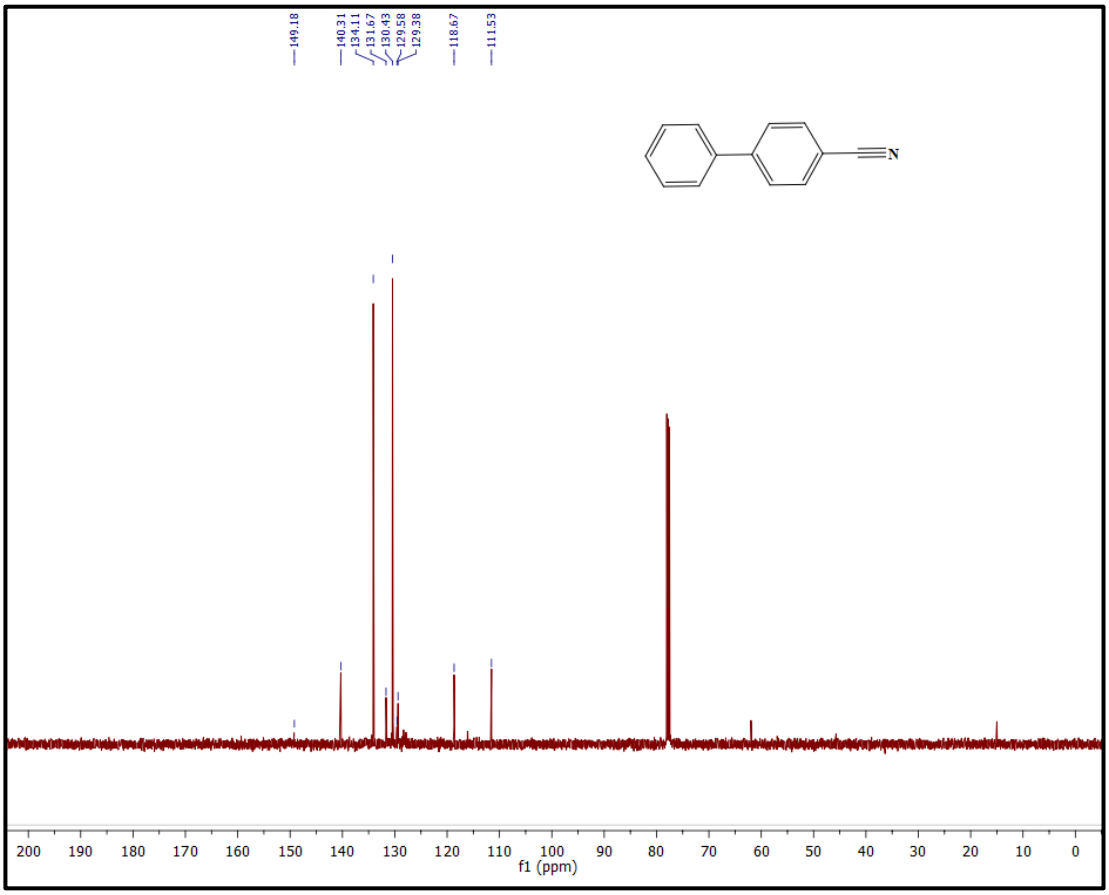

^{1}H and ^{13}C{^{1}H} NMR spectrum of [1,1'-biphenyl]-4-carbonitrile

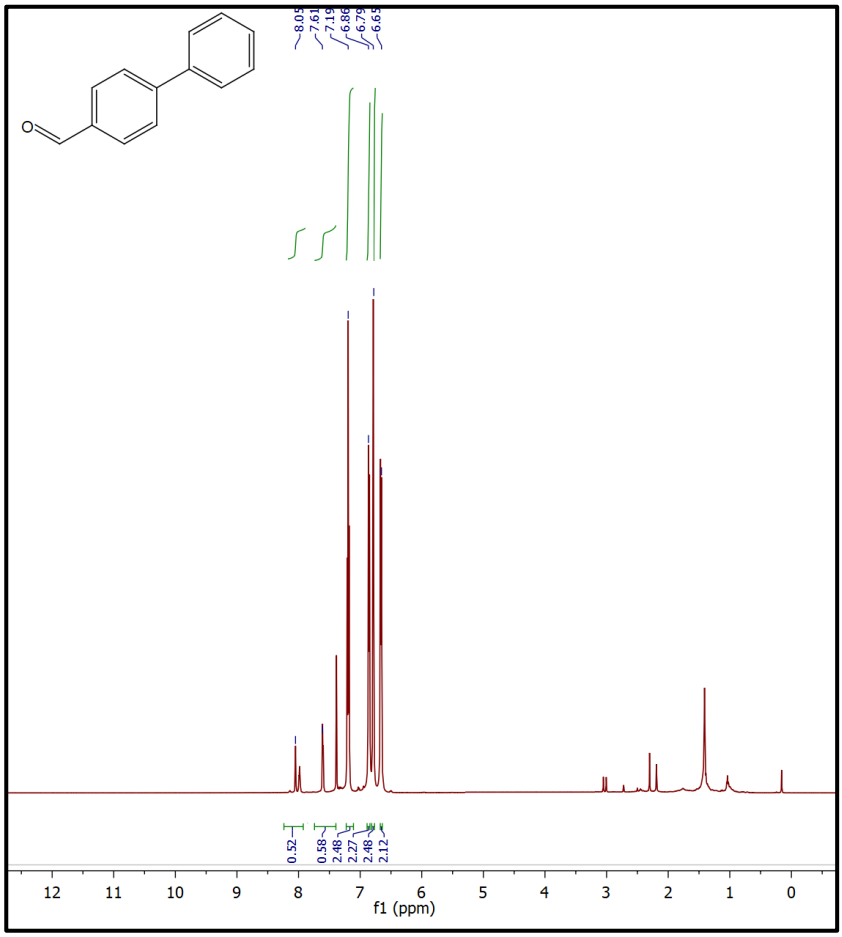

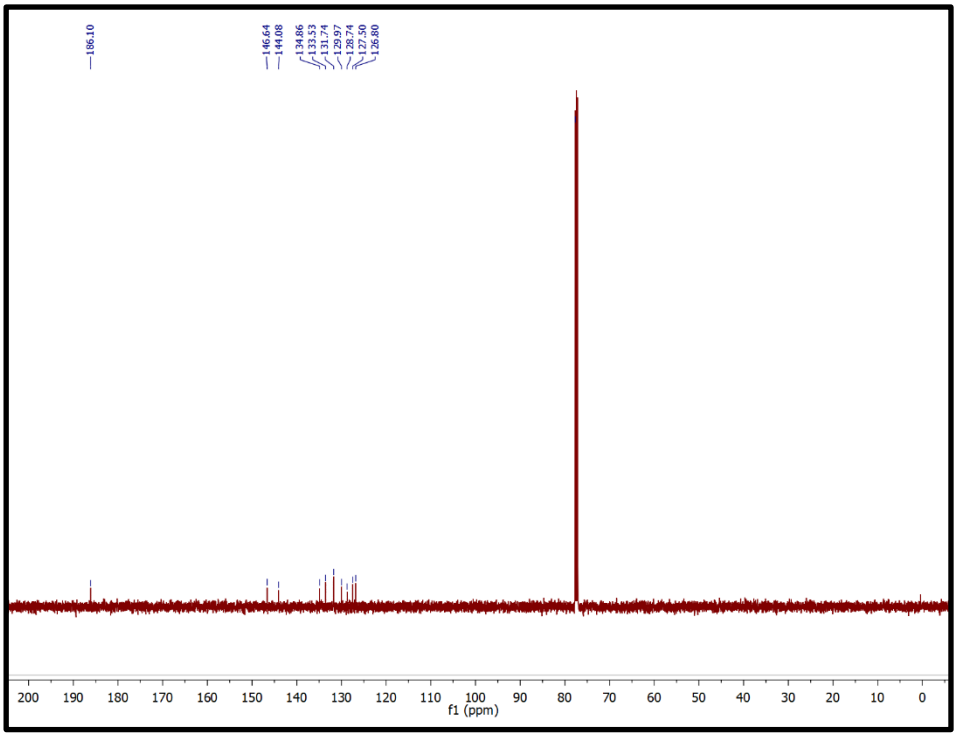

^{1}H and ^{13}C{^{1}H} NMR spectrum of [1,1'-biphenyl]-4-carbaldehyde

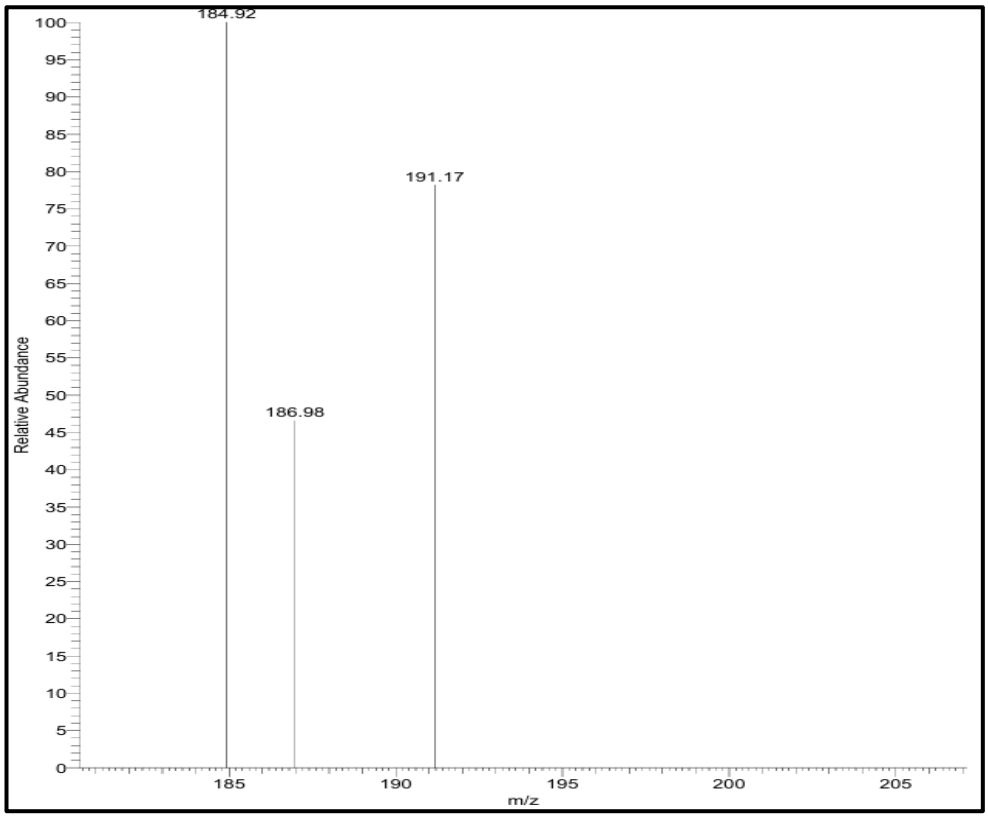

ESI-MS spectrum of 3-methoxy-1,1’-biphenyl (Exact mass= 184.09)

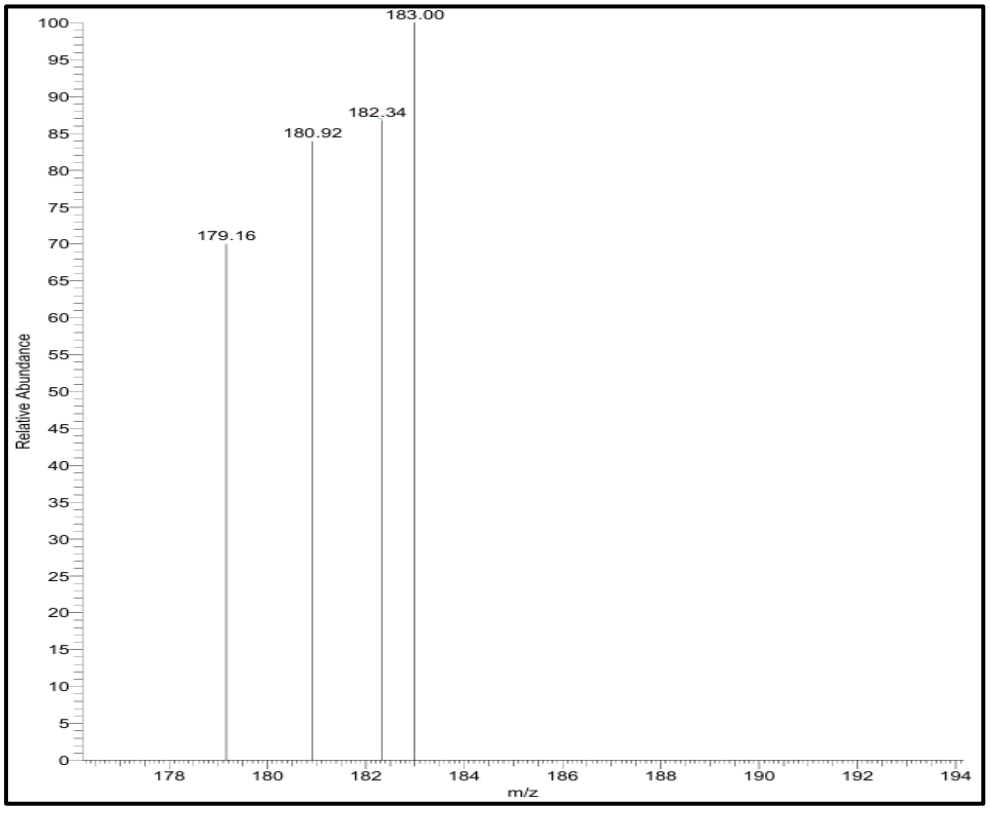

ESI-MS spectrum of 4-Ethyl-1,1’-biphenyl (Exact mass= 182.11)

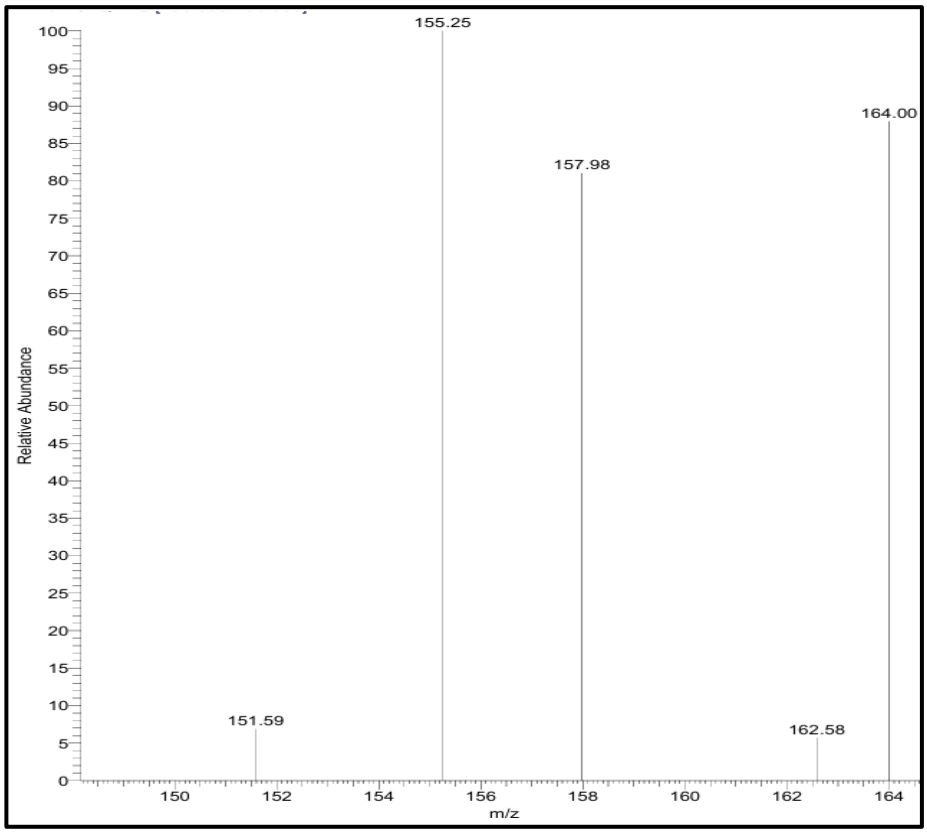

ESI-MS spectrum of 1,1′-biphenyl (Exact mass= 154.08)

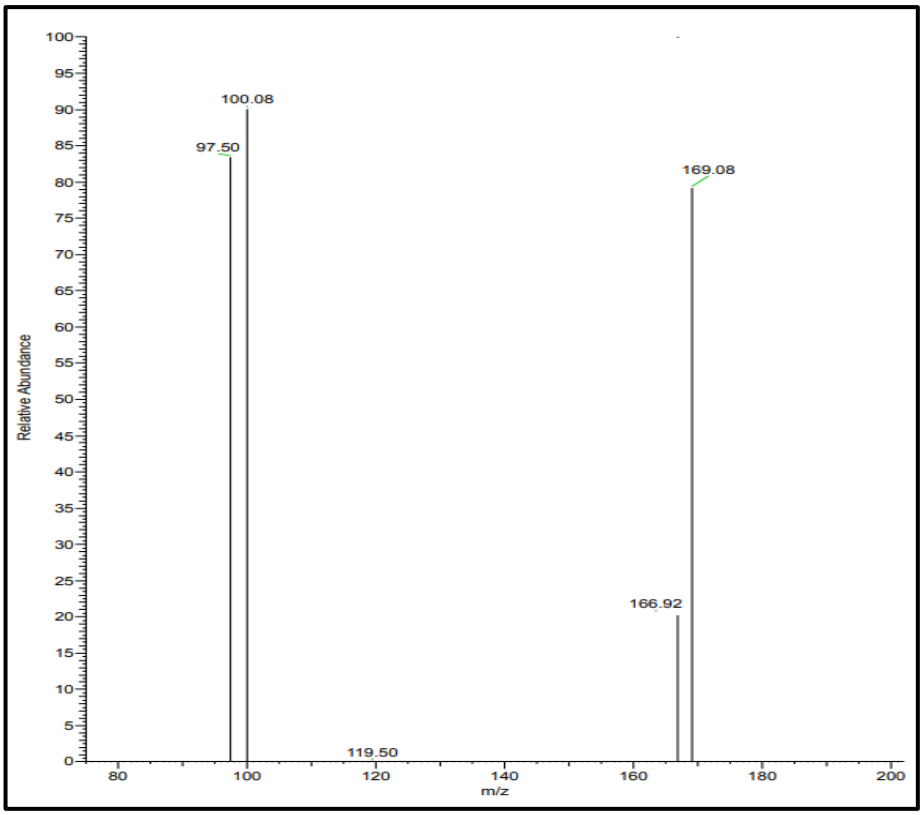

ESI-MS spectrum of 3-methyl-1,1′-biphenyl (Exact mass= 168.09)

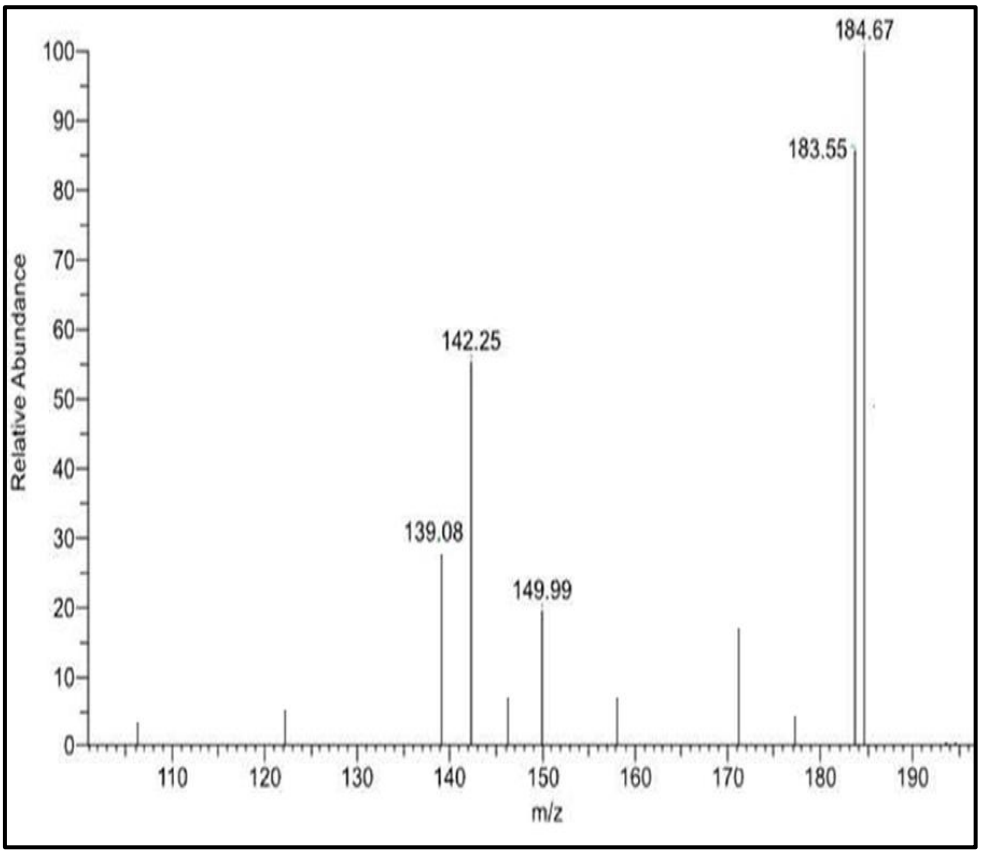

ESI-MS spectrum of 4-methoxy-1,1’-biphenyl (Exact mass= 184.24)

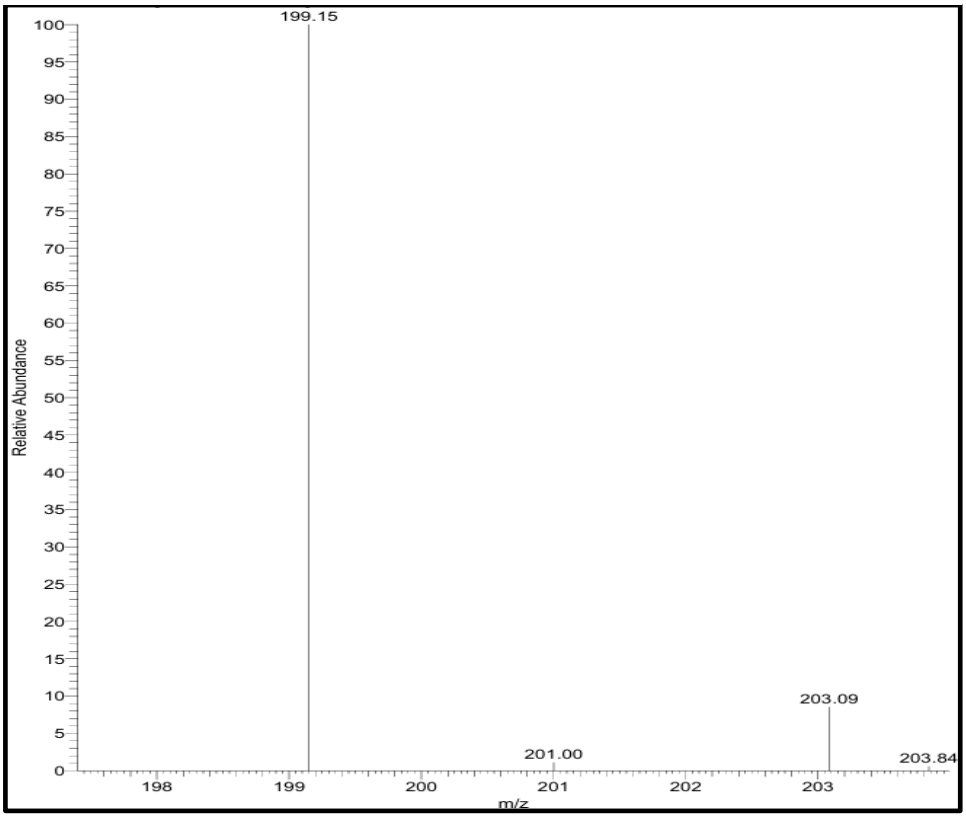

ESI-MS spectrum of [1,1'-biphenyl]-4-carboxylic acid (Exact mass= 198.07)

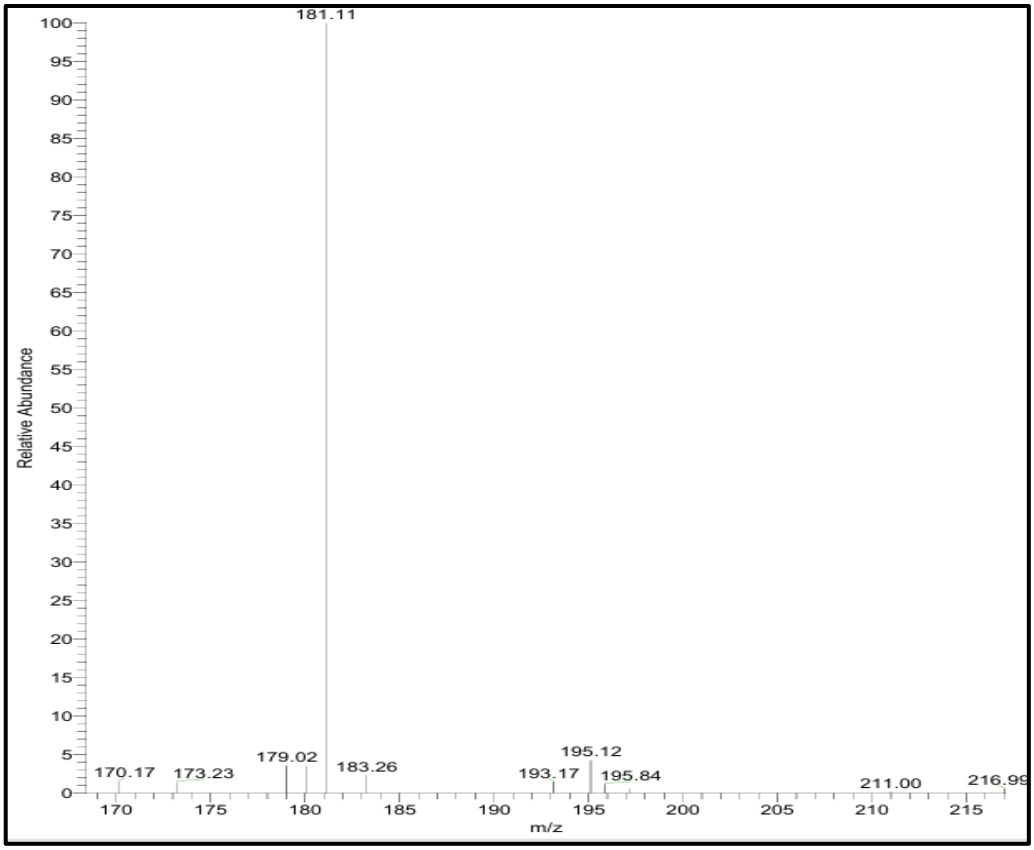

ESI-MS spectrum of [1,1'-biphenyl]-4-carbaldehyde (Exact mass= 182.07)

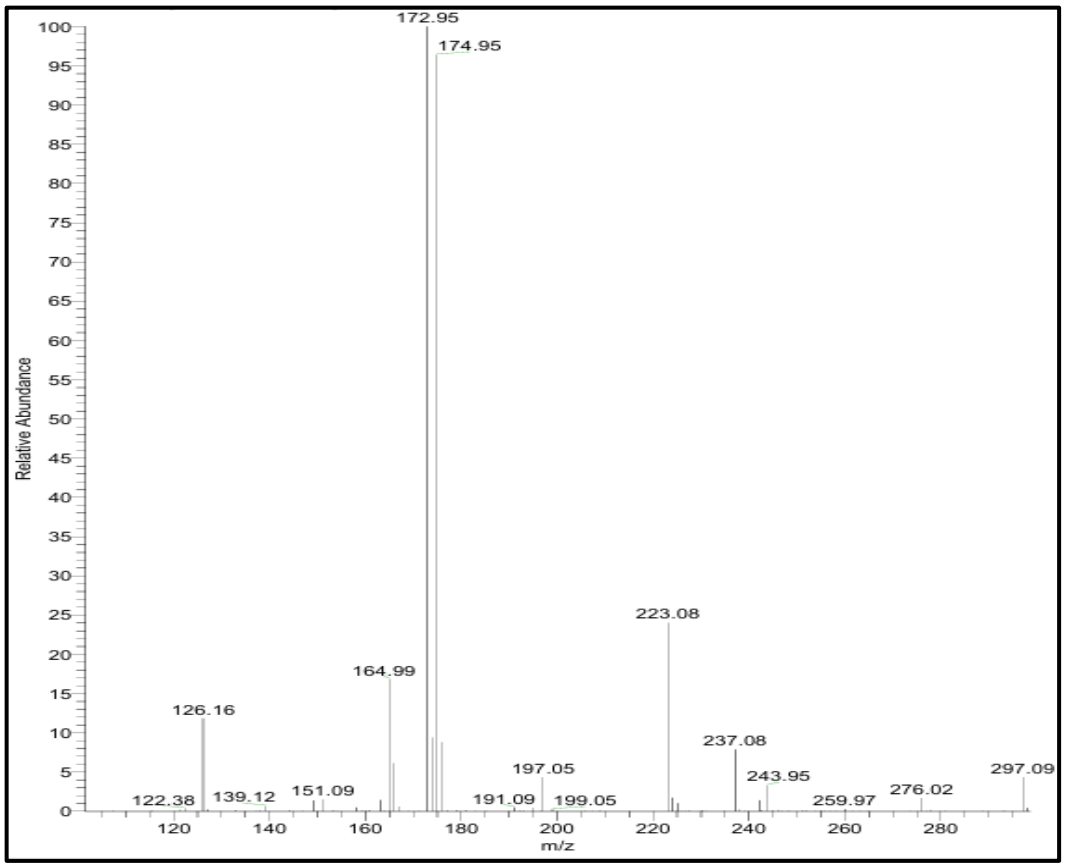

ESI-MS spectrum of 4-phenylpyridin-2-amine (Exact mass= 170.08)

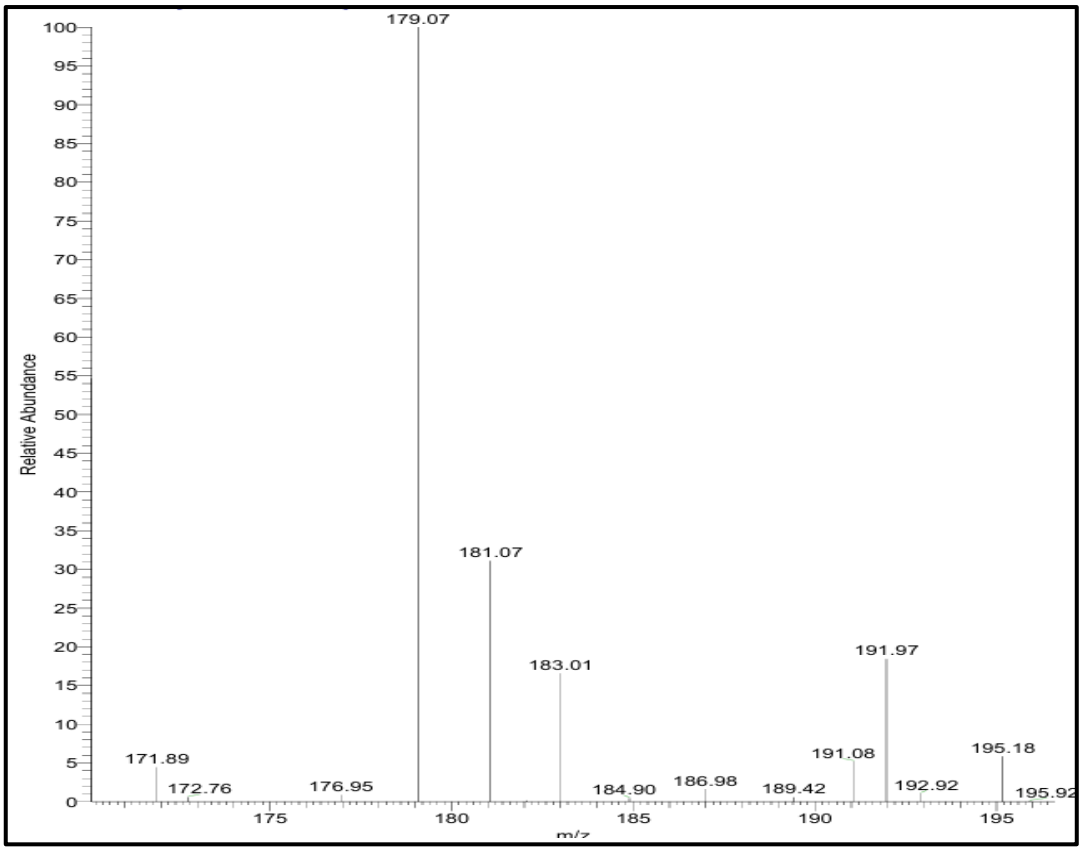

ESI-MS spectrum of [1,1'-biphenyl]-4-carbonitrile (Exact mass= 179.07)

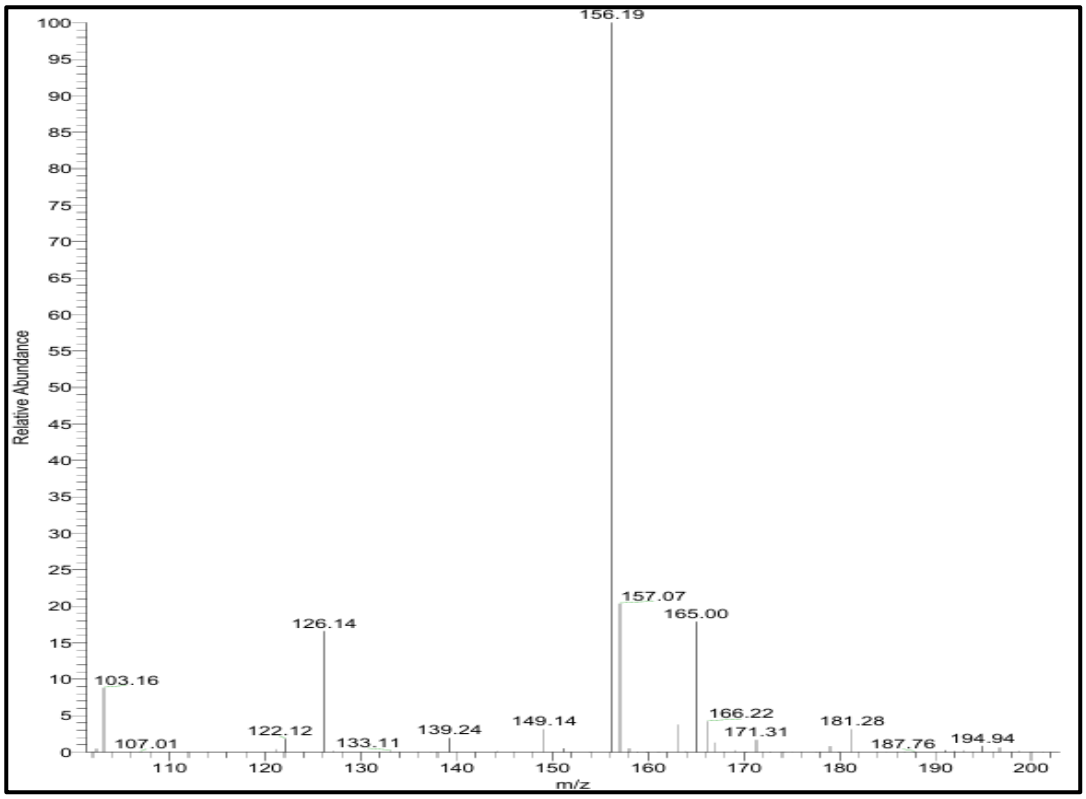

ESI-MS spectrum of 3-phenylpyridine (Exact mass= 155.07)

References:

1. R. S. Melo, P. Banerjee and A. Franco, J. Mater. Sci.: Mater. Electron., **2018**, 29, 14657 14667.
2. M. N. Kiani, M. S. Butt, I. H. Gul, M. Saleem, M. Irfan, A. H. Baluch and M. A. Raza, ACS Omega, **2023**, 8, 3755–3761.
3. J. Bora, M. Dutta, A. J. Kalita, A. Suleman, U. Chutia and B. Chetia, New J. Chem., **2025**, 49, 14119–14129.
4. P. Akbarzadeh, N. Koukabi and E. Kolvari, Mol. Divers., **2020**, 24, 1125–1137.
5. S. Payamifar, F. Kazemi, B. Kaboudin, *Appl. Organomet. Chem.* **2021**, *35*, e6378.
6. M. Keyhaniyan, A. Shiri, H. Eshghi, A. Khojastehnezhad, *New J. Chem.* **2018**, *42*, 19433–19441.
7. A. Shetty, D. Sunil, T. Rujiralai, S. P. Maradur, A. N. Alodhayb, G. Hegde, *Nanoscale Adv.* **2024**, *6*, 2516–2526.
8. M. Nasrollahzadeh, R. Bakhshali-Dehkordi, T. A. Kamali, Y. Orooji, M. Shokouhimehr, *J. Mol. Struct.* **2021**, *1244*, 130873.
9. Y. Dong, J. J. Jv, Y. Li, W. H. Li, Y. Q. Chen, Q. Sun, J. P. Ma, Y. B. Dong, *RSC Adv.* **2019**, *9*, 20266–20272.
10. C. K. Manna, R. Naskar, B. Bera, A. Das, T. K. Mondal, *J. Mol. Struct.* **2021**, *1237*, 130322.